General Disclaimer

One or more of the Following Statements may affect this Document

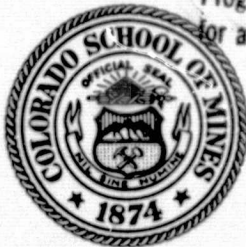E7.6 - 1 0.0.2 9
CR-145421

GEOLOGIC AND MINERAL AND WATER RESOURCES INVESTIGATIONS

IN WESTERN COLORADO USING ERTS-1 DATA: FINAL REPORT

NASA Contract NAS5-21778

Compiled and Edited by
Daniel H. Knepper
Department of Geology
Colorado School of Mines
Golden, Colorado 80401

Contributors:

D.L. Sawatzky   D.L. Bruns
D.W. Trexler   D.H. Knepper
R.J. Weimer   S.M. Nicolais

August 1974
Type III Report for Period 30 June 1972 - 1 August 1974

Remote Sensing Report 75-1

Prepared for

GODDARD SPACE FLIGHT CENTER

Greenbelt, Maryland   20771

REMOTE SENSING PROJECTS

DEPARTMENT OF GEOLOGY

COLORADO SCHOOL OF MINES • GOLDEN, COLORADO

1. Report No.	2. Government Accession No.	3. Recipient's Catalog No.
4. Title and Subtitle Geologic and Mineral and Water Resources Investigations in Western Colorado Using ERTS-1 Data: FINAL REPORT		5. Report Date
		6. Performing Organization Code
7. Author(s) Compiled and Edited by Daniel H. Knepper		8. Performing Organization Report No. 75-1
9. Performing Organization Name and Address Colorado School of Mines Golden, Colorado 80401		10. Work Unit No.
		11. Contract or Grant No. NAS5-21778
		13. Type of Report and Period Covered
12. Sponsoring Agency Name and Address G. Richard Stonesifer ERTS Technical Monitor, Code 430 NASA/Goddard Space Flight Center Greenbelt, Maryland 20771		Type III 6/30/72 to 8/31/74
		14. Sponsoring Agency Code

Original photography may be purchased from:
EROS Data Center
10th and Dakota Avenue
Sioux Falls, SD 57198

15. Supplementary Notes

16. Abstract ERTS-1 imagery of central and western Colorado contains an extraordinary amount of basic geologic information. Most of this information can be extracted from bulk processed, black and white positive transparencies by a skilled interpreter using conventional photogeologic techniques. Photo-optical image enhancement methods can be used to selectively enhance specific geologic phenomena, but overall image degradation results. Detection and mapping of lithologic contacts, geologic structures and landforms is relatively insensitive to spectral band, but the time of year the imagery was acquired profoundly affects detectability and information content. Geologic structures, particularly linear structures, are the most readily extractable type of geologic information on ERTS-1 images. Areas of high frequency of linear intersections show a strong correlation with the location of metallic mineralization in the Colorado Mineral Belt. "Reddish" color anomalies mapped on ERTS-1 images also correlate with areas of known mineralization in the San Juan Mountains.

17. Key Words (Selected by Author(s))	18. Distribution Statement
structural geology rock discrimination mineral exploration atmospheric effects	

19. Security Classif. (of this report)	20. Security Classif. (of this page)	21. No. of Pages	22. Price*

*For sale by the Clearinghouse for Federal Scientific and Technical Information, Springfield, Virginia 22151.

PREFACE

On 30 June 1972 a contract was awarded to the
Colorado School of Mines for research in the interpretation
of ERTS-1 imagery and supporting aircraft data and their
application to mineral and water resources investigations.
This work was done by faculty members and graduate student
research assistants in the Department of Geology and by
research scientists in the Planetary Geology Laboratory at
Martin-Marietta Corporation/Denver Division. The objectives
of the investigation were:

1) the extraction of basic geologic information
   from ERTS imagery,

2) the application of this basic geologic informa-
   tion to the study of mineral resources, volcanic
   phenomena, and water resources in central and
   western Colorado, and

3) input to the study of the effects of the
   atmosphere on ERTS MSS imagery.

ERTS imagery of central and western Colorado contains
an extraordinary amount of basic geologic information. Much
of this information can be extracted straight from the four
bands of MSS imagery using standard photogeologic interpreta-
tion techniques. Use of stereoscopic analysis greatly
increases the amount and accuracy of the extracted information.

Image enhancement techniques, such as color additive viewing, color separation and density slicing, can be effectively applied to the enhancement of specific image phenomena related to geology. However, image enhancement produces an image that is generally less useful for general interpretation.

The distribution and location of lineaments and color anomalies mapped from ERTS-1 images can be correlated with the location of mineralization in the Colorado Mineral Belt of central and western Colorado. Relatively simple structural (lineament) analysis of ERTS-1 images of less geologically well-known areas should prove productive as an initial step in mineral exploration.

The detectability of lithologic contacts and geologic structures on ERTS-1 imagery is relatively insensitive to spectral band. Imagery acquired at various times of year, however, show marked variations in detectability. The information content of a given set of ERTS-imagery is also insensitive to spectral band.

TABLE OF CONTENTS

LIST OF ILLUSTRATIONS

LIST OF TABLES

INTRODUCTION

This report summarizes the work conducted by the Colorado School of Mines under NASA Contract NAS5-21778 for the purpose of investigating the application of ERTS-1 imagery and supporting aircraft remote sensing data to geologic and mineral and water resources in western Colorado. The primary objectives of the investigation were to:

(1) Evaluate the use of ERTS-1 imagery for the discrimination and identification of rocks and soils, geologic structures and landforms,

(2) Study the potential of applying ERTS-1 imagery in the fields of general geologic mapping, structural and tectonic analysis and mineral resources, and

(3) Evaluate various interpretative and image enhancement techniques.

A secondary objective of the investigation was to gather various atmospheric measurements during selected ERTS-1 passes to be used by the Environmental Research Institute of Michigan (ERIM) in its on-going study of the affects of the atmosphere on remote sensing data.

Research conducted during this investigation by no means completely covers the range of geologic or geology-related topics that may be studied using ERTS-type remote sensing data. Since space imagery is a relatively new addition to our arsenal of investigative tools, we have focused our efforts mainly on the fundamental properties of ERTS-1 imagery: (1) the basic geologic information content of ERTS-1 imagery, (2) the way this information content varies with changes in imaging parameters (band, time of year, etc.), and (3) the potential of applying basic geologic information to selected disciplines of geologic inquiry.

Interpretative methods and the techniques of enhancing the interpretability of ERTS-1 imagery, employed during the investigation were mostly restricted to procedures that can be used by the average user of ERTS-1 imagery. Since most geologic users do not have expensive computer/display facilities nor can they afford to have sophisticated data processing applied to the digital imagery data (assuming they knew what kind of operations they needed to have performed on the data), our geologic analyses have been conducted on standard bulk processed imagery data and photographic products that can relatively easily be prepared from the bulk processed imagery, using standard and modified photointerpretation techniques.

Although submission of this final report terminates ERTS-1 research conducted under NASA Contract NAS5-21778 (Goddard Space Flight Center) at the Colorado School of Mines, analysis of ERTS-1 imagery of Colorado will continue to be conducted by faculty and students studying the geology of Colorado and by investigators working on Skylab/EREP research (NASA Contract NAS 9-13394) at the school. This latter research is concerned primarily with comparing the geologic utility of ERTS-1 imagery and Skylab/EREP data in terms of quality and quantity, with peripheral considerations of cost of acquisition.

PROJECT HISTORY

Initiation of the geologic and mineral and water resources investigations in western Colorado using ERTS-1 data by the Colorado School of Mines (C.S.M. ERTS Project, Proposal 026) commenced 30 June 1972 with the taking affect of NASA Contract NAS5-21778, Goddard Space Flight Center, Greenbelt, Maryland. Phase I of the investigation (Data Analysis Preparation) was conducted during July and August 1972, and consisted of the organization of the overall program and the various faculty and graduate student research projects that would be conducted and preparations for receiving, indexing and analyzing ERTS-1 data. Phase II of the investigation (Preliminary Data Analysis) was conducted during September, October and November 1972 and the results of the early studies was reported a Type II Report for the period 31 June-11 November 1972 (NASA-CR-132754).

Phase III (Continuing Data Analysis) was conducted from December 1972 through March 1974. Due to an oversight, a comprehensive Data Analysis Plan was not approved by NASA until June 1973, so the official recognition of the end of Phase III was considered 15 October 1974 (approvement of DAP + 16 months), rather than 15 March 1974. Additional

funds requested by the C.S.M. ERTS Project allowed Phase III to be extended through August 1974. These additional funds were used to follow three lines of investigation begun on the original contract funding.

PERSONNEL

Research undertaken on the C.S.M. ERTS Project was conducted by faculty and graduate student of the Colorado School of Mines and research scientists in the Planetary Geology Laboratory of the Martin Marietta Corporation-- Denver Division, under subcontract to C.S.M. Table 1 shows the research personnel involved in the C.S.M. ERTS Project and the approximate dates they were affiliated with the project.

Only one major personnel change occurred during the course of the C.S.M. ERTS Project. The original Principal Investigator, Dr. Robert G. Reeves, left the Colorado School of Mines in December 1972. From the date of his departure until June 1973, Dr. Daniel H. Knepper served as Acting Principal Investigator, at which time he became officially recognized by NASA as the C.S.M. ERTS Project Principal Investigator for the duration of the contract.

Table 1. List of personnel on C.S.M. ERTS Project with
approximate dates of affiliation.

PROGRAM MANAGER	FROM	TO
Dr. Harry C. Kent	30 June 1972	-termination
PRINCIPAL INVESTIGATOR		
Dr. Robert G. Reeves	30 June 1972	-31 December 1972
Dr. Daniel H. Knepper	1 January 1973	-termination
CO-INVESTIGATORS		
Dr. Robert M. Hutchinson		
Dr. Daniel H. Knepper	30 June 1972	-31 December 1972
Dr. Donald L. Sawatzky		
Dr. David W. Trexler		
Dr. Robert J. Weimer		
GRADUATE ASSISTANTS		
Mr. Dennis L. Bruns	30 June 1972	-31 December 1973
Mr. James L. Evans	30 June 1972	-
Mr. Stephen M. Nicolais	30 June 1972	-31 May 1974
RESEARCH SCIENTISTS/MARTIN MARIETTA CORPORATION		
Mr. James R. Muhm	1 July 1972	-31 July 1973
Mr. Roland L. Hulstrom	"	"
Mr. Kenneth E. Worman	"	"
Mr. Daniel C. Wychgram	"	"

ERTS-1 AIRCRAFT SUPPORT DATA

NASA MISSIONS 205 AND 211

Two high altitude aircraft missions were flown in
support of the Colorado School of Mines ERTS-1 program.
Mission 205 was flown during June 1972 and Mission 211
during September 1972.

DATA ACQUISITION

Data were acquired by instruments on the RB57F
Aircraft (NASA 925) from an average altitude of 55,000'
above sea level resulting in elevations of nearly 50,000'
above mean terrain. The data on Mission 205 were acquired
on 2, 14, and 15 June 1972; Mission 211 data were acquired
on 16, 17 and 21 September 1972. The data include color,
color IR and multiband photography and daytime thermal IR
imagery. Table 2 gives the specifications for the photo-
graphy acquired.

DATA RECEIVED

Mission 205 data were received during October 1972;
Mission 211 data were received during November 1972.
The Mx 205 data includes 14 north-south flight lines of

TABLE 2. MX 205/211 Photographic Specifications.

CAMERA	LENS	FILM	FILTER	PHOTOGRAPHY
RC-8	6"	SO-397	2A	Color
RC-8	6"	2443	12	Color IR
Zeiss	12"	2443	12	Color IR
Hasselblad	40mm.	2402	25	Blue
Hasselblad	40mm.	2402	57	Green
Hasselblad	40mm.	2424	89B	B/W IR
Hasselblad	40mm.	SO-356	HF 3	Color
Hasselblad	40mm.	2443	12 + cc 20B	Color IR

-8-

photography flown from near the northern border of Colorado
to near the southern border of Colorado. The 18 lines on
Mission 211 were flown in the same general configuration.
Photography requested over the San Juan Mountains could
not be flown on either mission due to poor weather
conditions.

DATA QUALITY

Data from both missions are good. Excellent resolu-
tions and exposures characterize the photography and the
thermal IR imagery is generally good quality. Both
side-lap and end-lap are adequate for geologic work with
stereoscopic equipment. In addition, cloud cover is
generally only a small percentage of the area, and most
areas are cloud-free on one of the missions.

NASA MISSION 213

On 9-14 September 1972, the NASA NC130B acquired
remote sensor data over four selected subsites within
the Colorado School of Mines ERTS test site. These four
sites are Golden, Leadville, Canon City and the San Juan
Mountains. Each of these areas was the site of a detailed
ERTS remote sensing investigation. Color and color IR
photography was acquired to support ground evaluation of

ERTS data and multiband photography and MSS data were
acquired to help gain a better understanding of the use
of multispectral sensors.

COLOR AND COLOR INFRARED PHOTOGRAPHY

Color and color infrared (IR) photography were obtained
over all areas in the noncontingency flight request. The
results of the evaluation of this photography is summarized
in Table 3.

Table 3. Summary of Broad Mission Parameters Evaluated

Area	Flightline accuracy	% coverage	Cloud loss (%)	sufficient Sidelap	end lap (60%)
Canon City	Good	100	25	Yes	Yes
San Juan Mts.	Good	100	10	Yes	Yes
Golden	Good	100	5	Yes	Yes
Leadville	Good	100	5	Yes	Yes

Eighteen additional image quality factors also were
evaluated providing an objective measure of the overall data
quality. Both the color and color IR photography provided
generally good to excellent positive transparencies.

Highly-variable terrain brightness caused some problems
in getting good exposures in all the photographed terrain.
Due to this variation in terrain brightness, fifteen percent
of the photography was rated as having variable exposure

(i.e.-not normal exposure). However, this photography was rated as acceptable. It is concluded that the photographer handled the difficult situation very well and that the processing was good.

MULTIBAND PHOTOGRAPHY

Multiband photography was flown to discriminate between rock types and to aid in understanding the multispectral scanner data. Multiband photography was obtained in the Canon City and Golden areas using the following film/filter combinations:

CAMERA	FILM/FILTER
I^2S	ERTS configuration
Hasselblad 4	2424/89B
Hasselblad 5	2402/8
Hasselblad 7	2402/92
Hasselblad 8	2424/87C

Mission parameters were essentially the same for the I^2S and Hasselblad photography except that no sidelap was obtained with the I^2S camera. An evaluation of some significant parameters of the multiband photography are listed in the Table 4 below. Overall, the multiband photography seems to have been properly acquired.

Table 4. Evaluation of MX 213 Multiband Photography.

		I²S	Hass.4	Hass.5	Hass.7	Hass.8
Exposure (%)	Normal	90	81	81	81	81
	Under	5	19	19	19	19
	Over	5				
	Variable					
Contrast (%)	Normal	80	81	81	81	81
	Flat	20	19	19	19	19
Tone		Good	Good	Good	Good	Good
Summary Evaluation		Good	Good	Good	Good	Good

MULTISPECTRAL SCANNER

Multispectral scanner (MSS) data were obtained over
selected areas at the Canon City and Golden sites.
Approximately 88 percent of the requested data was obtained.
Data loss was due to malfunctions of a few channels of
the MSS. The flight-line accuracy was excellent and cloud
loss was not significant.

AIRCRAFT DATA APPLICATIONS

Aircraft remote sensing data, mainly color, color IR,
and multiband photography, were applied to the CSM/ERTS-1
project in a variety of ways; a few specific examples are
listed below:

1) Areas where rock discrimination can be made on
ERTS-1 imagery were isolated and documentation was

made of the physical characteristics of the outcrops discriminated. Aircraft data were used to document tonal, textural, topographic, vegetation, etc., differences that allowed discrimination to be made.

2) Areas where similarly configured rock units occur, but where discrimination cannot be made, were isolated. Aircraft data were used to help determine the surface conditions that hindered discrimination.

3) Areas where known structural features (folds, faults, joint sets) occur were isolated on ERTS-1 images. It was then determined whether the known structures can be detected. Aircraft data were used to determine the cause of textural and tonal differences noted, if any.

4) Areas where known landforms occur were isolated on the ERTS-1 imagery. Aircraft data were used to document the geometry and dimensions of the landforms as well as to help determine the cause of texture and tone noted on the imagery.

5) Areas where known mineral deposits occur were isolated on ERTS-1 imagery. Aircraft data were used to help document the surface manifestations of the deposits and the ERTS imagery was analyzed for these manifestations.

6) ERTS imagery was studied for new geologic
   information on 1 - 5 above. Aircraft data were
   used to help document the discovery of newly
   discovered geologic phenomena.

7) Aircraft data were applied to detailed and
   reconnaissance ground studies in specific geographic/
   geologic areas of interest.

BASIC GEOLOGIC INFORMATION

The Colorado School of Mines analyzed and evaluated ERTS-1 imagery for the purpose of discriminating and identifying geological phenomena in central and western Colorado. Many specific geologic phenomena can be discerned on ERTS-1 imagery, and almost all information that can be derived from ERTS-1 images can be viewed, in one way or another, in a geological context. For example, such seemingly non-geological features as cities, railroads and highways can be studied from the point of view of the geological factors in their location (or mislocation) and the potential problems that might be encountered as a result of normal geological processes (floods, earthquakes, land-slides, erosion). Similarly, fields and field patterns can be viewed in terms of the geology and geochemistry of their soils or in terms of the availability of surface and ground water necessary for productive farming.

However, the geologic information content of ERTS-1 imagery can be pared down to 3 basic catagories from which more specific information can be derived. This Basic Geologic Information consists of the location and distribution of:

1) rocks and soils (lithology)

2) geologic structures

3) landforms

This knowledge is <u>basic</u> to all geologic investigations, be they mineral exploration programs, dam sitings, highway routings, groundwater studies, or whatever.

Although the 3 catagories of basic geologic information can be studied separately (lithologic maps, tectonic maps, topographic maps), they must be considered together during the geologic interpretation of ERTS-1 imagery:

1) Tracing of lithologic contacts may define geologic structures.

2) The evolution of landforms is commonly controlled by rock type (lithology).

3) Geologic structures often produce recognizable landforms.

Therefore, some overlap is necessary in the discussions of the 3 catagories of basic geologic information that follow.

The capability of extracting basic geologic information from ERTS-1 imagery was investigated by several researchers working on imagery of a variety of geologic terrains in different parts of Colorado (Fig. 1). In addition, quantitative studies were conducted on the lithologic contact detectability and information content of ERTS-1 imagery and the statistical significance of linears and lineaments mapped on ERTS-1 images.
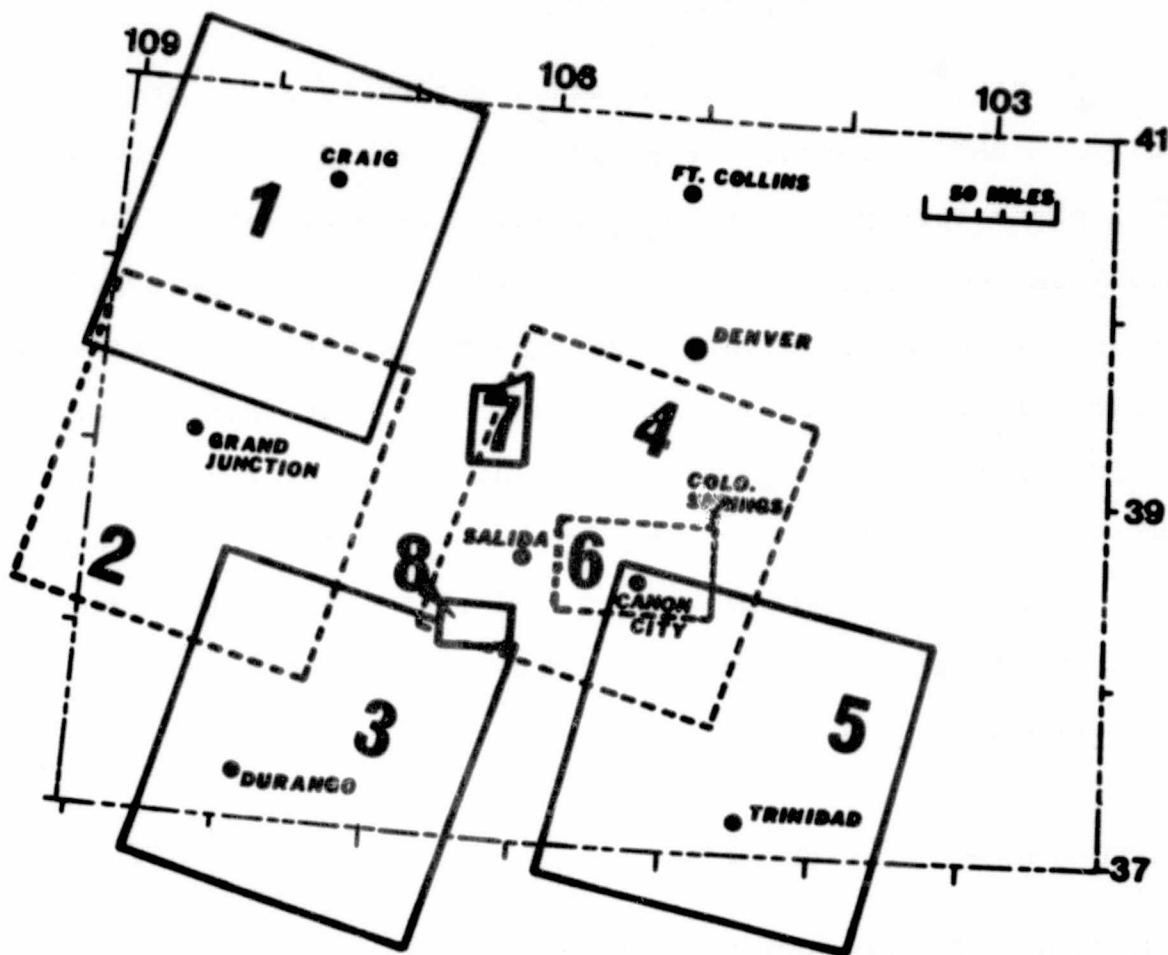
Figure 1. Index map of Colorado showing primary areas in
which ERTS-1 imagery was analyzed for basic geologic
information. 1 - Northwestern Colorado, D.W.
Trexler; 2 - Uncompahgre/Paradox area, R.J. Weimer;
3 - San Juan Mountains, R.W. Hutchinson and S.N.
Nicolais; 4 - Central Colorado, S.N. Nicolais and
D.L. Sawatzky; 5 - Raton Basin, R.J. Weimer; 6 -
Canon City area, D.H. Knepper; 7 - Mosquito Range,
D.L. Bruns; 8 - Southwest Bonanza area, D.L. Bruns.

- 17 -

LITHOLOGIC DISCRIMINATION

Mapping the location and distribution of rocks and soils on ERTS-1 imagery is largely controlled by the ability of a photo-interpreter to discriminate between lithologic units on the imagery. Rarely, if ever, can lithologic units be identified as to composition (quartz sandstone, carbonaceous shale, granite, etc.) on ERTS-1 images or, for that matter, on low-altitude photographs. Yet, different rock and soil types commonly result in different surface expressions, and these differences can be interpreted (lithologic discrimination) even though the specific units themselves cannot be identified.

RESULTS OF AREAL STUDIES

SAN JUAN MOUNTAINS AND CENTRAL COLORADO

ERTS-1 images of central Colorado and the San Juan Mountains (Fig. 1) were studied in order to determine the mapability of lithologic contacts in these geologically-contrasting areas. The images studied are shown in Table 5 and Figures 2, 3 and 4. Figures 5 and 6 are lithologic maps prepared by photo-interpretation of the images.
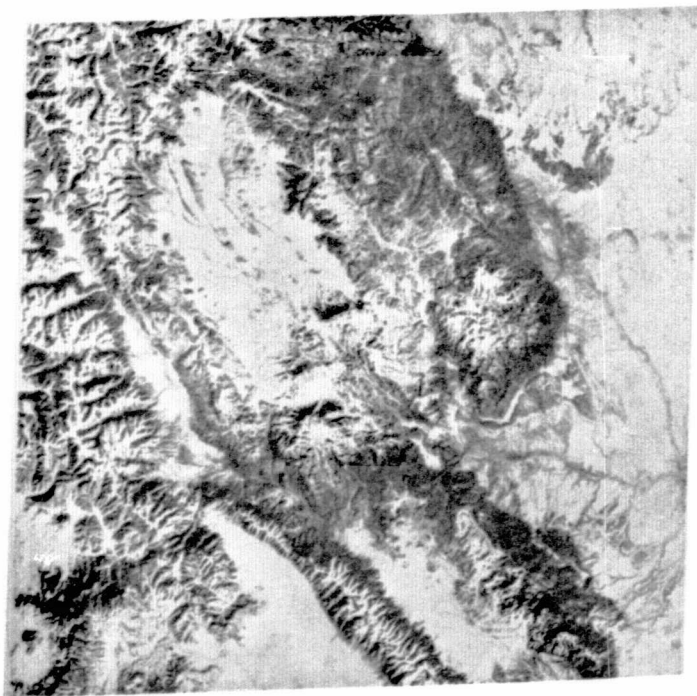
Central Colorado

Figure 2. ERTS-1 image 1172-17141-5.
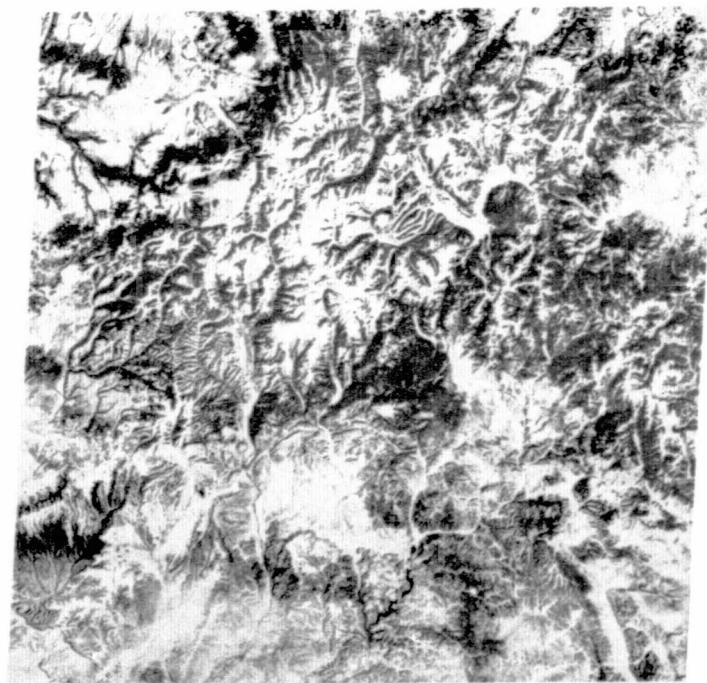
San Juan Mountains

Figure 3. ERTS-1 image 1191-17204-5.
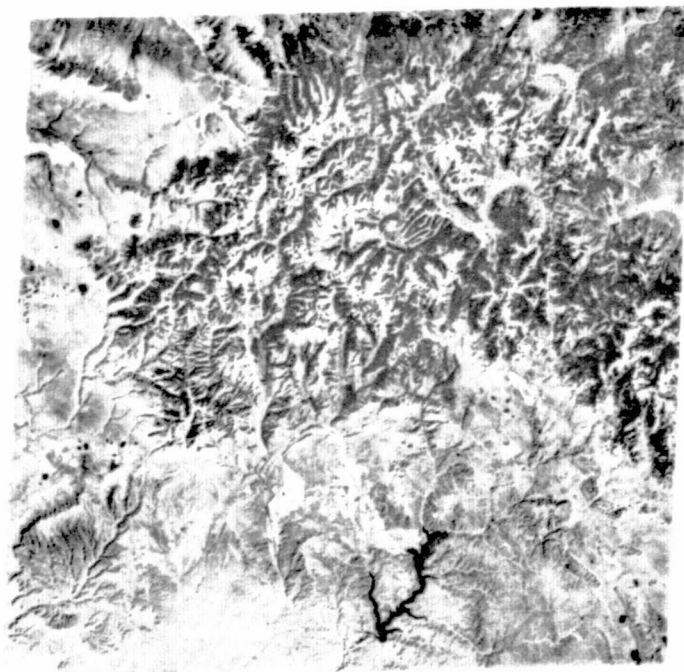
San Juan Mountains

Figure 4. ERTS-1 image 1425-17190-5.
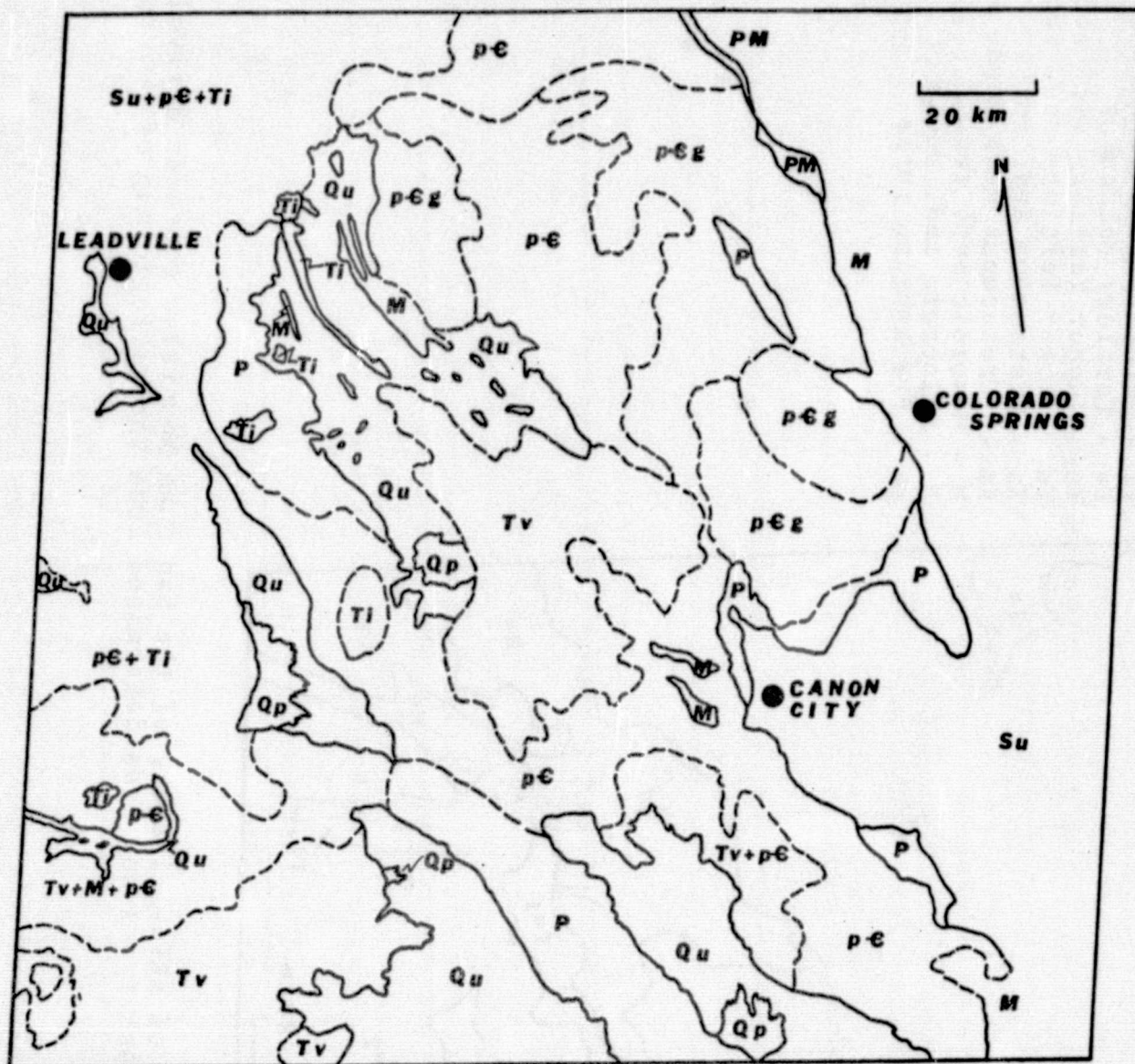
Su = Sedimentary rocks undivided
Qp = Quaternary pediment gravels
Qu = Quaternary sediments undivided
Tv = Tertiary volcanics
Ti = Tertiary intrusive
M = Mesozoic sedimentary rocks
P = Paleozoic sedimentary rocks
pЄg = Precambrian granite
pЄ = Precambrian rocks undivided

Figure 5.   Generalized lithologic map of ERTS-1 image 1171-
             17142 of central Colorado. Contacts derived by
             photo-interpretation; rock types and ages
             determined from the geologic map of Colorado
             (1:500,000) where possible.
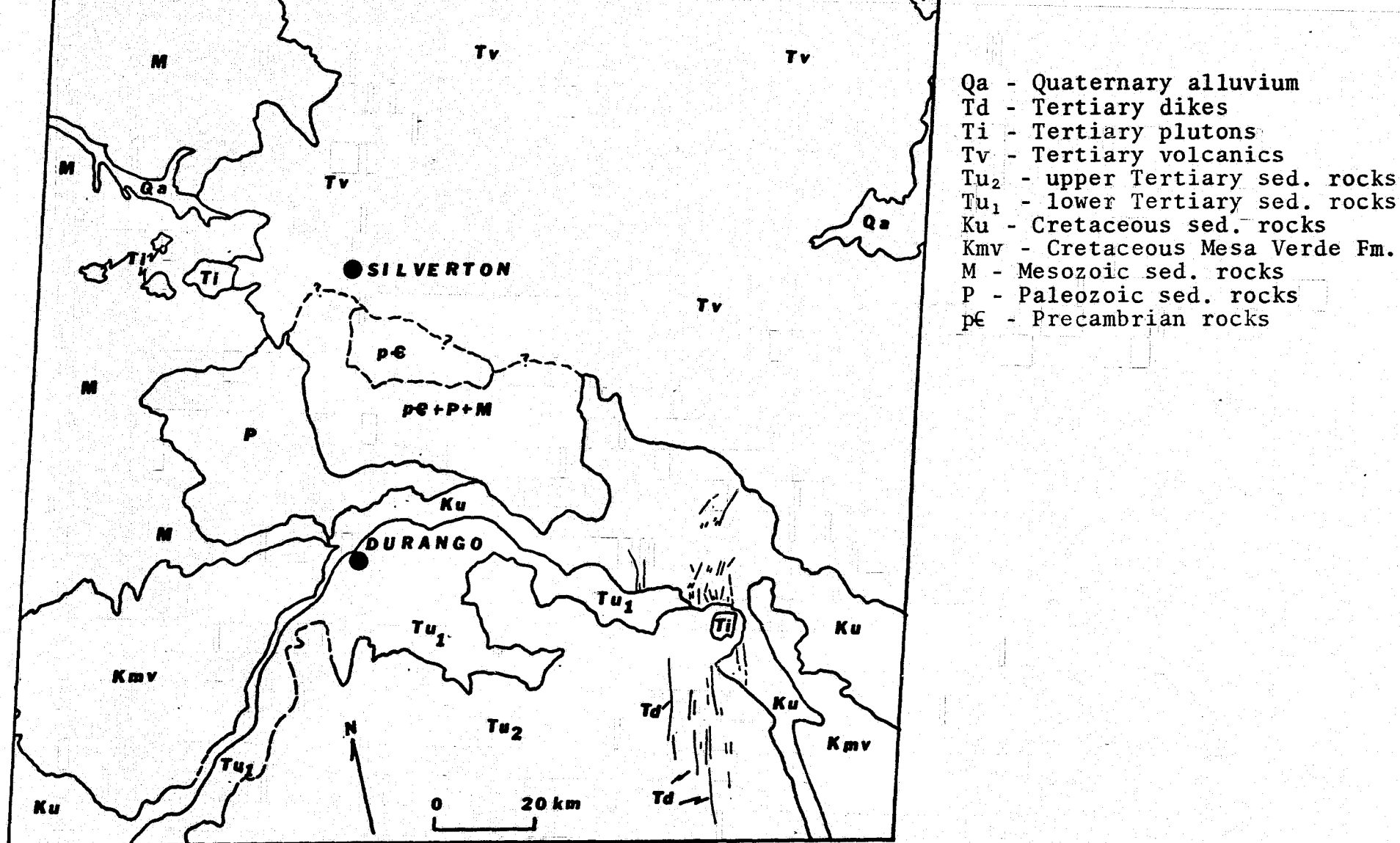
Figure 6. Generalized lithologic map of ERTS-1 imagery of the San Juan Mountains contacts derived by photo-interpretation; rock types and ages determined from the geologic map of Colorado (1:500,000).

Table 5. ERTS-1 imagery of Central Colorado and the San Juan Mountains analyzed for lithologic contacts.

AREA	IMAGE I.D.	COMMENTS
Central Colorado	1172-17142	snow-covered
San Juan Mtns.	1191-17204 1425-17190 1407-17193	snow-covered snow-free snow-free

Rock discrimination in the snow-covered scenes was generally poor especially in the western half of the central Colorado scene. Lithologic contact mappability in the snow-covered and snow-free scenes of the San Juan Mountain area were compared. The snow-free scene proved to be slightly better for rock discrimination in local areas.

During the photointerpretation of the ERTS imagery, rock discrimination and the placing of contacts was based almost entirely upon the geomorphic form and expression of the rock units, drainage textures and tonal differences. Many of the tonal differences are a direct result of the variations of vegetation with rock type and/or elevation. Except for specific areas (e.g.-local areas in and around Canon City, central Colorado scene) spectral differences in the snow-covered scenes studied were almost entirely due to vegetation density, vegetation type, land use patterns and variations in the amount of snow cover.

The ability to discriminate between two rock types on snow-covered ERTS scenes depends largely on the weathering characteristics and relative resistance to erosion of the rock types present. The contacts mapped were picked primarily on the spatial distribution of areas which appeared to have similar geomorphic forms, drainage textures and/or tones.

How well a contact between two rock types is expressed on the ERTS imagery studied depends upon the attitude of the contact (horizontal, inclined, vertical) and the composition and relative resistance to erosion of the adjacent rock types. Contacts between flat-lying sedimentary rocks or volcanic rocks (such as in the San Juan Mountain scene) on the steep slopes of mountains and on the sides of deep narrow canyons are generally very poorly expressed on the ERTS imagery due to the restricted outcrop exposure width (in a vertical view). Similarity in composition and resistance to erosion between the many volcanic units in the San Juan Mountains also renders discrimination difficult to impossible.

Among the most easily detected contacts in the scenes studied are:

1) bedrock vs. alluvium - San Luis Valley and Arkansas Valley (central Colorado scene)

2) sedimentary rocks vs. crystalline rocks - vicinity of Pikes Peak and Canon City - (Central Colorado scene)

3) Contacts between different sedimentary rocks in folded (Canon City) or tilted sequences (south edge of San Juan Mountains).

In most cases, detection and mapping of contacts is restricted to contacts between major lithologic groups or or sometimes between units within thick sequences of sedimentary rocks.

Contacts of dikes invading sedimentary rocks in the northeastern part of the San Juan basin are generally expressed as linear resistant ridges. Contacts between sedimentary rock units are generally expressed as a change in drainage texture and land forms (e.g. - hogbacks-valleys), especially if the rocks are tilted or folded. Although the contacts between crystalline and sedimentary rocks are usually easily detected, these contacts are difficult to impossible to detect in high, mountainous areas.

Contact between two adjacent crystalline rock types is often indistinguishable at the small scale of the ERTS imagery. The contact between the Precambrian granites, schists and gneisses of the Needle Mountains with the Tertiary volcanic rocks of the San Juan Mountains to the north is not very well expressed. The contacts between the many Tertiary intrusive bodies and the Tertiary volcanic country rocks in the San Juan region could not

be detected. However, there is a slight difference in tone
and drainage textures between the Pikes Peak granite and
the Precambrian gneisses and schists it intrudes.

In both the areas studied, actual or specific contacts
between known rock units often could not be discriminated.
However, a contact was often placed within a zone across
which there was a gradual change of drainage textures,
tones and general landforms. Although these contacts were
not exactly located, they more often than not did identify
a zone across which there is a major change in rock types.
Mapping lithologic contacts on snow-free scenes is much
the same as on snow-covered scenes, but tonal differences
on the imagery, especially in sparsely vegetated areas,
can be more directly related to lithologic differences.
Spectral differences between rock types and their residual
soils are best displayed on "true" color composites. Good
examples of rock type discrimination via spectral dif-
ferences can be found in the San Juan Basin and the Canon
City embayment.

RATON BASIN

The Raton basin is a structural basin in southern
Colorado and northern New Mexico about 80 km wide and
193 km long. The basin was selected as a study area
because its size permits coverage by one or two ERTS images

and, as a structural entity, the basin is typical of the intermontane structural basins in the Rocky Mountain area. The names applied to the major mountain ranges, valleys and geologic features are indicated on Figure 7.

Several images were reviewed with some preliminary mapping before selection of ERTS image E-1189-17091 for detailed study. Partial snow cover enhanced the topography and aided in geomorphic interpretations. Little difference could be noted between Bands 4, 5 and 6, but 6 was selected for mapping purposes. No stereoscopic coverage was available but a method of viewing both bands 5 and 6 with a stereoscope was employed and it aided significantly in the mapping.

The images were viewed from the point of view of no previous knowledge of the area. Therefore, it was necessary to determine the stratigraphic section and structure by employing normal photogeologic mapping techniques.

The discrimination of mappable rock units was based largely on topographic expression related to resistant or non-resistant units (landforms such as hogbacks, cuestas, valleys, ridges, drainages) and overall mountainous terrain vs low-lying terrain. Seven major mappable units were delineated (Fig. 8) as follows:

Unit 1. Resistant rocks in mountainous terrain with no visible layers or internal features. Because of structural dip in marginal sedimentary layers,
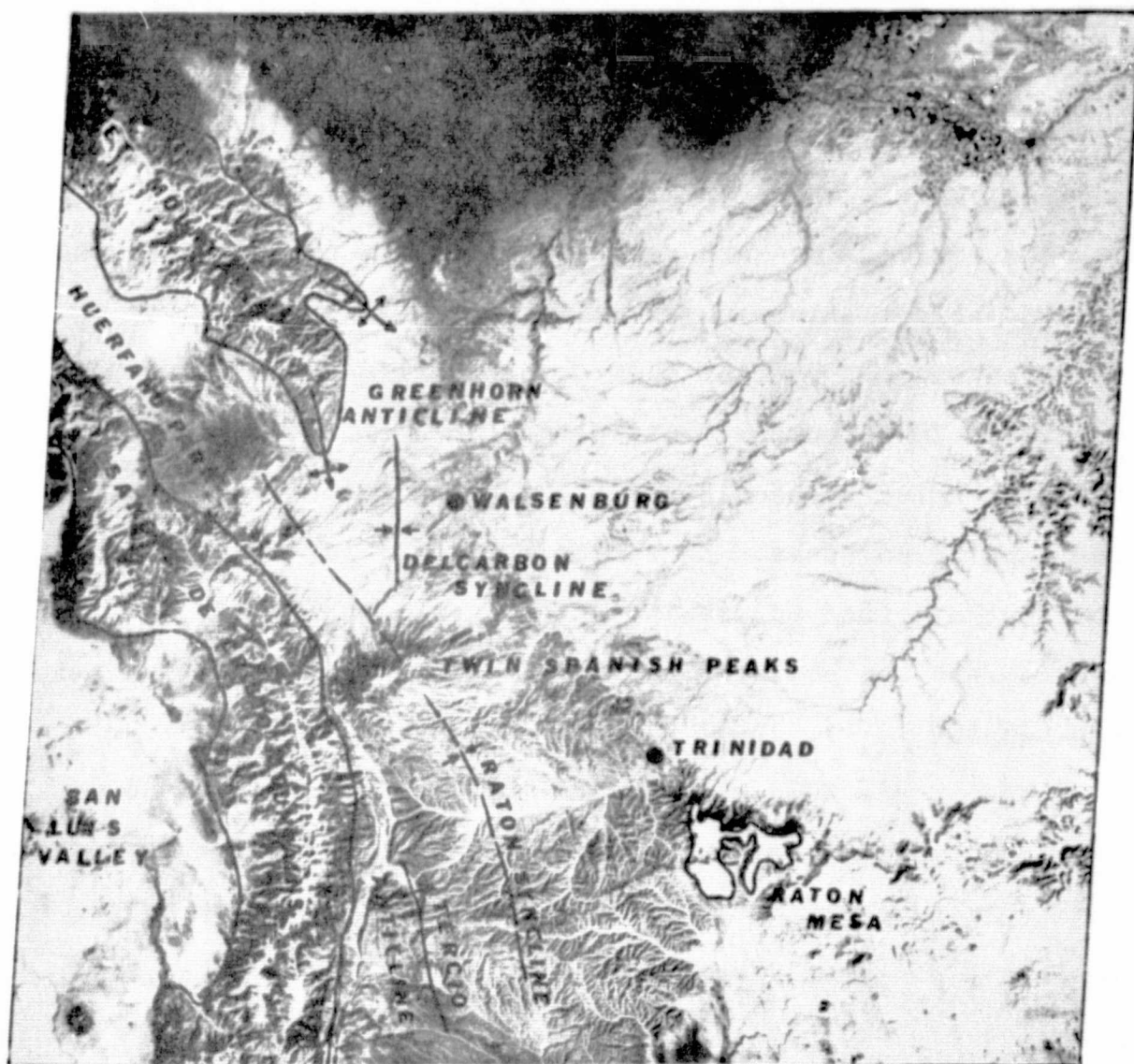
Figure 7. ERTS image 1189-17091-6 showing the major
geographic and geologic features of the Raton
basin area, south-central Colorado.
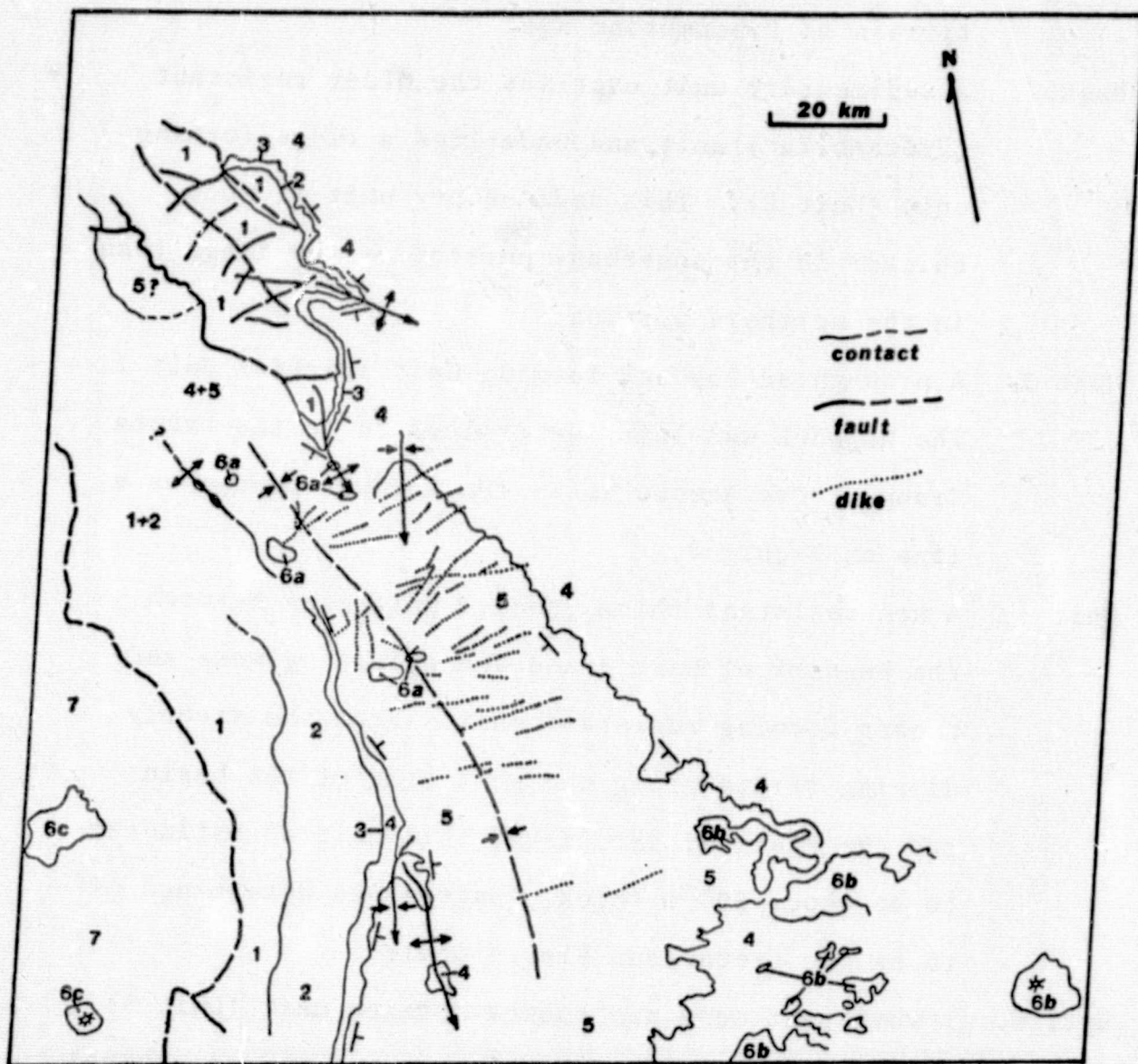
Figure 8. Geologic map of the Raton basin area prepared
from ERTS-1 image 1189-17091-6. See text for
explanation.

this unit is believed to be igneous or metamorphic terrain of Precambrian age.

Unit 2. A sedimentary unit overlies the older resistant (Precambrian) unit and underlies a ridge-forming unit (Unit 3). This sedimentary unit is much thicker in the southeast portion of the image than in the northern portion.

Unit 3. A pronounced hogback forming unit overlies Unit 2. The hogback was later determined to be the Dakota Group of Cretaceous age). Unit 3 was mapped as a line on Figure 8.

Unit 4. A non-resistant thick (shale) unit lies between the hogback of Unit 3 and the overlying mesa and cuesta-forming resistant unit. From the steeply dipping strata along the west side of the basin and the scale of the image, this unit is estimated to be about 800 m thick. Unit 4 was determined to be the Cretaceous Pierre Shale.

Unit 5. A resistant mesa and cuesta-forming unit (Unit 5) is exposed in the central portion of the structural basin. This unit was determined to be the Trinidad Sandstone, the coal-bearing Vermejo and Raton Formations and the Poison Canyon and Cuchara Formations. These units are Cretaceous and early Tertiary in age.

Unit 6. The sedimentary formations included in units 2-5
above are cut by igneous intrusions and covered
by volcanic flows.

Three different areas of igneous activity were noted:

a) Intrusive centers cutting the sedimentary units
2-5 mainly within the basin area. The intrusives
appear to be dikes, plugs and/or stocks. These
rocks possibly represent the oldest igneous
activity in the area.

b) Younger, nearly horizontal, flows were noted in
the southeast portion of the area. One well-
preserved (very young) cinder cone was also found
on the imagery.

c) A volcanic field with cinder cones occurs in the
southwest portion of the area. No age relation-
ship can be established between this field and
the one noted above. Both appear to be geologically
young (probably Quaternary).

Unit 7. The area of the San Luis Valley is covered by young
sedimentary rocks (Quarternary). Although present
elsewhere, this is the only area where these
youngest sediments were mapped.

UNCOMPAHGRE/PARADOX AREA

ERTS-1 image E-1156-17260 (Fig. 9) covers a large
portion of the Uncompahgre uplift and Paradox basin, and

Figure 9. ERTS-1 image 1156-17260-6 showing the major
geographic and geologic features of the
Uncompahgre/Paradox area, northwestern Colorado.

part of the Piceance basin of northwestern Colorado. All
four ERTS MSS bands were studied before band 6 was chosen
for detailed lithologic analysis. Figure 10 is a lithologic
map prepared from band 6 imagery; pseudostereoscopic
viewing, using band 6 imagery and one of the remaining
three bands for a stereo-pair, greatly increased the ability
to map lithologic contacts.

Six mappable units are easily discriminated on the
imagery (Fig. 10). Because of lack of soil cover and
vegetation in the topographically-low regions, tonal con-
trast between several of the units is excellent. The
characteristics of each unit are summarized as follows:

Unit 1) Resistant canyon-forming units are exposed in the
Black Canyon and Unaweep Canyon areas. This is
the oldest unit in the region and is regarded as
basement (Precambrian). Although probably
exposed, the unit could not be mapped in the deep
canyons that disect portions of the Uncompahgre
uplift.

Unit 2) All strata between the above unit and the base of
the thick shale mass with a light tone (unit 3)
were grouped together for mapping purposes. The
units are sandstone or limestone, are resistant to
weathering, and contain interbeds of shale (non-
resistant units). The tonal expression is
generally dark.
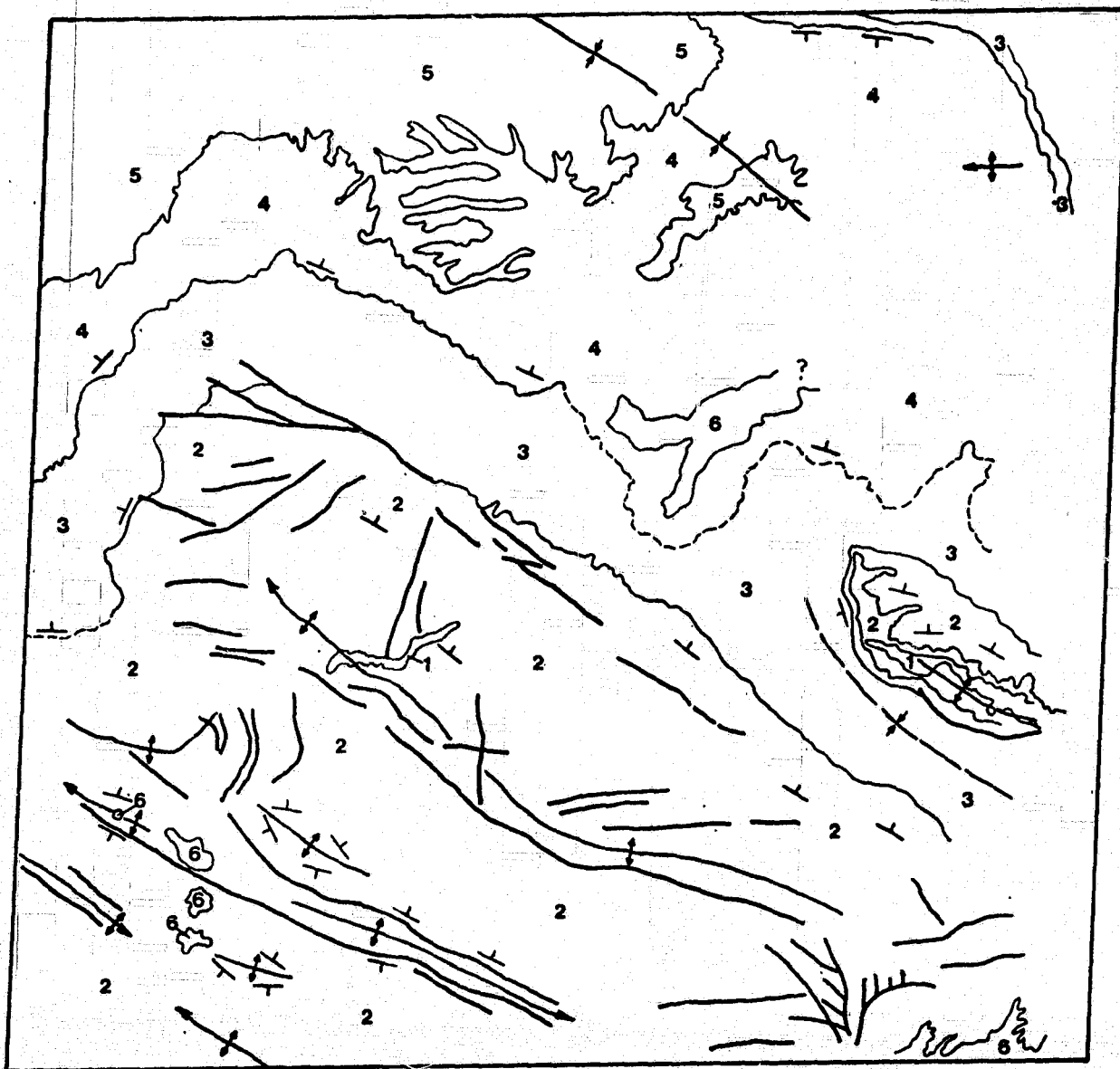
Figure 10. Geologic map of the Uncompahgre/Paradox area
prepared from ERTS-1 image 1156-17260-6. See
text for explanation.

These strata have been identified from geologic maps of the area as Triassic, Jurassic and Cretaceous in age. The uppermost resistant formation is the Dakota Sandstone.

Unit 3) The most conspicuous formation in the area is a thick mass of non-resistant shale recognized by the light tones on the image. The unit wraps around the north plunge of the Uncompahgre Uplift and is split into two outcrop belts by the Black Canyon Uplift.

Geologic maps of the area identify this shale mass as the Cretaceous Mancos Shale, approximately 1,500 m in thickness. The shale is light gray in outcrop and is of marine origin.

Unit 4) A resistant unit showing a dark tone on the image overlies Unit 3. The unit forms divides and characteristic land forms between the light tones of Units 3 and 5.

The unit contains sandstone, shale and coal and is identified from geologic maps as the Mesaverde Group (Cretaceous) and Wasatch Formation (Lower Tertiary). The thickness of the units is given as 1,500 m.

Unit 5) A second and younger formation with light tones is conspicuous in the northern portion of the image.

Unlike Unit 3, portions of this formation are resistant to erosion forming cliffs, slopes and canyon topography.

From geologic maps of the area, the unit is identified as the Green River Formation, composed largely of light gray and light green calcareous shales, oil shale, thin sandstones and marlstones of Eocene age.

Unit 6) Two areas of possible igneous rocks are identified on the image. An intrusive complex, forming a resistant mountain terrain, is present in the southwest portion of the image (La Sal Mountains). Several intrusives appear to cut the west-northwest anticlinal structures in the area. A second area of intrusives may be present east of the Black Canyon near the edge of the image.

The flat-lying undissected terrain in the north-central part of the area (Grand Mesa) is interpreted as lava flows. These appear to cap all of the older stratified units and, therefore, is the youngest.

Unit 7) Alluvial complexes, including pediments, can be observed along the major rivers. Much farming occurs associated with the rivers of the area. Because of the small scale, farming, etc., no effort was made to individually map these stratigraphic units.

around it, and a circular drainage pattern was also present around the Climax mining district. In general, however, the numerous Tertiary intrusives present in the region could not be distinguished from the Precambrian metamorphic rocks. The numerous sills intruded into the sedimentary rocks also could not be identified. It was estimated by comparison with a compilation geologic map of the area that only about 15% of the stratigraphic information available for detection on the ground could be extracted from ERTS imagery and the information extracted was general in nature. In the Mosquito Range and on the western edge of South Park, ERTS imagery taken during summer and winter were about equally useful for mapping lithologic information. The topographic variations present in the sedimentary rocks were enhanced by the low sun angle while such vegetational and rock color variations as existed were hidden by snow in the winter imagery. The reverse was generally true of ERTS imagery acquired during the summer; topographic variations were subdued and the vegetation and color differences present were more readily detected.

QUANTITATIVE EVALUATION

Since late July 1972, the Earth Resources Technology Satellite (ERTS) has been sending back scanner imagery of the earth in the green (band 4), red (band 5), and

photographic infrared (bands 6 and 7) portions of the

electromagnetic spectrum. Today, ERTS imagery of much of

the earth is available to geoscientists for application

to real and pressing geologic problems facing the U.S.

and the world. Because of the sun-synchronous orbit of ERTS,

imagery can be acquired over each area every 18 days,

producing an ever-increasing amount of imagery data from

which to choose. During a one year period, 20 potentially

usable sets of ERTS images could be obtained from each

imaged area. This would result in 80 individual ERTS images

for every area imaged; during the 2-year life of ERTS this

figure has doubled. Consequently, the geoscientist has the

problem of choosing from the available data, the imagery

that would best suit his purposes.

A study was conducted to determine if band and time

of year (month) were appreciably important factors in

being able to detect and map lithologic contacts on ERTS

imagery, and, if possible, to determine which bands and

times of year (months) produced the best results. The

results of the study reported here are not necessarily

everywhere applicable; however, the trends observed may aid

future ERTS investigators in choosing the best imagery

for lithologic mapping.

METHOD AND APPROACH

Twenty-four known lithologic contacts in central Colorado were selected for study. Each contact, or specific portion of a contact, was isolated on small-scale (1:100,000) color photos (Fig. 11), and the detectability (how easily seen) of each of the contacts on the photos was arbitrarily given a value of 1.0. These same contacts were then studied on each band of 4 sets of ERTS imagery taken at different times of year (Table 6 and Fig. 12), and the detectability of the contacts was evaluated relative to the color photos; the detectabilities of the contacts were always less than on the color photos.

Table 6. ERTS imagery sets of central Colorado used in study.

IMAGE I.D.	DATE	SUN AZIMUTH	SUN ELEV.	SNOW
1172-17141	11 Jan. 1973	151°	22°	Yes
1028-17135	20 Aug. 1972	129°	53°	No
1154-17143	24 Dec. 1972	153°	22°	Yes
1334-17142	22 June 1973	115°	62°	No

During the study of the contacts on the small-scale color photos, it was noted whether the contacts were expressed at the surface by (1) rock color (spectral), (2) topography, and/or (3) vegetation contrasts. This information was to be used to help explain any variation in the detectabilities that might be uncovered during statistical testing of the data.
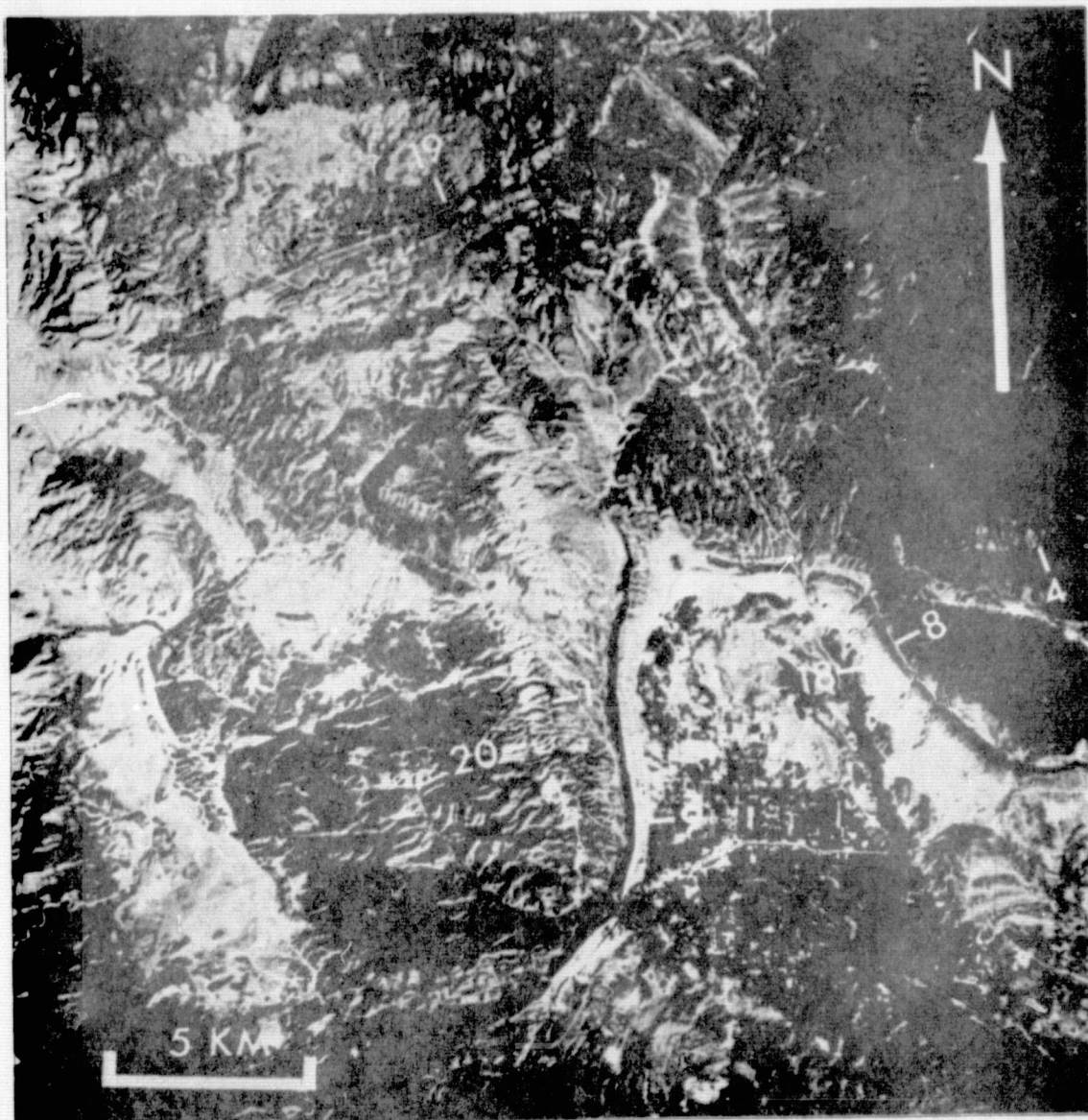
Figure 11.   Black and white reproduction of small-scale
color photo used to study lithologic contacts
in the Canon City area. Numbers identify some
of the contacts discussed in the text. NASA
Mission 211, Roll 31, Frame 0009.
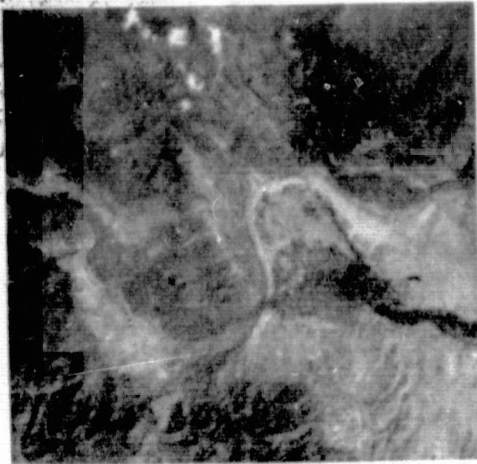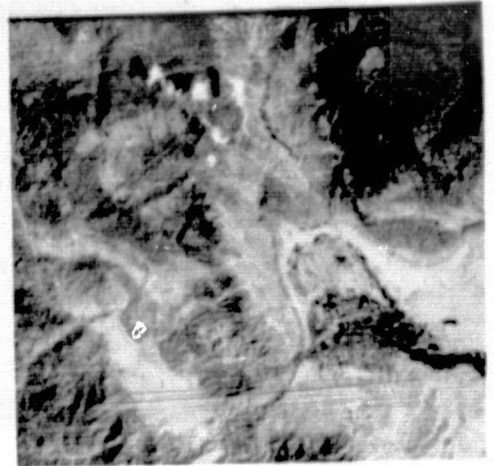
Green (.4-.5μm)   Red (.5-.6μm)
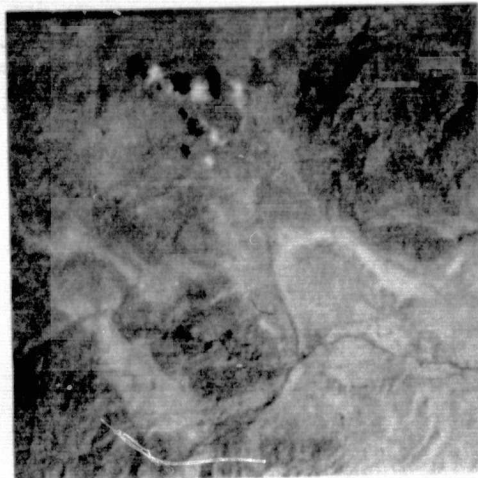
IR (.6-.8μm)

Figure 12A. Enlargements of portion of ERTS-1 image
             1028-17135 (20 Aug. 1972) showing same area
             as Figure 11.

Green (.4-.5μm)   Red (.5-.6μm)
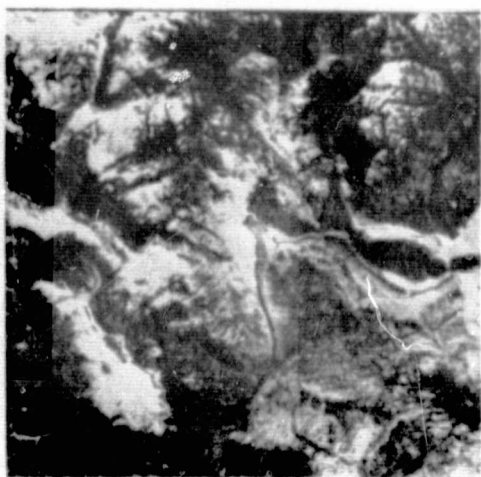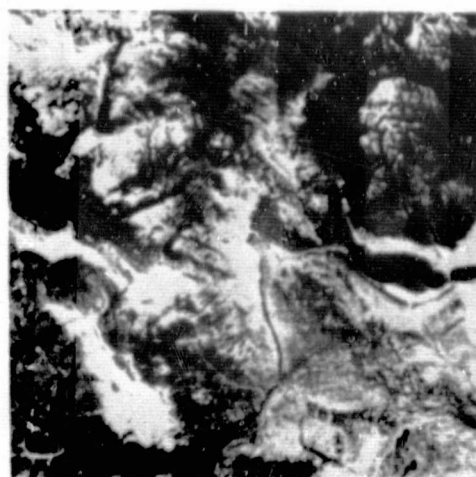
IR (.6-.8μm)

Figure 12B.   Enlargements of portion of ERTS-1 image
             1172-17141 (11 January 1973) showing same area
             as Figure 11.
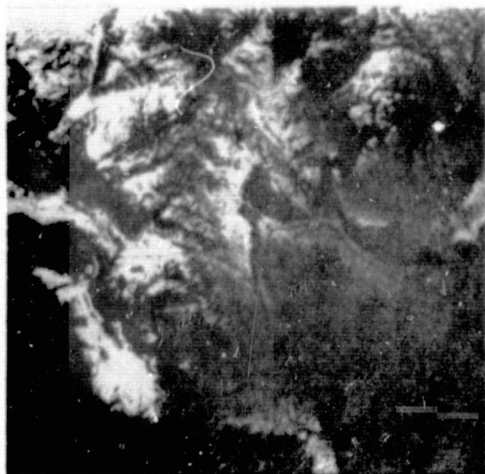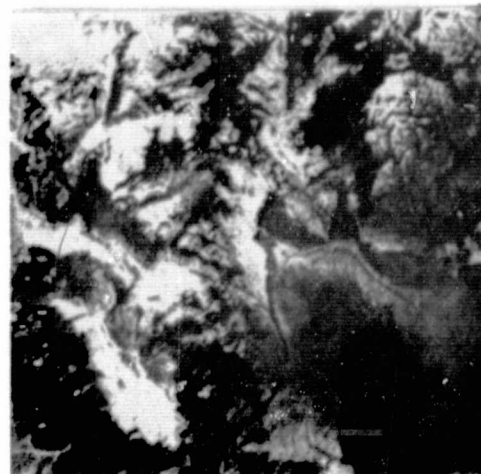
Green (.4-.5μm)
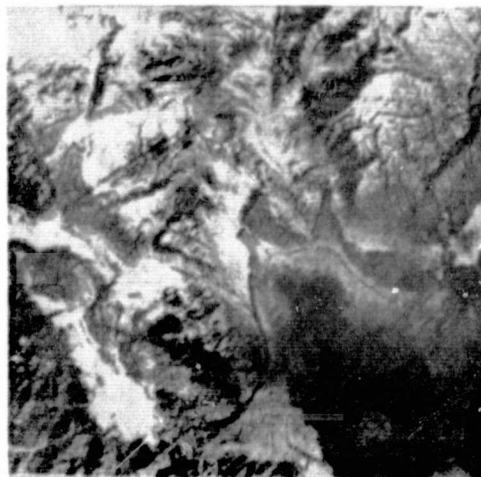
Red (.5-.6μm)

IR (.6-.8μm)

Figure 12C.   Enlargements of portion of ERTS-1 image
1154-17143 (24 Dec. 1972) showing same area
as Figure 11.
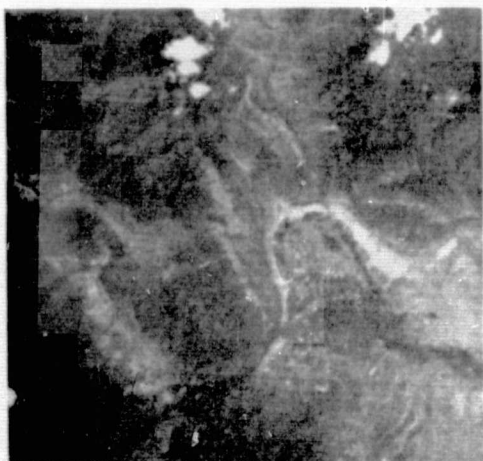
Green (.4-.5µm)
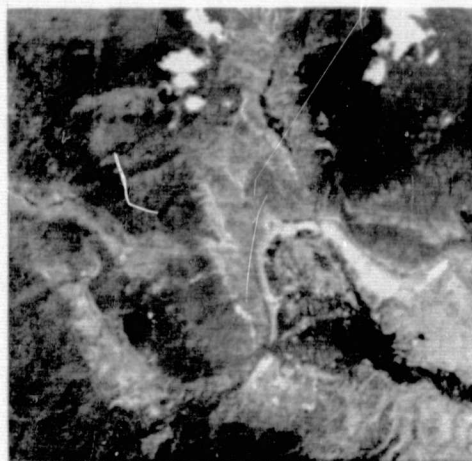
Red (.5-.6µm)
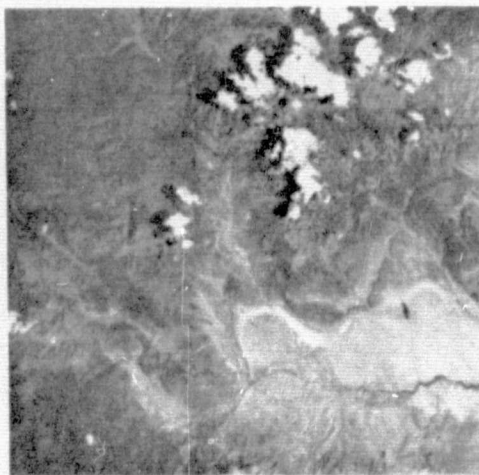
IR (.6-.8µm)

Figure 12D. Enlargements of a portion of ERTS-1 image
            1334-17142 (22 June 1973) showing same area
            as Figure 11.

Evaluation of the detectabilities was performed on 10" x 10" positive ERTS transparencies on a light table, using a 1 to 7X magnifying glass. The 4 sets of imagery were laid out in stacks on the light table according to image sets. One image was chosen from each stack and the 4 images were evaluated relative to the color photo and to each other. Next, all 4 bands of imagery from one image set (randomly chosen) were evaluated relative to the color photo and to each other. Finally, the remaining images in each set were evaluated using the evaluations made in the first two steps as a guide. All the evaluations were performed without knowing the image set and the band of the imagery being evaluated in order to reduce any conscious or unconscious bias in the evaluation procedure.

Occasional adjustments in the values of detectabilities for a given contact were necessary during the evaluation process. This occurred when a contact was found to have a detectability in between two previously evaluated images, but the two previous evaluations only differed by 0.1 (i.e.- no value to give the new image). The adjustments consisted of sliding the higher or lower detectabilities up or down, respectively, by a value of 0.1 in order to make room for the in-between image.

Figure 13 is an example of a portion of the evaluation matrix that was constructued.

ERTS IMAGE	CONTACT											
	1				2				3			
	J	A	D	Ju	J	A	D	Ju	J	A	D	Ju
BAND												
4	0	.7	.1	.9	0	.4	.3	.7	0	.2	0	.1
5	0	.6	0	.8	0	.3	.3	.9	0	.4	0	.3
6	0	.4	0	.3	0	.6	.2	.8	0	.1	0	.2
7	0	.4	0	.2	0	.3	.1	.8	0	.1	0	.1

Figure 13. Partial evaluation matrix generated during evaluation of detectability of lithologic contacts on ERTS imagery. J, January; A, August; D, December; Ju, June.

STATISTICAL TESTS

After all the detectability evaluations were completed for the 24 lithologic contacts, statistical tests were run on various subsets of the data matrix. These tests compare the mean detectability of a data subset with the mean detectability of another subset, producing information as to whether the means are statistically different at a given level of significance (α value). Three types of tests were used (3):

1) Standard F-test at $\alpha = 0.05$

2) Confidence intervals at $\alpha = 0.05$

3) Duncan multiple-range test at $\alpha = 0.05$

The standard F-test and the Duncan multiple-range test are relatively rigorous statistical tests. Confidence intervals are useful in visualizing the variability between a large number of populations.

Six different subsets of the data matrix were analyzed:

(1) Overall band--to compare the relative usefulness of the 4 ERTS-1 bands

(2) Overall image set--to determine if the time of year the imagery was acquired affects the detectability of contacts, regardless of band

(3) Overall contact--to determine if some contacts are easier to detect than others, regardless of band and time of year

(4) Contact/band--to determine if specific contacts are best detected on any particular band

(5) Contact/image set--to determine if specific contacts are best detected on any particular image set (time of year).

(6) Band/image set--to determine if any particular band is best for a given image set (time of year)

COMPARISON OF OVERALL BAND DETECTABILITY

The initial step in data analysis was to test the mean detectability (of lithologic contacts) between the four bands of ERTS MSS imagery. Table 7 summarizes the partially reduced detectability data used in the tests.

BAND	Σ OF DETECTABILITY SCORES	# OBSERVATIONS	AVERAGE DETECTABILITY	SUM SQUARES
4	18.7	91	.2054	8.01
5	24.9	91	.2736	11.83
6	18.9	91	.2076	7.73
7	16.7	91	.1780	6.91

Table 7. Summary of reduced detectability data for each band of ERTS MSS imagery.

All Bands

The detectability data from each of the four ERTS MSS bands were analyzed together to first determine if the mean detectabilities of the bands were statistically different. Results of the F-test rejected the null hypothesis that the means of the detectability of the four bands are equal (i.e. - the means of the four bands are not equal at the .05 level of significance). Subsequent tests dealt with the determination of how the mean detectabilities of the bands differ.

Bands 5 and 6

Inspection of the average detectability in each of the four bands (Table 7) suggests that the detectability in band 5 may be significantly better than in the remaining three bands. To test this, band 5 was compared with band 6, the next highest band in average detectability using the F-test. Results of the test indicate that bands 5 and 6 are statistically different at the .05 level of significance. Band 5, then, must also be different from (better than) bands 4 and 7.

Bands 4 and 6

The average detectability of bands 4 and 6 (Table 7) suggests that the mean detectabilities in these bands may not be statistically different at the .05 level of significance. F-testing of these bands confirmed this observation.

Bands 6 and 7 and Bands 4 and 7

The average detectability of band 7 (Table 7) suggests that band 7 may be somewhat worse than bands 4 and 6 for lithologic discrimination. However, statistical testing of band 7 with band 6 and band 7 with band 4 indicates that the mean detectabilities are not statistically

different at the .05 level of significance. These tests point out the usefulness of statistical analysis techniques over and above simple comparison of averages, although averages do give insight into how data from multiple populations differ when more sophisticated statistical test indicate that significant differences do exist.

Confidence Intervals of Mean Band Detectabilities

The meaning of the statistical tests of band detectabilities can be more easily visualized by studying confidence intervals constructed for the means of the various bands of imagery investigated (Fig. 14). The confidence intervals indicate that if you use this procedure, 95 percent of the time the actual population mean falls within the calculated interval, although sample means calculated during several tries at the experiment may vary from the mid-point ($\overline{x}$) on the interval.

Confidence intervals overlap when the factors being tested cannot be statistically separated at a given level of significance; the confidence intervals do not overlap when the factors are statistically different at a given level of significance.

Inspection of Figure 14 shows that the confidence interval of mean detectability in band 5 does not overlap the confidence intervals of bands 4, 6, and 7 and, hence,
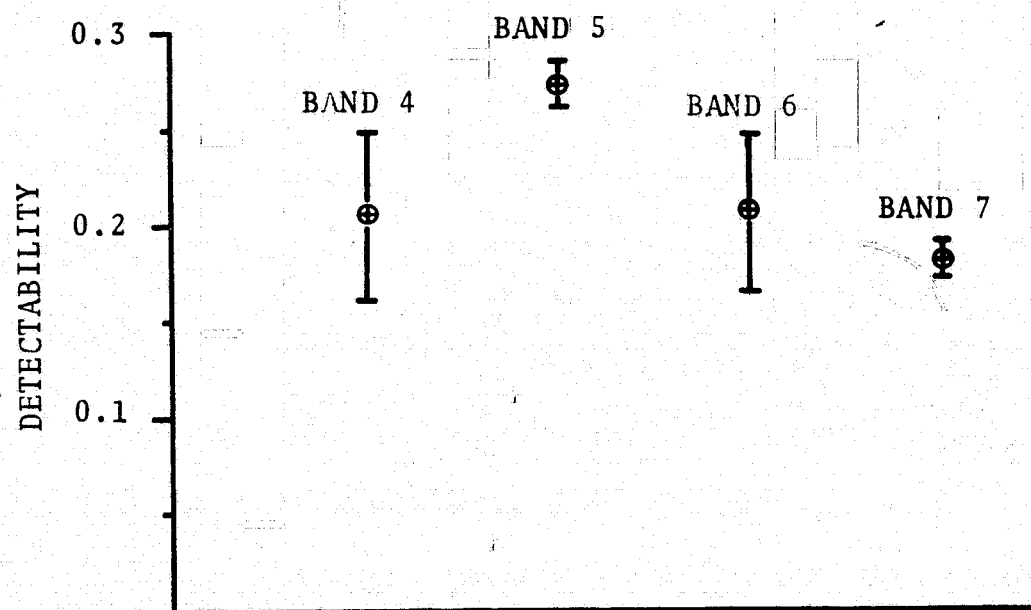
Figure 14. Confidence intervals of mean band
detectability of ERTS images studied.
$\alpha = .05$

is statistically different from these bands. The relatively small range in the band 5 confidence interval can be interpreted as indicating that the detectability in band 5 is consistently higher (better) than in the remaining bands.

Similarly, the small range in the band 7 confidence interval indicates consistently low values of detectability. However, the confidence intervals of bands 4, 6 and 7 all overlap and, therefore, cannot be statistically separated using 95 percent confidence intervals.

The broad ranges of the bands 4 and 6 confidence intervals may be interpreted as indicating that although the mean detectabilities in these bands cannot be statistically separated from band 7, there is greater variability in the detectaiblity of lithologic contacts in these bands. In other words, there are probably a meaningful number of lithologic detectabilities that are higher (better) than in band 4.

OVERALL IMAGE SET

It might be anticipated that the detectability of lithologic contacts would be highly sensitive to image set (time of year) since time of year affects many parameters including sun azimuth and elevation, vegetation, snow cover and soil moisture. The results of F-testing and confidence intervals indicate, however, that the time

of year has no significant affect on detectability. Table 8
summarizes the partially reduced detectability data from
the four sets of ERTS images.

Table 8. Detectability data for each set of ERTS MSS imagery.

IMAGE SET	Σ OF DETECTABILITY VALUES	# OBSERVATIONS	AVERAGE DETECTABILITY	SUM SQUARES
Jan.	20.0	96	.2083	9.68
Aug.	19.5	96	.2031	6.85
Dec.	15.9	96	.2092	7.09
June	23.8	96	.2479	10.86

All Image Sets

The detectability data from each of the four ERTS MSS
image sets were analyzed together to determine if the mean
detectabilities of the sets were statistically different.
The F-test indicated that the mean detectabilities are not
statistically different at the 0.05 level of significance.
Consequently, further tests between pairs of image sets
were not conducted.

Confidence Intervals of Mean Image Set Detectabilities

The 95% confidence intervals ($\alpha = .05$) for the mean
detectabilities of the four image sets are shown in
Figure 15. The figure shows that (1) all confidence
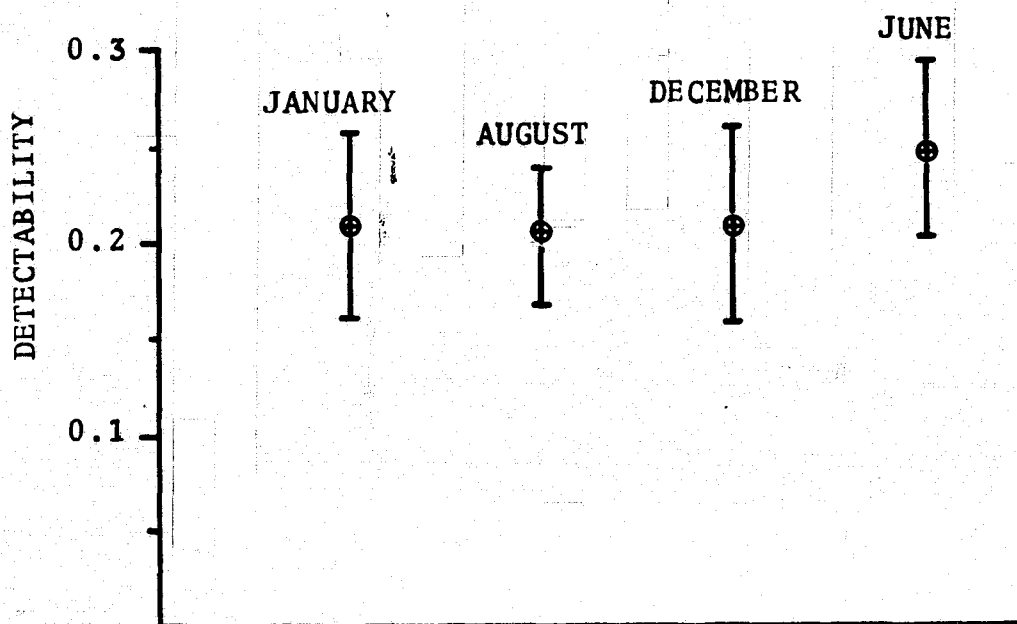
Figure 15. Confidence intervals of mean image set detectabilities of ERTS images studied. α = 0.05.

intervals overlap, (2) mean detectabilities ($\overline{X}$) do not vary greatly, and (3) the ranges of the confidence intervals are all relatively broad (compared to ranges of bands 5 and 7 in Figure 14).

The overlapping confidence intervals and the similarity in mean detectabilities between the image sets testify to the fact that the mean detectabilities are not statistically different at the .05 level of significance, as was discovered during the initial F-test. Unlike the confidence intervals for mean band detectability (Fig. 14), however, the ranges of the confidence intervals for mean detectability as a function of time of year (image set) are all relatively broad, suggesting that there is variation in the ability to detect lithologic contacts on images taken at different times of year.

OVERALL CONTACT

Confidence intervals of the mean detectability of each lithologic contact were constructed to study the variation in detectability. Figure 16 shows the confidence intervals.

The figure reveals that the detectability of individual lithologic contacts on ERTS MSS imagery is highly variable. Note that the ranges of the confidence intervals are, in general, very broad, but there is a tendency for those
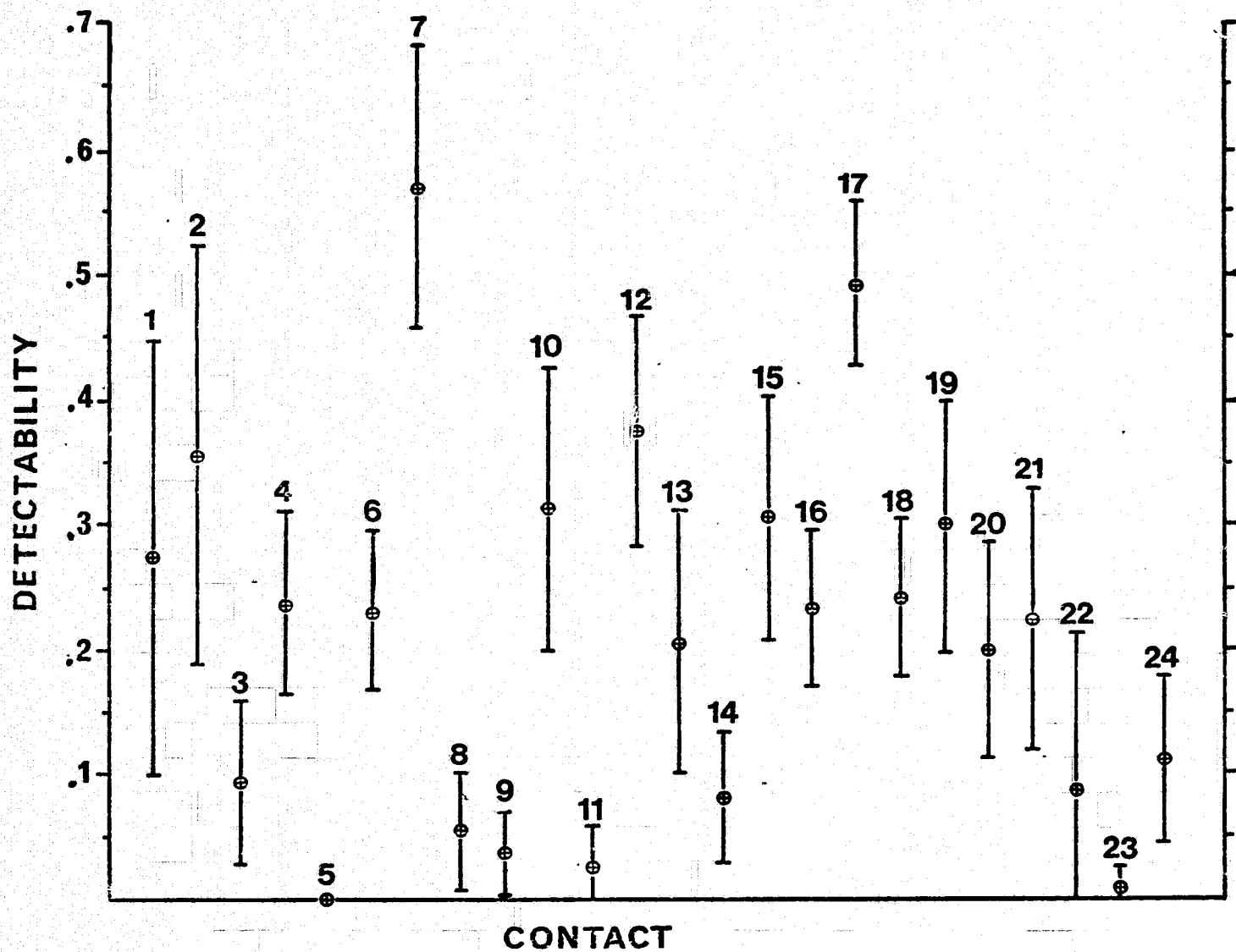
Figure 16. Confidence intervals of mean detectability of the 24 lithologic contacts studied. $\alpha = 0.05$.

contacts with low detectabilities ($\overline{X}$) to also have narrower confidence interval ranges. This suggests that some contacts are difficult to detect, regardless of the band or image set used in analysis. Similarly, other contacts are relatively easier to detect, but the detectability is more highly variable and depends more on the band and/or image set used for interpretation. This latter variability is probably related to the type and degree of surface expression of the individual contacts along their trace. Subsequent analyses were oriented towards determining whether image set or band is the most important factor in producing the observed variability on the imagery.

CONTACT/BAND AND CONTACT/IMAGE SET

Of the 24 lithologic contacts evaluated, 12 of the contacts are expressed at the surface by some combination of topography, color and vegetation. The remaining 12 contacts, with the exception of contacts 16 and 18, are expressed only by two of the terrain parameters. Contacts 16 and 18 are expressed by topography, color and vegetation, but the December imagery of these contacts is cloud-covered and could not be evaluated.

The 12 contacts expressed by topography, color and vegetation were chosen for further analysis to determine whether band or image set is the most important factor

affecting the detectability on ERTS-1 imagery. The
detectability of each of the contacts was statistically
analyzed with respect to band and to month using the Duncan
multiple-range test (3). This test can be used (1) to
determine whether statistical differences exist between
the measurements from several different populations and
(2) to determine the relative order of the population
measurements (best to worst; highest to lowest, etc.) where
statistical differences exist. Similar results can be
obtained by repeatedly testing pairs of measurements using
the simple F-test, but the individual tests are not
independent; a constant level of significance is maintained
using the Duncan multiple-range test. Figure 17 summarizes
the results of the Duncan tests.

For the 12 contacts analyzed, the band played no
statistically significant part in determining detectability
of specific lithologic contacts. However, the statistical
analyses show that the image set (time of year) does affect
the detectabilities of the individual contacts.

June imagery (or June and August where no statistical
difference is present between the two) was statistically
the "best" imagery for 4 of the 12 contacts. January
imagery was "best" for 4 of the 12 contacts. And December
imagery was "best" for 1 contact. Three of the contacts
were not statistically affected by the image set.

CONTACT	BAND DIFFERENCE YES	BAND DIFFERENCE NO	BAND ORDER 1	BAND ORDER 2	BAND ORDER 3	BAND ORDER 4	IMAGE SET DIFFERENCE YES	IMAGE SET DIFFERENCE NO	IMAGE SET ORDER 1	IMAGE SET ORDER 2	IMAGE SET ORDER 3	IMAGE SET ORDER 4	COLOR CONTRAST	TOPO. CONTRAST	VEG. CONTRAST
2		X					X		Ju	A	D	J	H	H	L
3		X					X		Ju/A	D/J			H	H	M
4		X						X					M	M	M
6		X						X					H	M	M
7		X					X		J	D	A/Ju		L	H	H
8		X						X					M	H	M
9		X					X		J	Ju/A/D			H	M	L
10		X					X		J	D	Ju/A		M	H	M
13		X					X		A/Ju	D/J			M	H	M
15		X					X		D	J	Ju/A		L	H	L
17		X					X		J	D/Ju/A			L	H	L
20		X					X		Ju	A/D/J			M	H	M

Figure 17. Summary of Duncan multiple - range tests used to determine statistical differences in contact detectability as a function of band and image set. Where differences exist, the order of decreasing detectability was also determined with 1 best, etc. Ju = June; J = January; D = December; A = August. H, high; M, medium; L, low contrast.

Figure 17 indicates that there is no obvious correlation between the type and degree of surface expression of a lithologic contact and the time of year the contact is most detectable. This is particularly surprising, since the three terrain components (color, topographic and vegetative contrast) might be expected to be highly sensitive to the seasons. For example, those contacts expressed at the surface by a significant topographic feature might be expected to be most easily seen on winter imagery acquired at relatively low sun-elevation angles (topography enhanced). Two possible explanations may account for the lack of such correlations in this study:

1) The evaluations of the degree of surface expression made on the color photos is too imprecise

2) There is a general lack of understanding of the relative importance of color, topographic and vegetative contrast in producing a detectable image expression.

It is believed that both explanations probably apply to this study.

BAND/IMAGE SET

The detectability of all contacts together as a function of band was tested for each of the four image

sets to determine if any specific band is "best" for a given image set. The Duncan multiple-range test was used.

Results of the testing indicate that the different bands of June imagery cannot be statistically separated at the 0.05 level of significance. This relationship is also indicated by the 95% confidence intervals (Fig. 18) of the mean detectability of the four bands of June imagery. Identical results were obtained in testing the August, December and January image sets. It must be concluded, therefore, the there is no statistically "best band" to be specifically used with any given image set. In other words, the detectability of lithologic contacts within each image set is relatively insensitive to what band is analyzed.

SUMMARY OF RESULTS

1.) Lithologic contacts are generally most easily seen on ERTS MSS band 5 imagery.

2.) In general, the time of year the imagery was acquired (image set) is not a significant factor.

3.) The detectability of individual lithologic contacts on ERTS MSS imagery is highly variable.

4.) The band of imagery studied is not important in the detection of individual contacts.
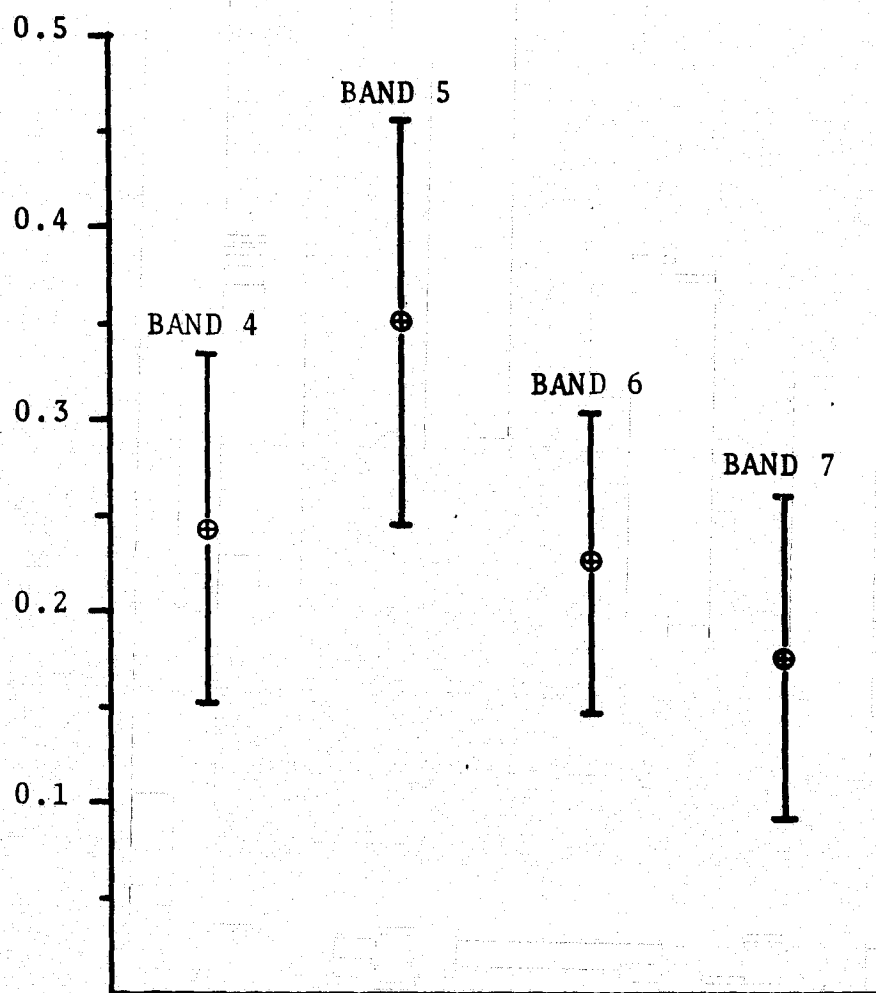
Figure 18. Confidence intervals of mean detectability
of the four bands of June ERTS imagery.
(1334-17142). α = 0.05.

5.) The image set (time of year) significantly affects the detectability of individual contacts.

6.) There is no "best" band of imagery to be used with a given image set.

DISCUSSION

Sources of variation in detectability can be divided into two catagories: (1) imaging parameters and (2) terrain parameters. Imaging parameters include spectral band and image set (time of year). These factors can be controlled to the extent that specific ERTS-1 imagery can be chosen for study.

Terrain parameters are those variable physical characteristics that together produce a surface expression of a given contact. Basically, surface expression can be divided into three types: (1) topographic, (2) spectral and (3) vegetative. Each is infinitely variable.

Rigorous investigation of the complex relationships between imaging and terrain parameters is beyond the scope of this study. However, a few observations are warrented.

Topographic, spectral and vegetative contrasts between adjacent lithologic units work together to produce a specific surface expression of the contact. In order to be detected on ERTS imagery, this surface expression must be translated

to image expression--tones, textures and geometrical relationships between tones and textures that can be detected.

In the strictest sense, only vegetative contrast varies with time; the topographic and spectral components of surface expression are relatively fixed. For example:

1) topographic relief or style does not vary

2) red rocks are red regardless of the time of year. Yet seasonal, daily, and hourly factors may act to enhance or subdue the surface and image expression of all three terrain components:

1) Shadowing at low sun-elevation angles enhances topography; high sun-elevation subdues topographic expression

2) Snow cover subdues or hides the actual spectral contrast between adjacent lithologic units; shadows produced by low sun-elevation angles may produce the same effect.

3) Vegetation contrast may be either enhanced or subdued due to snow cover, and vegetation contrasts vary with phenology.

Experience tells us that vegetation and color (spectral) differences between adjacent lithologic units should be more sensitive to imagery band than to time of year. A field geologist or photo-interpreter might add that:

1) many mappable units do not differ significantly in color; most are "reddish".

2) most lithologic contacts are masked by soil, alluvium and vegetation

3) topography and vegetation are the most useful mapping criteria.

Seemingly, the "best" ERTS-1 imagery for detecting lithologic contacts would be that imagery in which:

1) topographic expression is fully enhanced.

2) Vegetation contrast is at a maximum, either due to growth cycle differences or seasonal, daily or hourly enhancement factors.

3) Spectral contrast is at a maximum.

Maximum topographic enhancement occurs when sun-angles are the lowest possible. This occurs in mid-winter in Colorado, a time when snow cover is commonly complete.

Maximum spectral contrast occurs when the sun is high (contact not shadowed) and the contact is free of snow and vegetation (contact is exposed).

Maximum vegetation contrast occurs at different times of year depending on the (1) specific types of vegetation involved and (2) its geographic location. Elevation and topographic position are important controlling factors.

The question now posed is, "How do we select the best ERTS imagery for mapping lithologic contacts?" In other

words, when do the topographic, spectral and vegetative

contrasts produce the maximum surface expression. Clearly,

the problem is complex.

During the statistical testing of the detectability

data, it was discovered that:

(1) There is no "best" band within any of the image

sets studied

(2) There is no "best" band for any of the contacts

studied

(3) Overall, band 5 is best.

It appears that these results are controlled by

the sample size of the data sets used in the studies of

the affect of band on detectability. To analyze the

effect of band on each image set, only 24 observations

were used for each image set. To analyze the effect of

band on each individual contact, only 4 observations were

used (one of each image set). However, in analyzing the

overall effect of band, a total of 96 observations of

each band were available for analysis. The mean detect-

ability in band 5 was consistently higher in each test

than the mean detectabilities in the remaining 3 bands

but the difference was not statistically significant

except when 96 observations were used.

The results of the statistical tests and the considera-

tion of the dependence of the tests on sample size suggest

that, for detection of lithologic contacts, band is not a

very important factor. In fact, band does not become statistically significant until a great many observations are made. And even then, although the overall detectabilities may be slightly higher, there is no suggestion that the amount of information extracted from the band 5 imagery will be any greater than in any other band.

In physical terms, these results point out the fact that spectral contrast between adjacent rock units, when it is expressed at the surface, may not be discriminated by (1) multispectral remote sensing techniques in general, and (2) the bands used in the ERTS MSS system specifically.

Conceptually, vegetation differences should also be sensitive to band, yet the results of the tests suggest that either (1) the vegetation contrasts observed are not sensitive to band or (2) the vegetation contrasts observed are subdued by other factors controlled by image set (i.e.- snow cover, sun-angle).

Another set of statistical tests showed that:

(1) the detectability of individual lithologic contacts is sensitive to image set (time of year) and the best detectabilities occur on different image sets for different contacts.

(2) Overall, image set does not affect the detectability of the lithologic contacts in general.

These results are interpreted as meaning that the surface expression (and image expression) of some of the contacts

is best developed at one time of year, whereas other contacts are better seen at a different time of year. In fact, different contacts may be seen on different image sets (Fig. 19). If these contacts and image sets are considered together, as was done in the overall analysis, the differences cancel out, indicating that there is no best image set.

INFORMATION CONTENT

Analysis of the detectabilities of the lithologic contacts on the four bands of the four image sets studied does not tell anything about the information content of the various possible combinations of band(s) and image set(s). Conceivably, an image with relatively low detectabilities may contain more lithologic information (more contacts detectable) than an image with high detectabilities. Therefore, the information content of the images as well as the detectabilities must be considered if the optimum imagery (most information with least number of images) is to be determined.

The detectability data contain a clue to the information content of the ERTS imagery as follows:

(1) If a contact is detectable on a given image (detectability greater than zero), then the
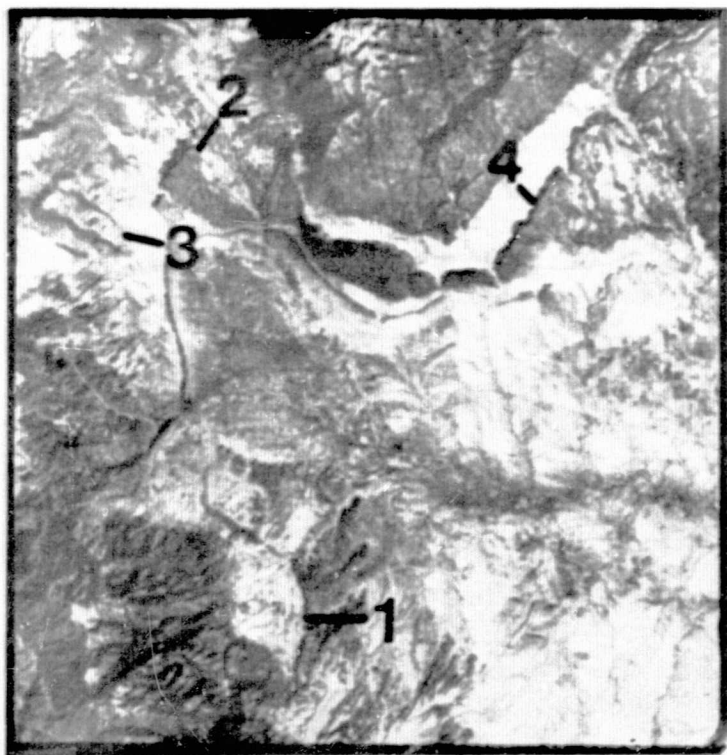
JANUARY (1172-17141-5)   JUNE (1334-17142-5)
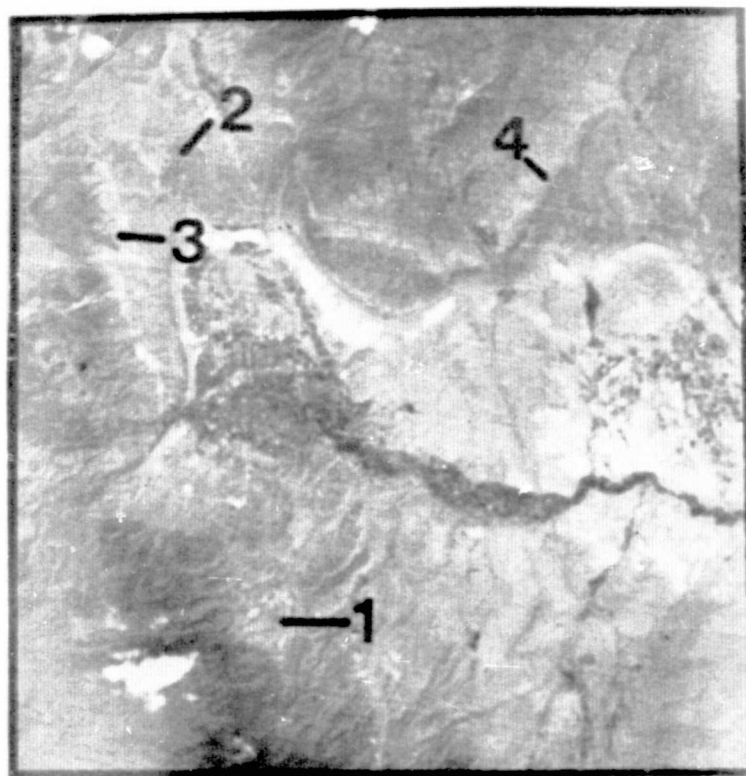
Figure 19. Winter and spring ERTS MSS imagery of the Canon City, Colorado area.
Several lithologic contacts are located for comparison.

information content of that image, for that contact, is plus one.

(2) If a contact is not detectable on the image (detectability equals 0), the information content of that image for that contact is zero.

Figure 20 shows the detectability data illustrated in Figure 13 after conversion to information content. Once

IMAGE SET	CONTACT											
	1				2				3			
	J	A	D	Ju	J	A	D	Ju	J	A	D	Ju
BAND												
4		1	1	1		1	1	1		1		1
5		1		1		1	1	1		1		1
6		1		1		1	1	1		1		1
7		1		1		1	1	1		1		1

Figure 20. Information content of ERTS images for 3 lithologic contacts. 1's indicate information is present; blanks indicate information is absent.

the detectability data have been converted to information content data, various subsets of the data matrix can be studied to determine the relative amounts of information that can be extracted using various combinations of bands and image sets. Only 19 of the 24 lithologic contacts studied were used in the information content analyses because 5 of the contacts could not be evaluated in the

December image set due to cloud cover. The highest
information content for these 19 contacts is only 95%
(18 of 19) because one contact was not seen on any of the
images studied. This contact may or may not be detectable
on sets of images not examined during this study.

Image Set/All Bands

The information content of each of the four image
sets is shown in Figure 21. Note that 89% of the contacts
studied can be found if only the June or August imagery
is studied, but that 95% (the maximum) can be found if
both June (or August) and December (or January) imagery are
studied. This relationship points out the fact that
imagery from different times of year contains different
lithologic information. In other words, all potentially
extractable information cannot be found by studying a
single image set.

Band/All Image Sets

The information content of each band of imagery is
shown in Figure 21. If either band 5, 6 or 7 of each image
set is studied, 95% of the contacts should be found. Only
slightly less information (89%) should be found using band
4 imagery from each imagery set. These figures show that
band appears less important than image set in information
content.

BAND (all image sets)	1	2	3	4	5	6	7	8	9	10	11	12	13	14	15	16	17	18	19	20	21	22	23	24	% INFO.
4	1	1	1	1		1	1	1	1	1		1	1	1	1	1	1	1	1	1	1	1	1	1	89%
5	1	1	1	1		1	1	1	1	1	1	1	1	1	1	1	1	1	1	1	1	1	1	1	95%
6	1	1	1	1		1	1	1	1	1	1	1	1	1	1	1	1	1	1	1	1	1	1	1	95%
7	1	1	1	1		1	1	1	1	1	1	1	1	1	1	1	1	1	1	1	1	1	1	1	95%

CONTACT

Figure 21a. Information content of four bands of ERTS-1 imagery. 1's indicate information is present; blanks indicate information is absent.

IMAGE SET (all bands)	1	2	3	4	5	6	7	8	9	10	11	12	13	14	15	17	19	20	24	% INFO.	
JAN.			1		1	1	1	1		1				1	1	1	1	1		63%	JUNE + JAN = 95%
AUG.	1	1	1	1		1	1	1		1	1	1	1	1	1	1	1	1	1	89%	JUNE + DEC = 95%
DEC.	1	1		1		1	1	1	1	1			1	1		1	1	1	1	79%	JUNE + AUG = 89%
JUNE	1	1	1	1		1	1	1		1	1	1	1	1	1	1	1	1	1	89%	JAN + DEC = 79%

CONTACT

Figure 21b. Information content of four ERTS-1 image sets. 1's indicate contact information present; blanks indicate information absent. All bands of each image set considered.

Band/Image Set

Obviously, the maximum amount of available lithologic information will be gained if each band of each image set is analyzed. But can the maximum amount of available information be gained if only 1 or 2 specific images are studied? To check this, a matrix showing the information content of each of the 16 ERTS-1 images was prepared (Fig. 22) and the percentage of the contacts that can be seen on each image was computed.

From Figure 22 it can be seen that the most information that can be gained by analysis of a single ERTS-1 image is 89% (June, band 5 and June, band 6). However, 95% of the information can be gained by studying all 16 images, all June and January images (8), all June and December images (8), all band 5 images (4), all band 6 images (4) or all band 7 images (4) (Figs. 11 and 12). Clearly, the fewer the number of images it is necessary to study to gain the maximum amount of available information, the greater the savings in time and expense.

In order to check whether it may be possible to gain the maximum amount of information using only 2 specific images, the information content (% of contacts found) of each of the 120 permutations of band and image set was calculated. It was found that the maximum amount of

BAND 4

IMAGE SET	1	2	3	4	5	6	7	8	9	10	11	12	13	14	15	17	19	20	24	% CONTACTS
Jan.				1		1	1			1		1			1	1	1	1		47
Aug.	1	1	1	1		1	1			1		1	1	1	1	1	1	1	1	79
Dec.	1	1		1		1	1	1	1	1		1	1		1	1	1	1		74
June	1	1	1	1		1	1	1				1	1	1	1	1	1	1	1	79

BAND 5

IMAGE SET	1	2	3	4	5	6	7	8	9	10	11	12	13	14	15	17	19	20	24	% CONTACTS
Jan.				1		1	1		1		1	1			1	1	1	1	1	58
Aug.	1	1	1	1		1	1			1	1	1	1	1	1	1	1	1		79
Dec.		1		1		1	1		1		1	1		1	1	1	1	1	1	68
June	1	1	1	1		1	1	1		1	1	1	1	1	1	1	1	1	1	89

BAND 6

IMAGE SET	1	2	3	4	5	6	7	8	9	10	11	12	13	14	15	17	19	20	24	% CONTACTS
Jan.				1		1	1	1	1		1	1			1	1	1	1		58
Aug.	1	1	1	1		1	1			1		1	1	1	1	1	1	1		74
Dec.		1		1		1	1			1		1	1		1	1	1	1	1	63
June	1	1	1	1		1	1	1		1	1	1	1	1	1	1	1	1	1	89

BAND 7

IMAGE SET	1	2	3	4	5	6	7	8	9	10	11	12	13	14	15	17	19	20	24	% CONTACTS
Jan.				1		1	1		1	1		1			1	1	1	1		53
Aug.	1	1	1	1		1	1	1		1		1	1	1	1	1	1	1	1	84
Dec.		1		1		1	1			1		1	1		1	1	1	1		58
June	1	1	1	1		1	1			1	1	1		1	1	1		1	1	74

Fig. 22. Information content of each ERTS-1 image studied. 1's indicate information present; blanks indicate information absent. Percentage of the 19 contacts for which information is present at far right.

information (95%) could be extracted from any of 11 pairs of the ERTS-1 images studied. These pairs are:

1) January, band 5 + June, band 5
2) December, band 5 + June, band 5
3) January, band 6 + June, band 6
4) December, band 4 + June, band 5
5) December, band 4 + June band 6
6) December, band 4 + June, band 7
7) January, band 5 + June, band 6
8) December, band 5 + June, band 6
9) June, band 5 + January, band 6
10) June, band 5 + January, band 7
11) June, band 6 + January, band 7

It is apparent from the above analysis that all of the lithologic information available on the ERTS-1 images can be gained by interpreting only 2 carefully selected images. Furthermore, the images to study is strongly dependent on selection of images from two contrasting times of year; band is not a very important factor. Since the overall detectabilities in band 5 imagery was statistically higher than in the remaining bands, imagery from band 5 only might be expected to provide the overall best information (i.e.-highest detectabilities and highest information content). Therefore, analysis of January and June band 5 or December and June band 5 imagery should be the overall "best" for mapping lithologic contacts in central Colorado.

CONCLUSIONS

Interpretation of the results of the statistical analyses performed in this study cannot be casually extrapolated to all ERTS-1 images in all areas of the world for all lithologic contacts. To the contrary, these results pertain to only those lithologic contacts studied on the specific ERTS-1 image sets used in this investigation. Indeed, it is not conclusively known whether the results apply equally well to all of central Colorado, even though a variety of types of contacts was studied. Agreement with empirical analyses of many ERTS-1 images in central and western Colorado, however, suggest that the ressults are representative for this area.

1.) The capability to detect and map some lithologic contacts on ERTS-1 images is highly sensitive to the time of year the images were acquired.

2.) The relationship between time of year and the relative effects of color, topographic and vegetative contrasts in producing a surface expression and image expression of a lithologic contact is not well understood. Before widely useful predictive models can be prepared, this relationship needs to be researched in depth, particularly if automatic mapping techniques are to be advanced beyond the present state.

3.) If only one set of ERTS-1 MSS images is available for study, the lithologic contacts may be more easily seen on band 5, but it is possible that more contacts may be seen on another band. All 4 bands should therefore be studied.

4.) If multiple sets of imagery are available for study, most of the lithologic contacts that can be found on ERTS-1 MSS imagery will be detectable on a combination of imagery from two contrasting times of year. In this case, all 4 bands of imagery from each image set need not be studied. The maximum amount of available information should be found by examining only one band from each image set. Band 5 imagery would apparently be the best choice, although other combinations might provide the same amount of information.

5.) In central Colorado, all of the lithologic contacts capable of being imaged by ERTS can be found by using either:

    a) January band 5 + June band 5

    b) December band 5 + June band 5

It is not known whether lithologic contacts not seen on these image pairs may be detectable on some other image set.

GEOLOGIC STRUCTURES

The term "geologic structure", as used in this report, refers to the folds, fractures and major tectonic elements of the earth's crust that formed during deformation by geologic processes. Geologic structures are the most readily extractable type of geologic information contained in ERTS-1 images, and the capability of studying several tectonic elements and their associated folds and fractures in a single image is, perhaps, the greatest asset of ERTS-1 imagery in the field of geology.

RESULTS OF AREAL STUDIES

SAN JUAN MOUNTAINS AND CENTRAL COLORADO

ERTS-1 images of central Colorado and the San Juan Mountains (Fig. 1) were studied in order to determine the mappability of various geologic structures in these two geologically-contrasting areas. The images studied are shown in Table 5 and Figures 2, 3 and 4. Figures 23 and 24 are structural maps prepared by photointerpretation of the imaged areas.

The geologic structural information contained on ERTS imagery of central Colorado and the San Juan Mountains is generally expressed by one or more of the following:

a) topography

EXPLANATION

——— photo lineament

— — strong photo lineament   ⌐ ⌐ circular or arcuate
                                        ⌐ ⌐ lineament
—?— possible photo lineament

Figure 23. Structural geologic map of central Colorado
            prepared from ERTS-1 image 1171-17142.
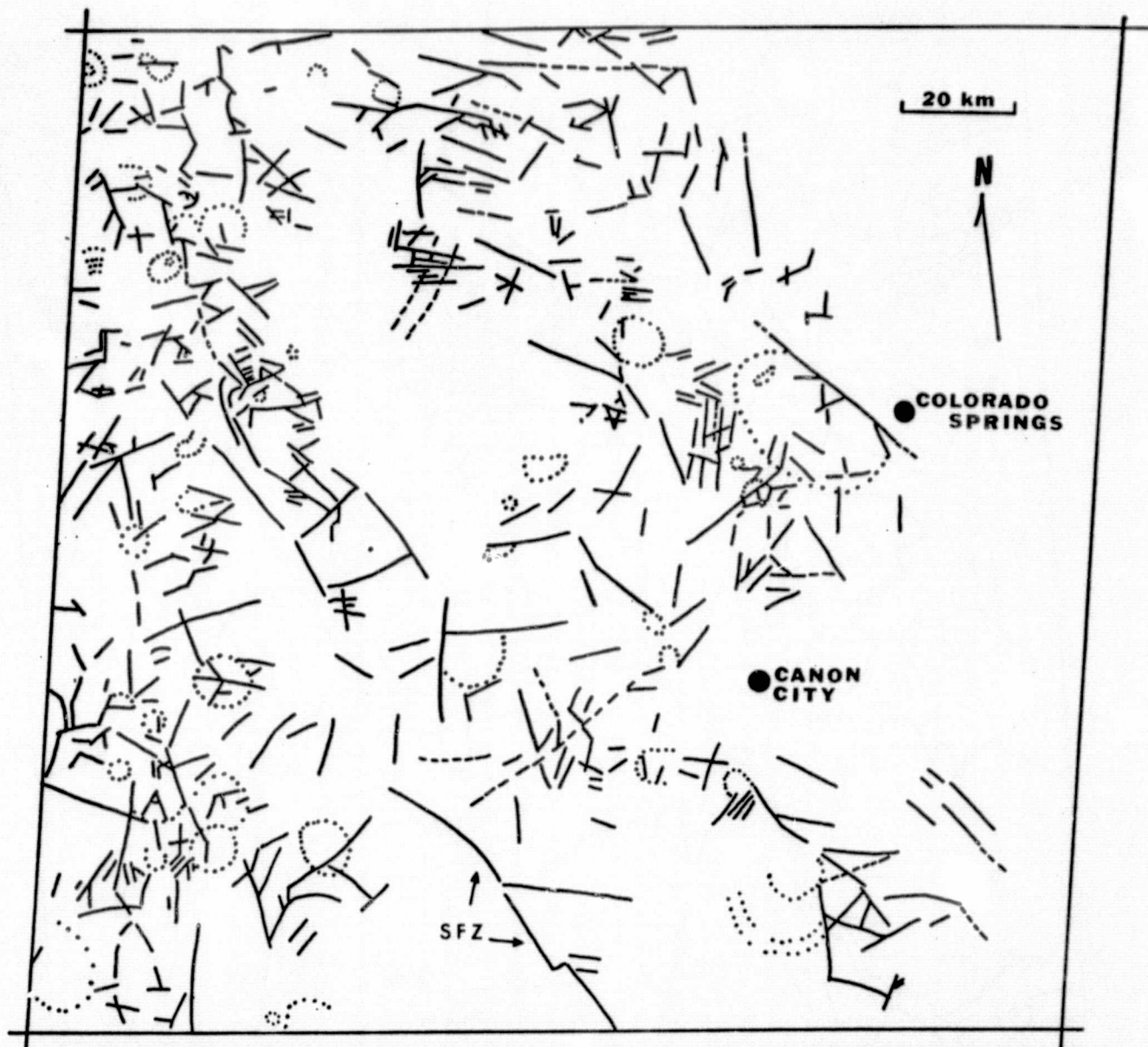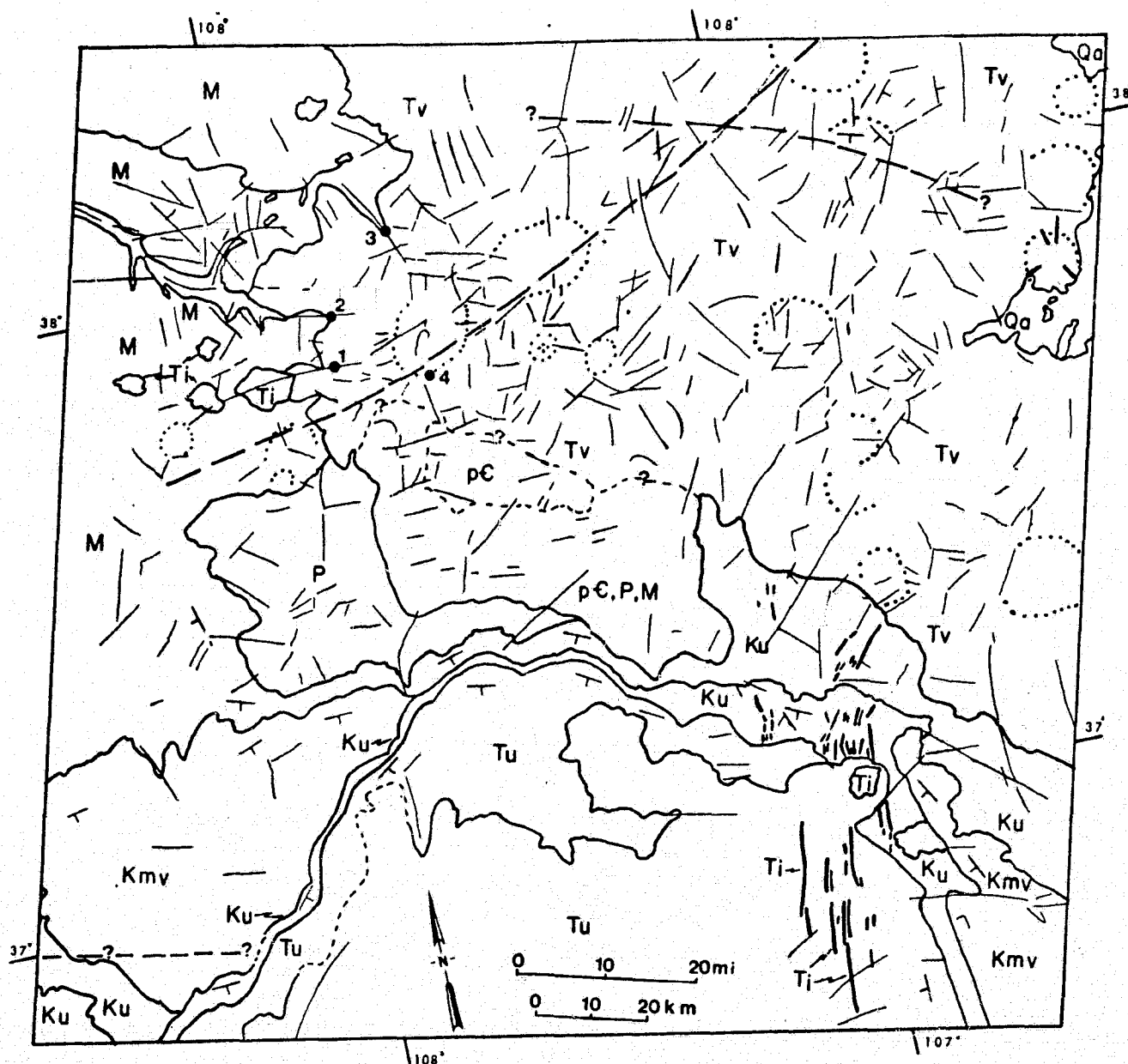
EXPLANATION

—— photo lineament

— — strong photo lineament

— ? — possible photo lineament

⌒ circular or arcuate
      lineament

Figure 24. Structural geologic map of the San Juan
            Mountain area prepared from ERTS-1 images
            1191-17204, 1407-17193 and 1425-17190.

b) strike and dip of stratified rocks

c) outcrop patterns

d) drainage patterns

e) tonal patterns.

The most apparent structural features are lineaments
defined by topography, drainage patterns and linear tonal
changes which are interpreted to have geological significance.
Although many lineaments can be related to known faults,
shear zones, major joint trends and lithologic contacts, there
are commonly many more lineaments on an ERTS scene than can
be definitely related to a known structural features.

Fractures (faults, shear zones and major joint trends)
are generally well-expressed in crystalline rocks as straight
topographic lows formed by preferential or more rapid
weathering along the fracture. Faults in gently dipping
sedimentary rocks are most easily seen on low sun-angle,
snow covered ERTS scenes. These faults generally appear as
tonal alignments; the same faults are much less obvious on
the snow free scenes.

Major faults and fault zones often appear as linear
breaks in topography. The straight escarpment resulting
from late Tertiary faulting along the Sangre de Cristo
Fault zone (SFZ, Fig. 23), is a good example.

If the interpreter is careful, most roads, fence lines,
contrails and other cultural linear features will not be
interpreted to be lineaments. These non-geological linears

are best seen, and appear most frequently, in non-forested areas of low topographic relief. Roads, railroads and fence lines appear as long, narrow, relatively straight tonal changes. Contrails are generally diffuse and cut across the scene with no relationship to topography.

Although many more lineaments can often be mapped than there are known faults, some of these additional lineaments may reflect previously undetected faults or extensions of known faults; other new lineaments may be related to fracture and joint systems that may have played a major role in the development of linear drainage systems.

In addition to lineaments, circular and curvilinear features are also apparent on the ERTS imagery and these features most often represent volcanic or intrusive centers in Colorado. In the San Juan region, evidence for the volcanic nature of the San Juan Mountains is supplied by the striking topographic expression of the Silverton, Lake City and Creede calderas (S,L, and C, Fig. 24). These structures are distinctively outlined by the annular to semi-annular drainages that have developed on and adjacent to bounding ring faults formed during caldera collapse.

It should be noted that the small scale of ERTS imagery prevents the interpreter from seeing many faults. Consequently, many small scale faults, and especially the many veins and vein systems in the central Colorado and San Juan Mountain areas (many of which are faults of small

displacement , cannot be detected on the ERTS imagery.

Fold structures in sedimentary rocks can often be identified by topography, outcrop patterns, drainage patterns and opposing dip slopes. The large anticlines and synclines of the Canon City region are very well-expressed on the central Colorado area. Large sedimentary basins, such as the San Juan basin, may also be well expressed. The overall structure of the northern and western edge of the San Juan basin is easily delineated on ERTS imagery by mapping dips in the sedimentary sequence.

RATON BASIN

The structural features of the Raton basin were determined in conjunction with establishing the stratigraphic column of the area (see p. 26). Both first (large) and second (small) order geologic features were noted and recorded on the geologic map (Fig. 8). Figure 7 shows the major geographic and geologic features of the area.

First Order Geologic Features

a) A major asymmetric structural basin was mapped with the steep flank on the west and a gentle east flank. The synclinal axis trends north-

northwest but bifurcates to north marking two separate synclines.

b) A second basin is present in the southwestern portion of the area. The basin margins appear to be fault controlled because no sedimentary formations (Units 2-5) are observed between the resistant rocks (Precambrian) forming the core of the mountain ranges and flat floored basin.

c) Two major mountain ranges containing older resistant rocks (Precambrian) are noted:

1) The Wet Mountains in northwest portion of the area with the south plunge forming the Greenhorn Mountain anticline. This structure splits the Raton basin into the eastern Delcarbon syncline and the western Huerfano Park syncline.

2) A western mountain range (Sangre de Cristo) with a sedimentary sequence along the eastern flank but not along the western margin. This relationship suggests a tilted fault-block uplift or a younger fault system along the western margin placing Precambrian in contact with Late Tertiary or Quaternary sedimentary rocks.

d) Two major fault systems are recognized along the margin of the two mountain ranges. Most pronounced is faulting along the west margin of the Sangre de

Cristo Range (2 above). The second major fault
zone is present along the west flank of the Wet
Mountains. The major faults trend north-northwest,
but north-south and northeast trends modifying the
dominant trend is observed.

Second Order Geologic Features

Minor folds and faults were mapped in several parts
of the area:

a) Axes for the minor folds are shown on Fig. 8
are observed in sedimentary rocks. These folds
are typical of exploration targets drilled in
petroleum exploration programs. In the case
history for exploration of these folds, drilling
for petroleum found the anticlines to be non-
productive.

b) Minor fault patterns are clearly visible in the
Greenhorn Anticline--Wet Mountain area. The
faults trend northwest, northeast and east-west.
Only those lineaments that control drainage on
both sides of a divide or that cause a drainage
pattern anomalous to the normal pattern are
considered to be faults.

The igneous dikes cutting the sedimentary
sequence in the basin generally parallel the

northeast trend of faulting observed in the older
basement rocks of the Wet Mountains.

UNCOMPAHGRE/PARADOX AREA

Figure 9 shows the major geographic and geologic
features of the Uncompahgre/Paradox area. During analysis
of ERTS-1 images of the area for lithologic discrimination,
numerous geologic structures ranging in size from small
anticlines to large block uplifts were mapped (Fig. 10).

A major uplift trending N.70°W. with faulted margins
dominates the central portion of the image area. The
uplift, called the Uncompahgre uplift, is largely covered
with sedimentary rocks and appears to be a tilted block
with a long low dip on the north flank and an abrupt narrow
south flank. The structure plunges to the northwest.
Minor faults with east-west, northwest and northeast trends
cut the sedimentary rocks. Deep canyons are probably
eroded through the sedimentary cover into the basement
complex, but these older rocks are mapped only in the
Unaweep Canyon. The faults appear to be basement-controlled
faults associated with vertical uplift.

Two major structural basins flank the Uncompahgre
uplift. The Piceance basin to the northwest contains the
thick sedimentary sequence of units 3 through 6 with very
minor folding. The north flank of the basin shows steep
dip in unit 4 along the Grand Hogback.

The Paradox basin to south has numerous anticlinal
trends expressed in surface exposures of stratigraphic
unit 2. Units 3 through 6 are absent with the possible
exception of small unmapped areas of the lower part of
Unit 3. The axes of the minor anticlines trend about
N.70°W. The Paradox Valley anticline has straight cliff
exposures suggesting faulted margins. The synclinal axis
of the structural basin cannot be mapped on this image.

The Black Canyon uplift is expressed in units 1-3
along the east margin of the image area. Although much
smaller, the overall form of the structure is similar to
the Uncompahgre Uplift. It is a tilted block with a gentle
northeast flank, an abrupt faulted south flank and a
gentle northwest plunge into the Piceance Creek basin.
The Gunnison River has eroded a deep canyon along the axis
of the structure exposing the basement (Precambrian). A
syncline with Unit 3 at the surface separates the Black
Canyon from the Uncompahgre Uplift.

MOSQUITO RANGE

For identifying geologic structures, particularly
faults, ERTS imagery taken during winter was found to be
more useful than that taken during summer and fall.
However, some structural information in the mountains
above timberline was lost in wintertime imagery because

of deep snow cover. Therefore, ERTS imagery taken during all times of the year, needs to be examined to produce the maximum amount of structural information. The low sun angle affect in the area during wintertime probably accounts for the usefulness of wintertime ERTS imagery. It is possible that ERTS-type imagery obtained just before sunset during the summer would be very useful for structural studies as it would provide low sun-angle enhancement of topography with a different sun direction from that of winter imagery. Where stereo coverage is available, strike and dip of sedimentary rocks in the Mosquito Range could be easily mapped.

Another factor which varies with time of year is the presence of cloud cover. There are more cloud-free days during winter than during summer and, therefore, more usable ERTS imagery is obtained over central Colorado during the winter. Cloud-free, snow-free ERTS imagery over the Mosquito Range of central Colorado is relatively rare.
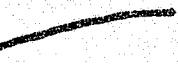
Faults mapped on ERTS imagery were compared to faults mapped during previous geologic investigations in the northern portion of the Mosquito Range. Approximately 50% of the major faults (faults two miles or more in length) could be mapped from the ERTS imagery, including most of the Mosquito-Weston, London, and Union fault systems which are the best known and among the most economically and

tectonically important faults in the region (Fig. 25).
Virtually none of the minor faults (faults less than two
miles in length) was identified in ERTS imagery.

Several circular features were mapped on ERTS imagery
(Fig. 25). One of the features was found to correspond to
a small Tertiary stock. Another surrounds the known area
of intrusion and mineralization at Climax, Colorado. Three
other such circular features did not correspond as closely
with areas of known igneous intrusives. One of these, the
circular feature at Prospect Mountain northeast of
Leadville, enclosed an area of Precambrian sedimentary
rocks with several small intrusives. The intrusives are
found on the periphery of the circular feature rather
than in the center, but the circular feature does seem to
reflect their presence. A second circular feature north-
east of Prospect Mountain, at Mount Arkansas, seems to
most nearly reflect the presence of an area of Precambrian
gneiss and schist surrounded by Precambrian granite in
three directions and by faulted Paleozoic sedimentary
rocks to the west. Examination of United States Geological
Survey aeromagnetic and gravity maps of the area (4) indicate
that there probably is no buried Tertiary intrusive related
to this circular feature. The third circular feature
encloses the Mount Lincoln-Mount Democrat area north of
Alma. In this area, Precambrian metamrophic rocks, Paleozoic
sedimentary rocks, and Tertiary intrusives, including the
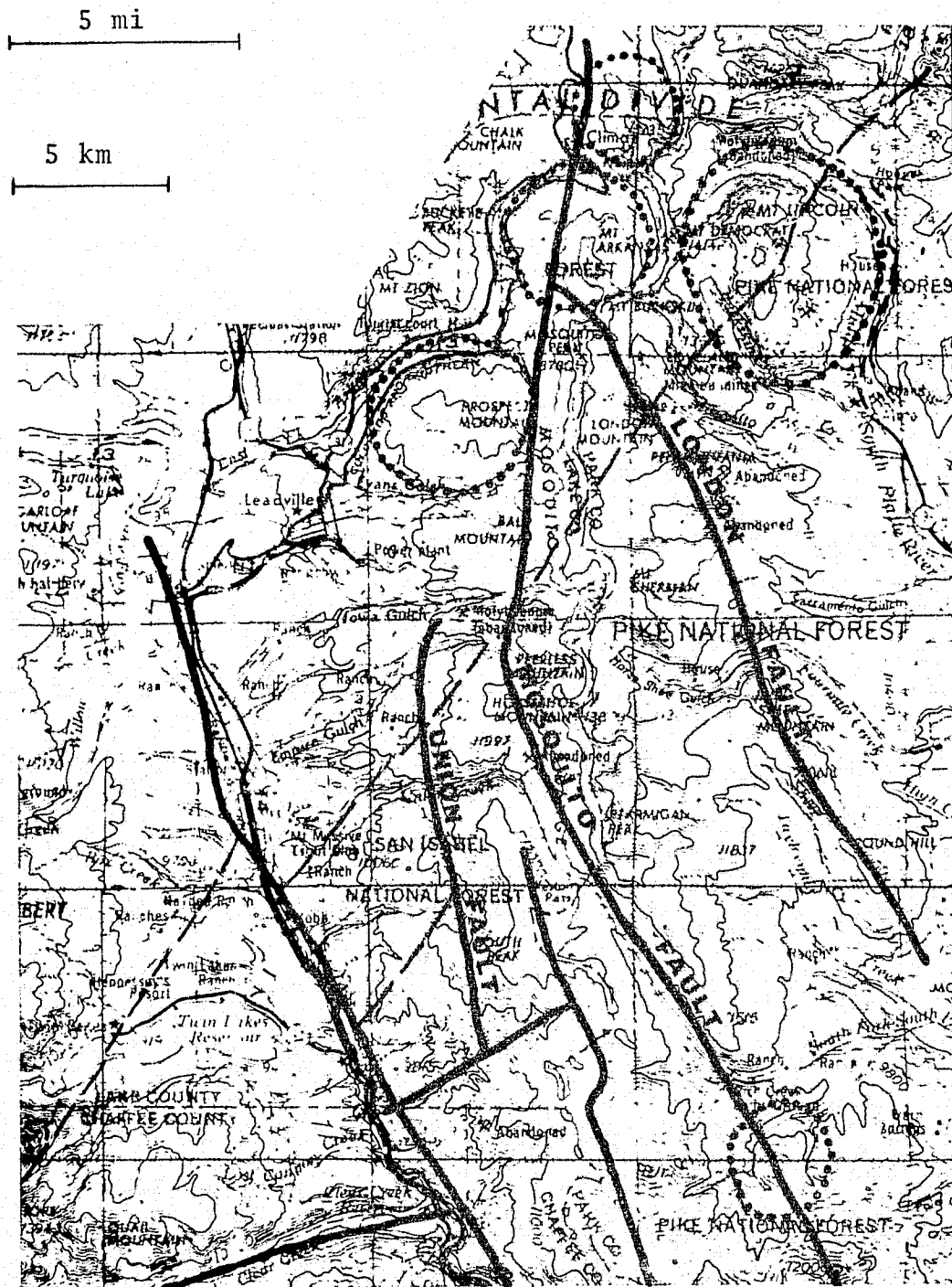
Circular
Feature

Fault

Lineament

Figure 25. Circular features and major faults mapped
from ERTS imagery of the Mosquito Range area.

Buckskin stock, are present. The circular feature mapped from ERTS imagery does not closely follow any of the surface contacts. Examination of gravity and aeromagnetic maps of the area show a gravity low northeast of and under the northeast portion of the circular feature, and a magnetic high over the location of the Buckskin stock, with a weaker arcuate magnetic high which corresponds well with the periphery of the circular feature as mapped from ERTS imagery. This suggests that the circular feature may reflect the presence of an unexposed intrusive body of which the Buckskin stock and other small intrusives in the area are but a small portion.

NORTHWESTERN COLORADO

Lithologic contacts, geologic structures, and geomorphic features as detected on ERTS imagery are closely related phenomena. This fact is well-illustrated in a study of folds in an oil-producing area in northwestern Colorado (Fig. 26). The area includes portions of the Piceance basin, Uinta Mountains, White River Plateau, and Green River basin; the Green River oil shales are exposed in the south-central portion of the image.

Positive transparencies of the four MSS bands (1:1,000,000) were studied stereoscopically and also pseudo-stereoscopically using bands 5 and 7 of the same
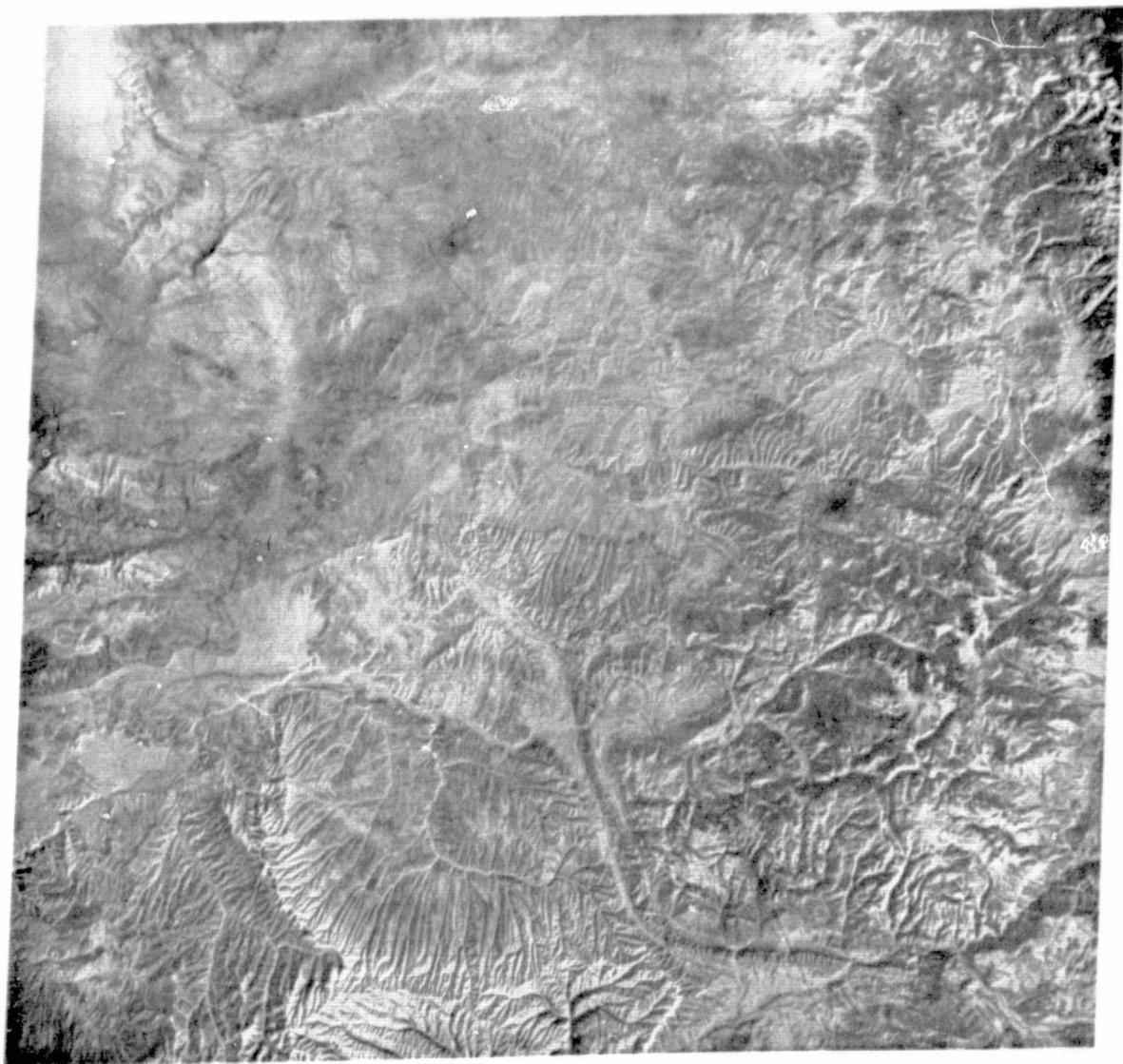
Figure 26.   ERTS-1 image 1156-17253-7 of northwestern
Colorado. Photo-interpretation of the 4 MSS
bands of this scene revealed the 63 folds
shown in Figure 27.

image as a stereo pair. The troughlines and crestlines of 63 folds were identified and plotted on a clear acetate overlay (Fig. 27).

The question was then asked, "What physical parameters at the surface made it possible to identify the folds on the ERTS imagery?" To get at the answer the imagery was re-examined and the folds were classified according to size and detectability (Table 9) and physical characteristics (Table 10). Only four surface manifestations of the folds were found to be important in identifying the fold structures on the ERTS imagery:

1. Tonal pattern - includes apparent lithologic banding caused both by differences in rock and soil spectral reflectance and by differences in vegetation type and density, primarily the latter.

2. Broad-scale topographic expression.

3. Opposing dip slopes - a small-scale form of topographic expression.

4. Stream patterns.

Most of the mapped folds are relatively small (56) and obscure (32) on the imagery (Table 9). As can be seen from Table 10, some folds will be obvious on ERTS imagery if they are expressed by lithologic banding or topography, however, it is very clear that in order to extract the maximum amount of fold information from the imagery, it
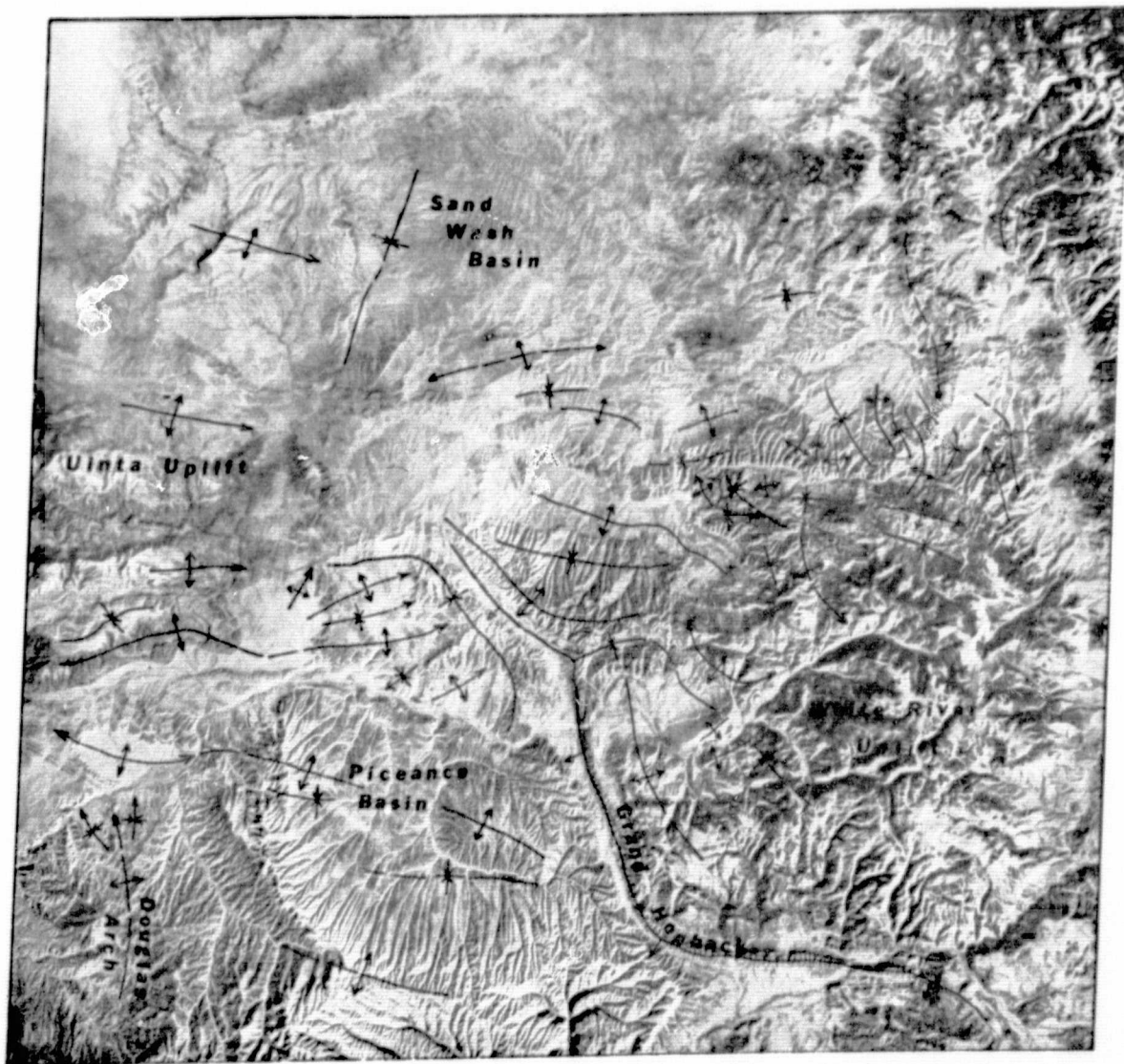
Figure 27.   ERTS-1 image 1156-17253-7 showing the axial traces of 63 folds.

DETECTABILITY

	Obvious	Evident	Obscure	TOTAL
LARGE Major folds that can be traced for tens of kilometers	3	1	3	7
SMALL Minor or secondary folds mostly on flanks of LARGE folds.	12	15	29	56
TOTAL	15	16	32	63

SIZE

Table 9 . Size and detectability of the 63 folds mapped on ERTS image 1156-17253.

PHYSICAL CHARACTERISTICS DEFINING FOLDS

DETECTABILITY	Tonal Pattern	Topographic Expression	Dip Slopes	Stream Patterns
Obvious	9	15	0	1
Evident	3	14	5	2
Obscure	0	0	32	4
TOTAL	12	29	37	7

Table 10. Number of folds identified on ERTS-1 image 1156-17253 classified according to detectability and the surface characteristics that defined them. Note that a number of folds were manifest by more than one surface characteristic and, hence, the total number of folds is greater than 63.

is necessary to interpret small-scale, subtle geomorphic features such as stream patterns and dip slopes. Furthermore, it is apparent that geomorphic expression is the most important factor in identifying folds on the ERTS imagery.

Since the image originally used for the fold interpretation was acquired during mid-winter, it was thought that perhaps topographic enhancement caused by the low solar inclination angle combined with partial snow cover may have caused the geomorphic (topographic) factors to appear more important in fold mapping than might be the general case. Therefore, a snow-free, high sun-angle image of the same scene was interpreted. The results were that fewer folds could be detected and that those folds that were found were less well-expressed. It was concluded that geomorphic features are, in fact, the most important factors in the detection of folds on the ERTS imagery of northwestern Colorado and that images acquired during mid-winter provide the best data.

LINEAR FEATURES IN ERTS IMAGERY

Two ERTS images of central Colorado, E-1172-17141 (Figure 28) and E-1154-17143, were selected for analysis of linear geologic structure information content. The two images were selected for their excellent expression of linear features. Their main attributes are low sun elevation
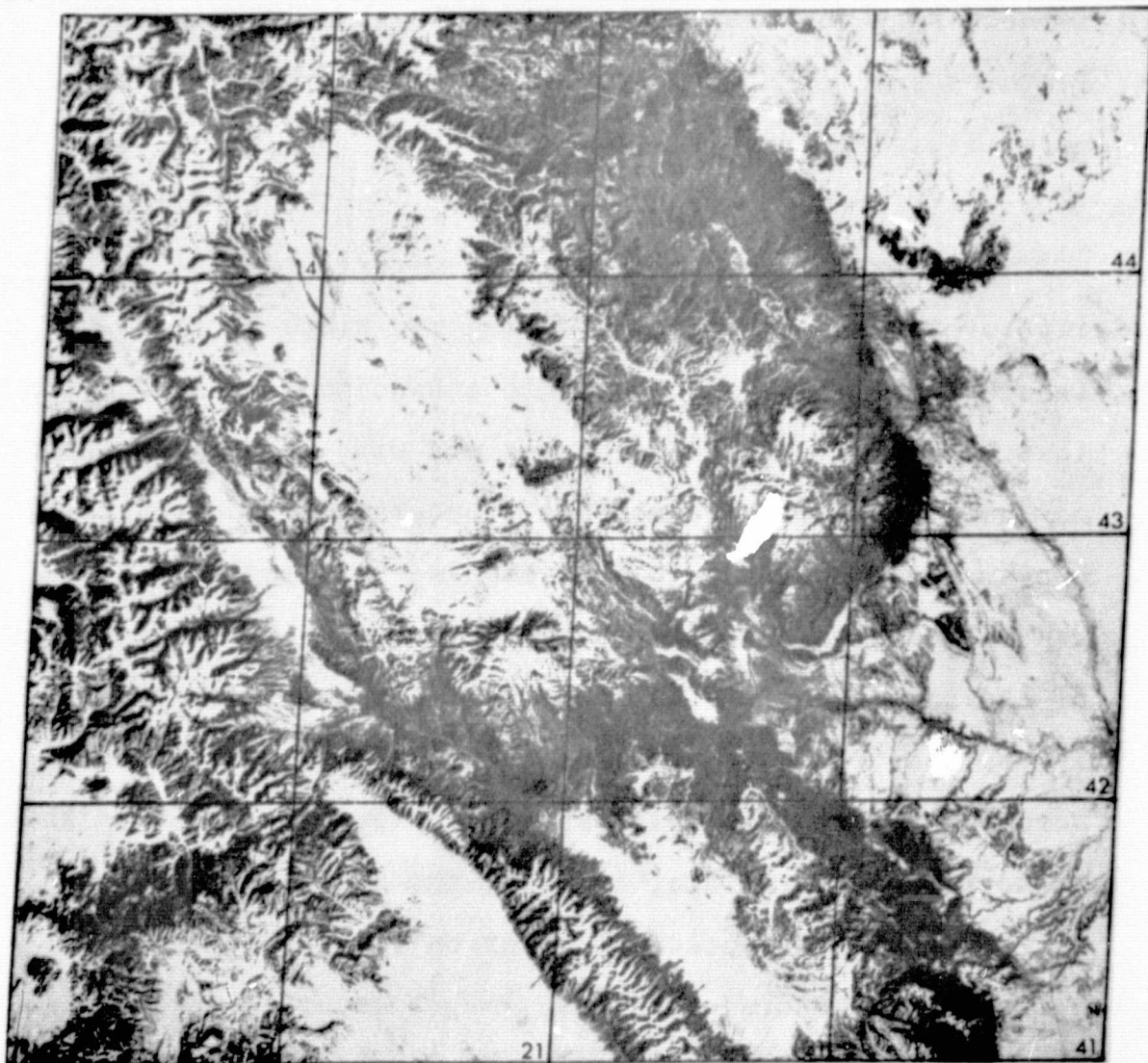
Figure 28.   ERTS image, E-1172-17141, of central Colorado.   Date
January 11, 1973, sun elevation is 23 degrees, sun
azimuth is 150 degrees.   Grid subdivisions will be
referred to in the text.

and near maximum snow cover. Since a significant propor-
tion of linears is the result of shadow enhancement of
topographic features, the lowest sun elevation was selected;
it was the minimum available nearest the winter solstice,
approximately 23 degrees. This sun elevation is not the
optimum for maximum shadow enhancement of the topography in
central Colorado, because slopes less than this are not
shadow enhanced. In addition to this restriction, there
is selective shadow enhancement of linears as a function
of deviation from the sun azimuth, which was approximately
S.30W. (See Reference 5 for a detailed discussion of uses
and limitations of shadow enhancement of topographic
linears). On the other hand, some linear features,
especially those which are the margins of dark areas or
are long linear dark areas, were enhanced by the snow cover.
Snow cover enhances the dark-area margins (particularly
between coniferous forests and dormant grassland) and
shadow margins by increasing the contrast between the dark
and light areas. Furthermore, the snow decreases the
contrasts in illuminated areas and provides a uniform high
reflectance in areas of otherwise variable reflectance. On
the contrary, snow cover might obliterate some linears by
smoothing low topographic features. All things considered,
when imagery from other seasons was subjectively evaluated,
its information content and detectability of linears were

found to be very much less, which discouraged further analysis for new information not available in snow-covered imagery.

The image that has the more widespread and deeper snow cover, E-1174-17141, also has the greater detectability. The reason seems to be in the greater contrasts as explained above. However, despite some cloud cover, E-1154-17143 has more information (more linears) compared to the other image.

Band 6 images seem to have the greatest detectability of all the ERTS bands. In these winter scenes, contrasts between vegetation types and between vegetated and less vegetated areas are the least and are further diminished by snow cover. In addition, detectability is improved in Band 6 because shadows are darker because of low radiance in this bandwidth as compared to other bandwidths.

There is little doubt that the linear trends in images are not always a true representation of linear trends determined from fault maps and/or rock joint trend maps. Other studies have shown that less than half the linears in one photograph can be related to known structures. Not all geologic linears are represented as linears on the image, say, for example, as vegetation or topographic linears. This may be due to preferential enhancement of some trends by geomorphic processes. Some linears parallel to streams seem not to be controlled so much by lithology or structure, but by direction of drainage evaluation,

determinable by the line from the local headwaters to the local outflow area of the stream. It seems very probable that stream patterns contribute a great deal of randomness to strike frequency distributions, while structurally controlled trends provide less information. Thus, the "signal-to-noise" ratio is low. The detrimental effects of snow cover and sun attitude have already been discussed.

STRIKE-FREQUENCY ANALYSIS

The purpose of the strike-frequency analysis was to determine the dominant azimuthal trends of the linears measured on the imagery in order to study the geographical distributions of the trends and their geologic origins. Firstly, linears were marked and traced on a clear overlay of a 9 in. by 9 in. positive transparency (scale - 1:1,000,000) viewed in transmitted light (Figure 29). Only linears of obviously cultural origin were not entered into the analysis. As will be demonstrated, there may be some valid bases for being more selective of linears to be entered into the analyses and, thereby, the possibility of improving correlations between two or more data sets.

Following preparation of the overlay, the linears were hand digitized for length and azimuth to the nearest degree. When lengths of linears were measured, they were grouped into length classes of 0.1 inch (0.254mm) with a
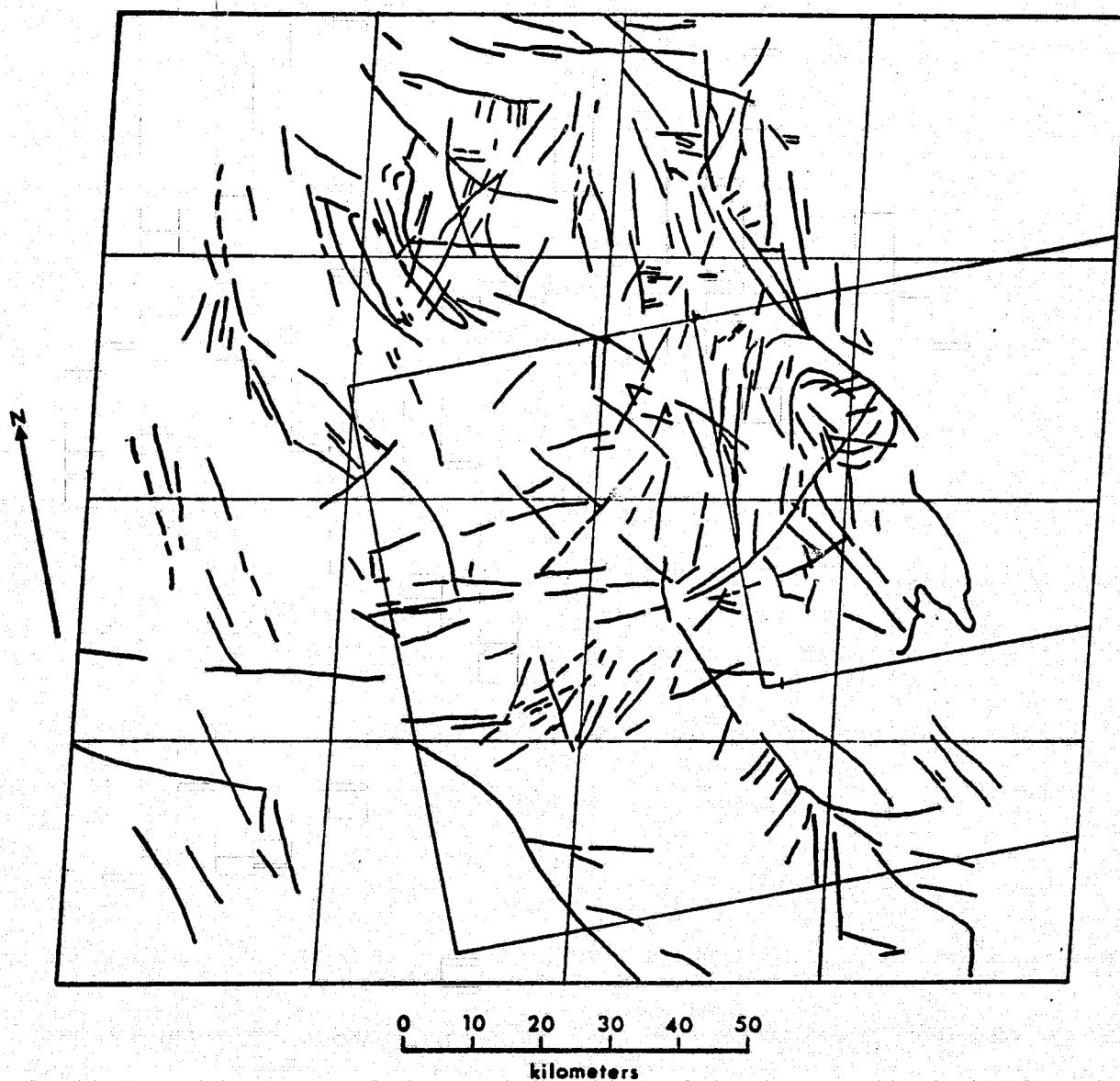
Figure 29. Linears traced from ERTS image E-1172-17141.
Gridded areas are as in Figure 28. Larger
rectangular subarea is of the Pueblo relief map.
Smaller subarea is of the Southern Front Range.

maximum of 2 inches (5cm) being found. Strike-frequency histograms of the azimuths of the linears and their length-weighted azimuths were made with the aid of a computer program developed for the study. Azimuthal trends were selected at those azimuths where maxima in the strike-frequency histogram occurred. In addition, to aid in the selection of trends, significance values were calculated for the frequency maxima by the algorithm appended to this section.

Various degrees of smoothing of the frequency histograms were performed by the method of moving sums as even large data sets had very irregular histograms. Because of the loss of information in the summing process, various summing intervals were investigated for optimum enhancement of dominant trends. Maxima and minima of the histogram constitute an irregular wave form, and where two maxima or two minima are closer together than the summing interval, they are merged into one and some information is lost or filtered out (Figure 30). It should be noted that the summing interval for the original data set is 1 degree of azimuth.

In the discussion that follows, strike frequency histograms have significance values plotted on the ordinate and azimuths on the abscissa as in Figure 30. Relative frequency values determined by moving averages at each degree of azimuth were converted to significance values by the appended algorithm. Two smoothing intervals were
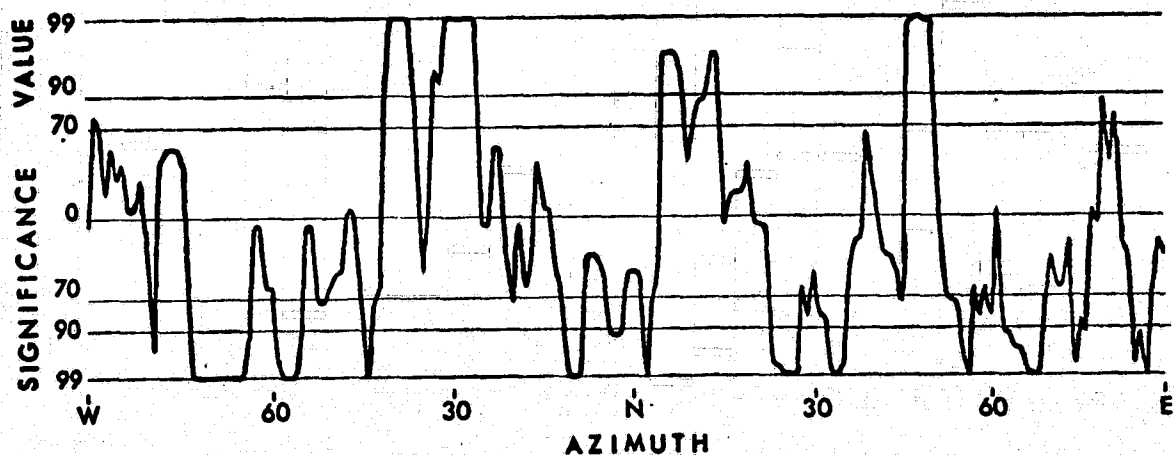
(a) Smoothing interval is 5 degrees of azimuth.
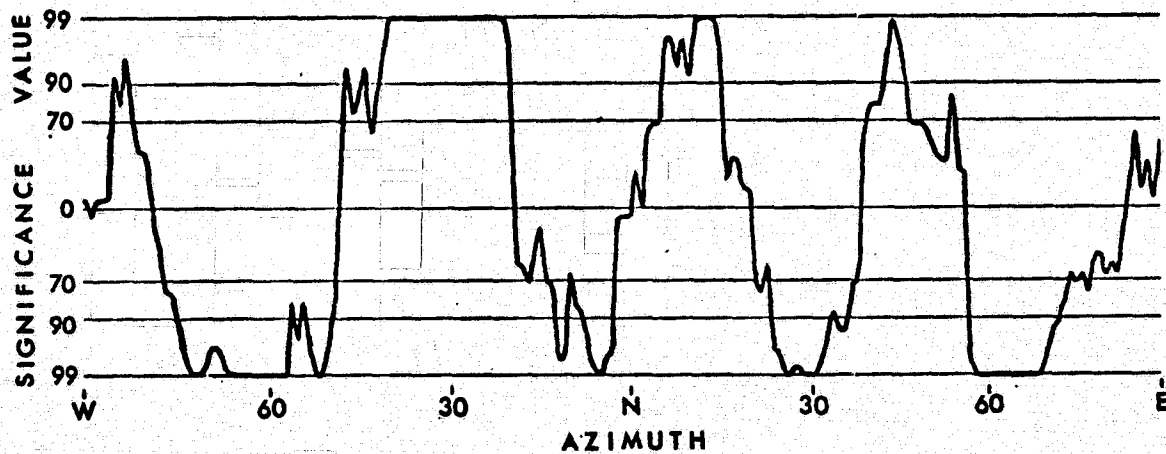
(b) Smoothing interval is 18 degrees of azimuth

Figure 30. Example of merging of narrow maxima and minima by increasing the azimuthal summing or smoothing interval.

selected for emphasizing the trends found in the histograms. An 18-degree interval (10% of azimuth half-circle) was selected to emphasize broader trends. A 5-degree trend (3%) was selected to emphasize trends of narrower azimuthal range.

Selection of trends was not easy nor entirely consistent because of the irregularity of the frequency histograms. However, the procedure of selecting trends was to associate them with significant maxima surrounded by significant minima. Thus, in the worst case, a trend or significant maxima might consist of numerous significant "spikes" surrounded by values of low significance. A study of some randomly generated linears indicated that such data sets have fewer maxima above the 90 percent significance value than real data sets. In this study, if a real data set fell short of producing 99-percent maxima then 90-percent maxima were used for trend selection. A brief discussion of the numerical meaning of the significance value is given in the appended section.

It was found that the "signal-to-noise" ratio of the histogram is considerably increased by length weighting linears before entering them into the strike-frequency analysis. Thus, where any azimuth had a frequency value of one, in the unweighted analysis, this value became the value of the length class (increasing from 1 in steps of 1). This

method provided no new trends over the non-length weighted analysis, but did enhance the trends; that is, increased the "signal-to-noise" and improved their significance values (Figure 31). While no new trends appeared as a result of length weighting, it is very possible for a few long linears to produce a trend in a length-weighted analysis, but none in an unweighted analysis.

Correlation of the strike frequency histograms of two or more data sets was done by inspection. Automatic correlation was attempted by application of the technique of autocorrelation, but generally correlation coefficients of less than 0.25 were produced. The failure of the autocorrelation technique seems to lie in the abundance of non-correlative frequency values of low significance (the 'noise' discussed before), even though the significant maxima or minima might be highly correlated. Attempts to individually correlate the quadrants of the frequency histogram produced some higher correlation coefficients (0.25 to 0.50), which indicate that computations of moving intervals of correlation might have produced better and more usable results.

AZIMUTH TRENDS IN THE WHOLE IMAGES

Approximately 300 linears were measured in each of the two images studied. Strike-frequency histograms at unweighted azimuths for each image are shown in Figure 32 and for the
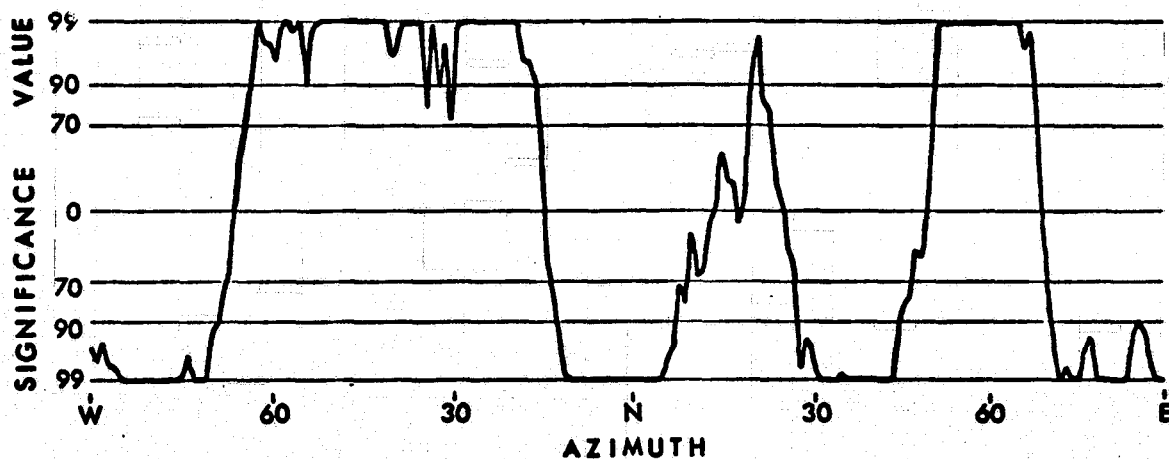
(a) Length-weighted azimuthal data
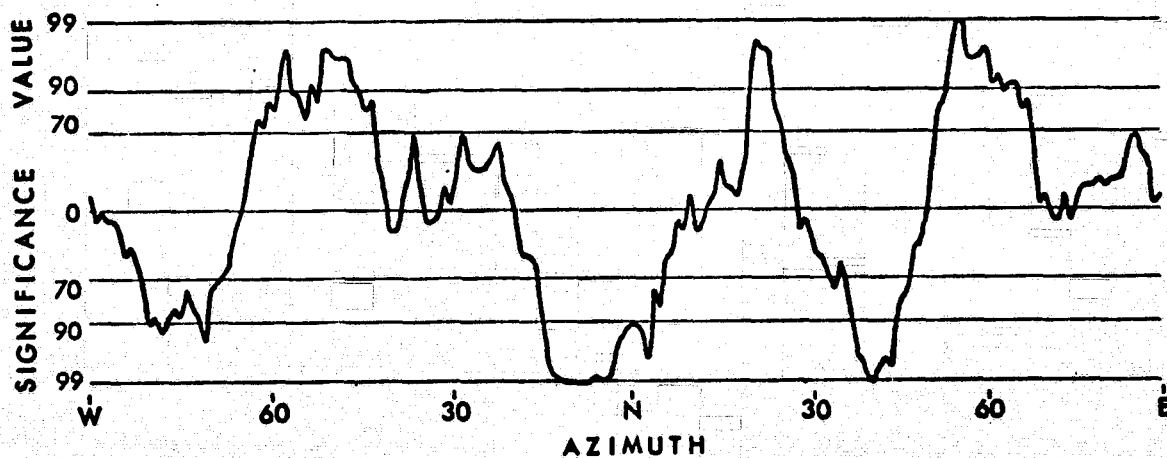
(b) Unweighted azimuthal data

Figure 31. Illustration of effect of length-weighting on significance of trends in strike-frequency histograms, 18-degree smoothing.

combined images in Figure 33. The larger interval of
smoothing (18 degrees) was used for Figure 32 and two
intervals (5 and 18 degrees) in Figure 33. The trend in
Figure 33a is a very broad and significant one ranging
from N.30W. to N.35W. and corresponds to the major structural
and topographic trends in central Colorado (Figure 34).
Figure 33b reveals that at the smaller smoothing interval
there may be 5 to 7 closely grouped trends constituting the
broader trend. The trends are wholely in counterclockwise
deviation to the sun azimuth of N.30W., indicating that
there are relatively fewer slopes, as well as other
linears, with trends in the west-northwest and east-northeast
quadrants.

AREAL DISTRIBUTIONS OF TRENDS

Inspection of the areal subdivisions of the linear
map (Figure 29) indicates that each contain one or more
distinct and easily detectable trends, more so than in
the greater imaged area. Also, the trends in each sub-
division are not part of image-wide trends but of trends
localized to that subdivision and a few neighboring ones.

The local trends of each of the 10 subdivisions are
plotted in Figure 35. The frequency of local trends for
each 10 degree interval of azimuth for the combined images
is shown in the histogram in the figure. The frequency
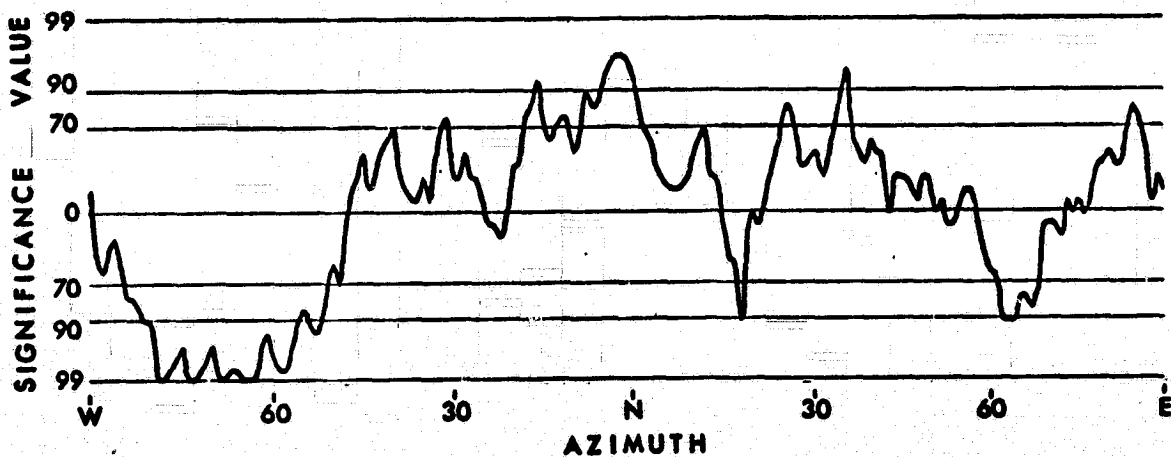
(a) E-1154-17143
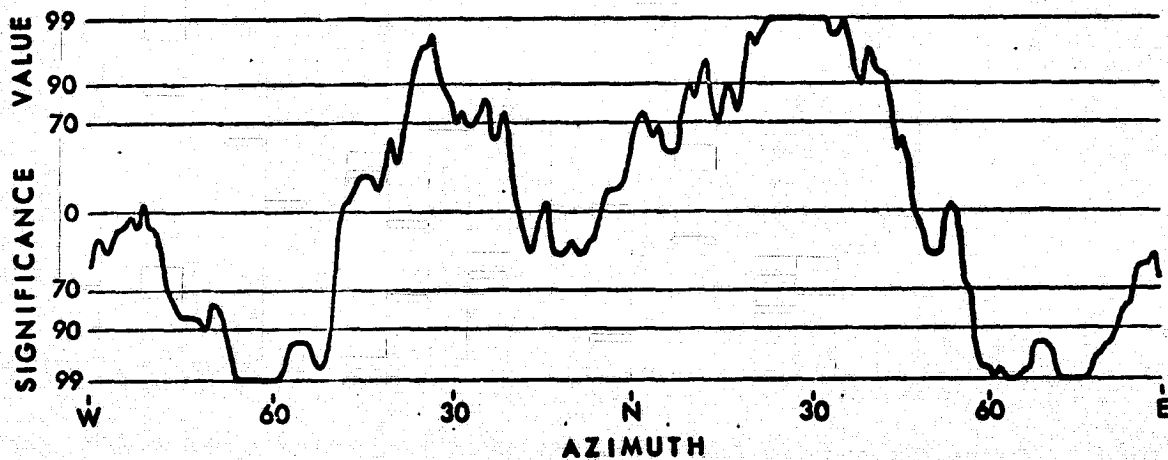
(b) E-1172-17141

Figure 32. Strike-frequency histograms of linears in two ERTS
images of central Colorado. The area covered is
shown in Figures 29 and 34.
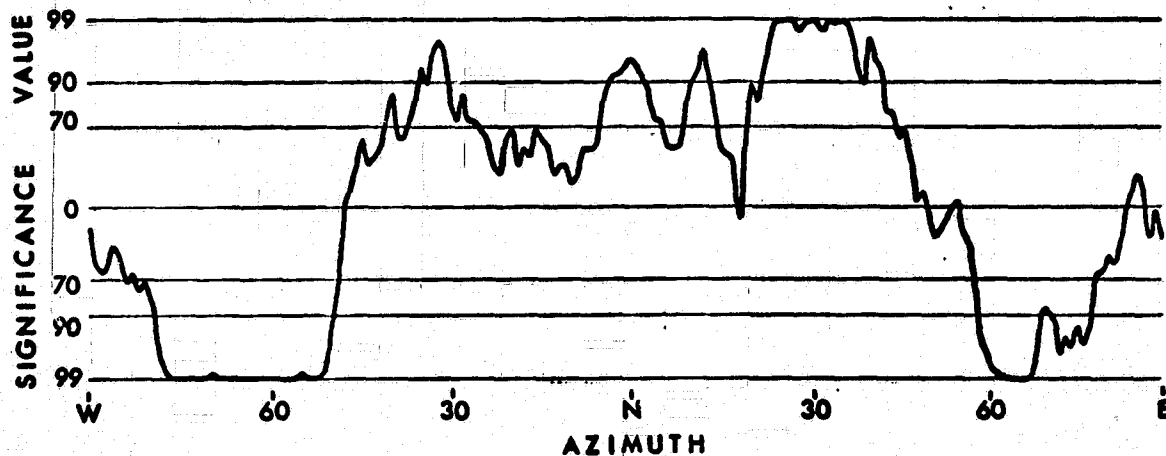
(a) Smoothing interval is 18 degrees.
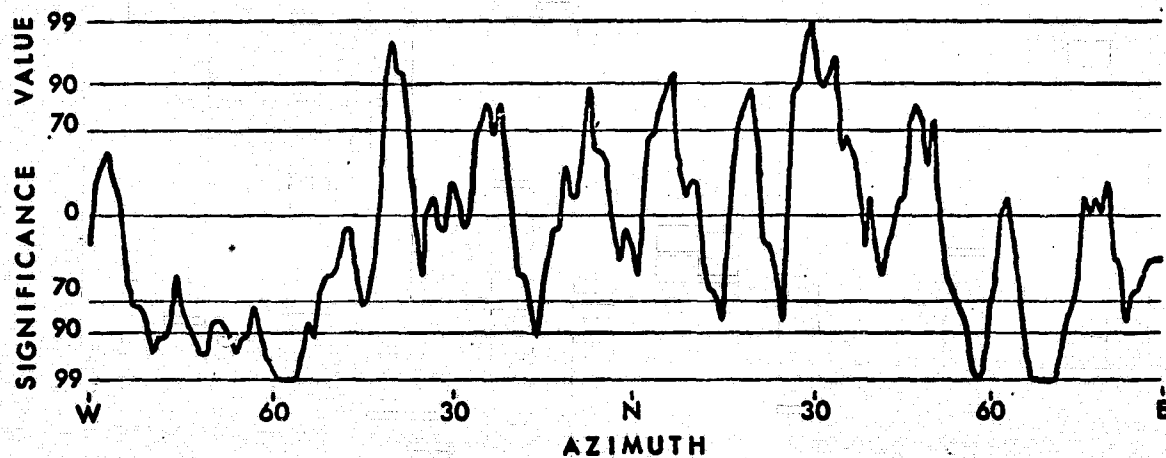
(b) Smoothing interval is 5 degrees.

Figure 33. Strike-frequency histograms of linears combined
from both ERTS images, E-1154-17143 and E-1172-17141.
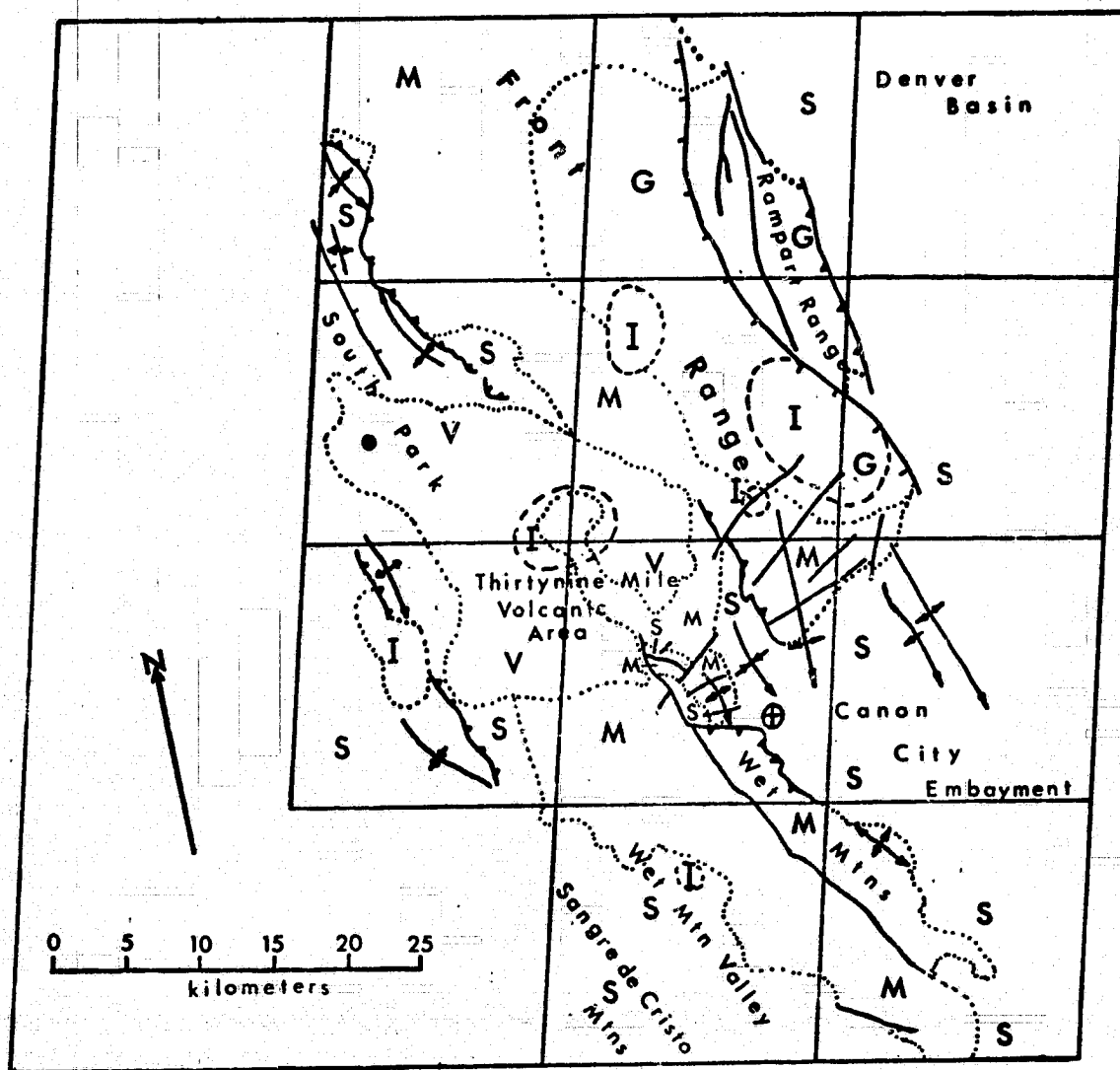
Figure 34. Geologic map of imaged area showing major faults and folds and gross lithologic terrains. Plain, hachured, and toothed lines are faults. Hachures indicate reverse faults, teeth indicate thrust faults. Lines with arrows are folds. Lithologic terrains are defined by dotted lines and are sedimentary (S), metamorphic (M), granitic igneous (G), volcanic (V), igneous or volcanic intrusive centers (I).
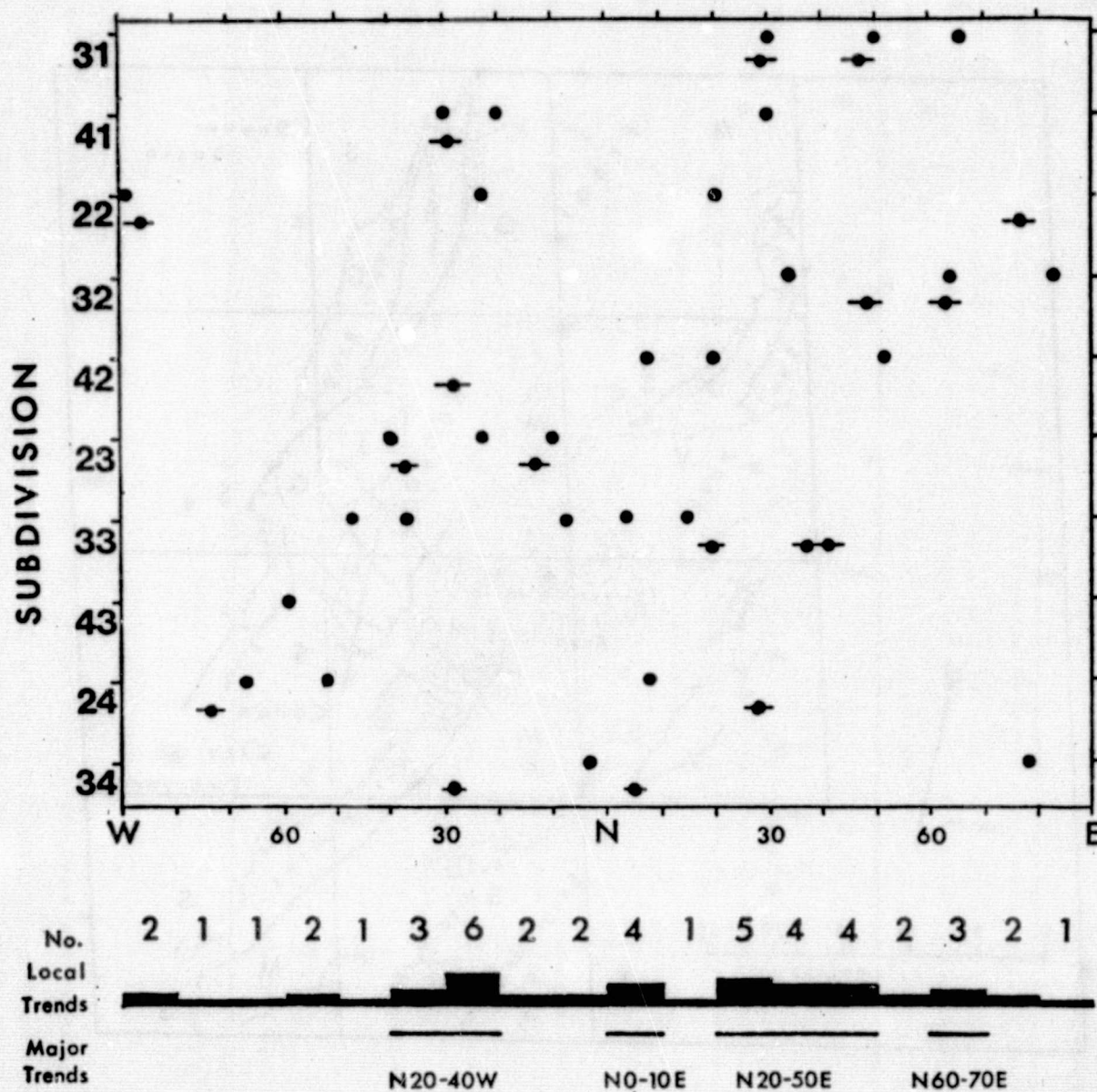
Figure 35. Areal distribution of local trends in 10 subdivisions of E-1172-17141 (barred dots) and E-1154-17143 (plain dots). Histogram shows number of trends for both images per 10 degree sector of azimuth. Heavy lines below histogram indicate 4 prominent trends for total area of all subdivisions.

Figure 36. Number of local trends within each subdivision that fall within the four major trends of Figure 8. Numerator is for E-1154-17143 and denominator is for E-1172-17141.

histograms for each image are nearly the same. The result is that the local trends, while spread across the azimuth half-circle, do emphasize four major trends: N.20-40W., N.0-10E., N.20-50E., and N.60-70E. When the occurrence of the local trends within the major trends is plotted areally, as in Figure 36, a correspondence to the major structural features in Figure 34 can be made. The N.20-40W. and N.0-10E. trends are associated within the Cenozoic folds and faults of South Park and Canon City Embayment and in the older igneous and metamorphic terrains of the Front Range. The N.20-50E. trend is predominant in the southeast quarter of the area. The N.60-70E. trend is associated with the Cenozoic volcanic terrain and is also dominant in the Front Range in the north part of the image. In the volcanic terrain, there is a definite control of topography by volcano-depositional features (6). In the north, the area is of high relief associated with the Tarryall Mtns. and the North Fork of the South Platte River. Generally, local trends occur in no more than about 40 percent of the area.

LENGTHS OF LINEARS

All linears of E-1172-17141 that lie within the area of the Pueblo, Colorado, Quadrangle plastic relief map (scale-1:250,000) were grouped by length. For comparison, a linear

map of the relief map was made and the linears were also

grouped by length. Frequency distributions of linear

lengths in the two data sets are shown in Table 11.

LENGTH – km	0	5	10	15	20	25	30	35	40	45	
Relief Map	174	279, 118, 33, 22, 11, 6, 2, 4, 1, 2								1	
E-1172	32	46, 31, 26, 25, 7, 8, 5, 4					1			1	

Table 11. Frequency of linears for each length class con-
verted to kilometers for ERTS image E-1172-17141
(in area of relief map) and for Pueblo relief map.

The ERTS linears consist of topographic and non-

topographic linears illuminated at a sun elevation of 23°

and azimuth of N.28W. in a heavily snow-covered scene. The

Pueblo linears are essentially high-relief topographic linears

illuminated at a sun elevation equivalent to 15 degrees and

accumulated at illuminations from four directions, S.45E.,

South, S.45W., and West. The relief map was painted white

to remove tonal contrasts not due to illumination angle.

Thus, the relief map linears were mapped under optimum

conditions.

The scale of the ERTS image studied is 1:1,000,000 and

that of the photograph of the Pueblo Relief Map is 1:800,000.

Smaller features are detectable in the ERTS scene than in the relief map photograph because the resolution of the relief map itself is lower.

Over three times as many linears were extracted from the relief map as from the ERTS scene. While the modal and longest lengths are nearly the same between the two sources of data, the ERTS images yielded a greater average and median length (Table 12). It is believed that the

Source	No.	Total Length	Average Length	Median Length	Modal Length	Longest
E-1172-17141	186	1417	7.6	6	3	42
Pueblo Relief Map	653	2561	3.9	3	3	42

Table 12. Statistics of lengths of linears in E-1172-17141 and Pueblo relief map in kilometers.

higher resolution of the ERTS images permits the connection of what would be disconnected line segments on the relief map in the range greater than the modal length and less than the greatest length.

LENGTH AND TREND

The two data sets discussed in the previous section were analyzed for length preference as a function of azimuth. Length trends (of length-weighted azimuths) are shown in Figure 37b and 38b. Comparison of the length trends with the azimuthal trends in Figure 37a and 38a indicates that
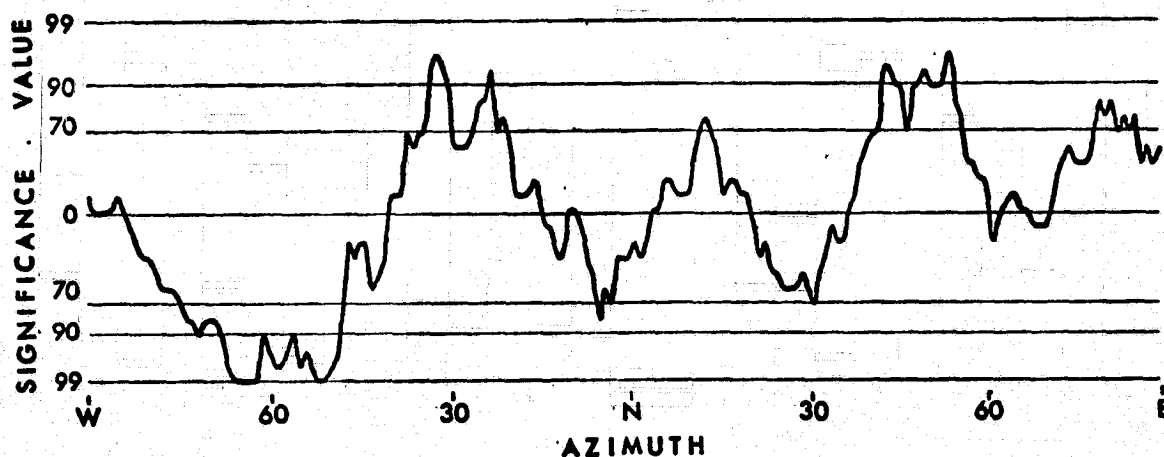
(a) unweighted azimuthal trends
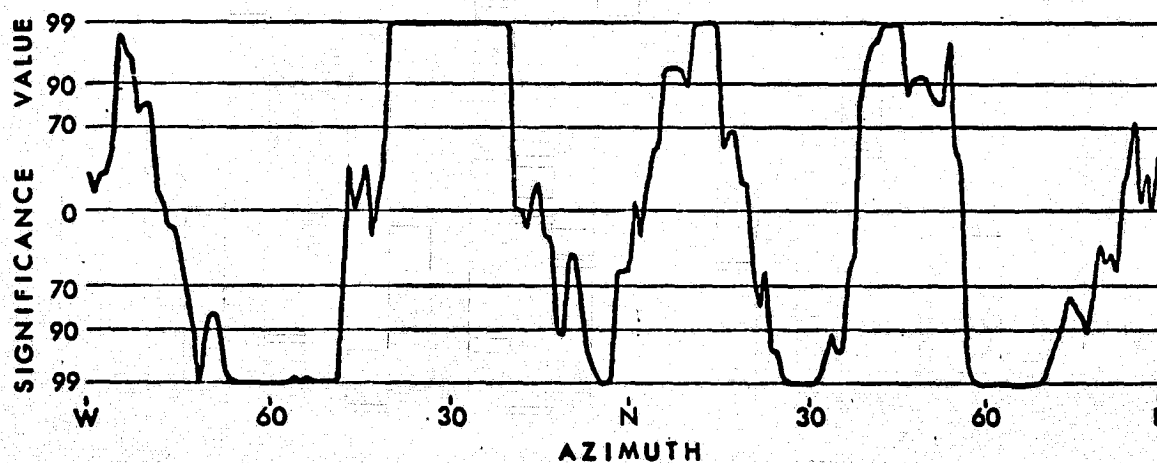
(b) length-weighted azimuthal trends

Figure 37. Linear trends in ERTS image E-1172-17141 for
area of Pueblo relief map as outlined in
Figure 2, 18 degree smoothing.
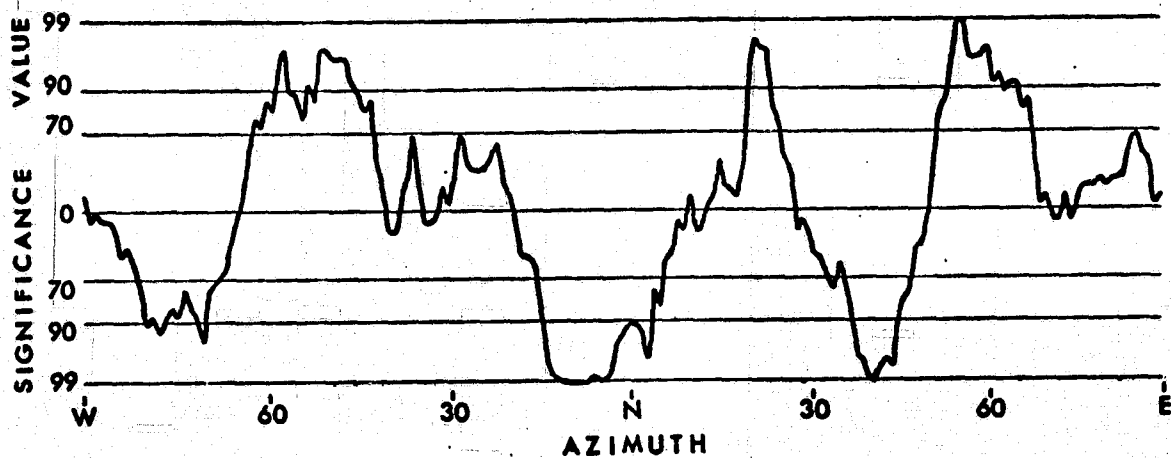
(a) Unweighted azimuthal trends
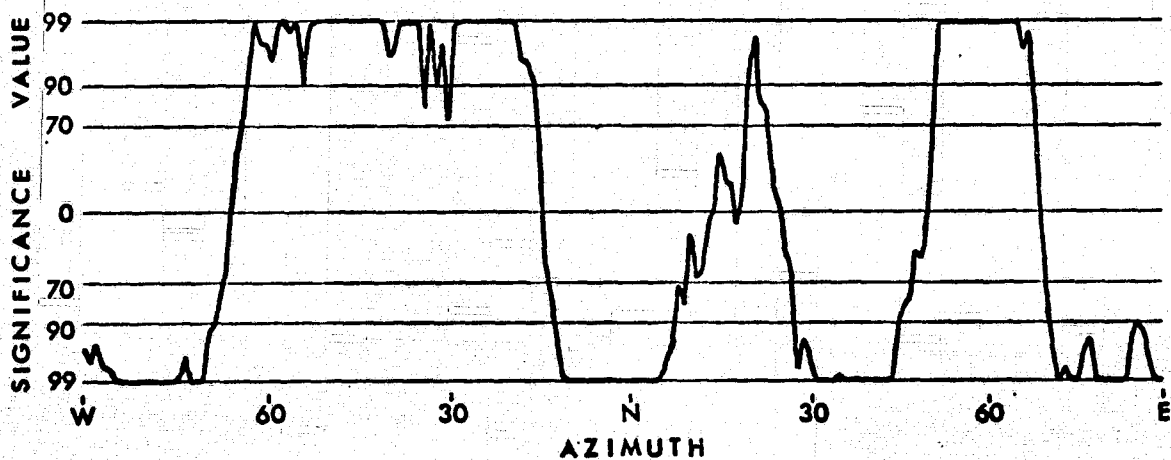
(b) Length-weighted azimuthal trends

Figure 38.   Histograms of linears in Pueblo relief map as
             outlined in Figure 29, 18 degree smoothing.

no new trends occur as a result of length-weighting of linears, but enhancement of the maxima and minima does occur. Figures 39a and 39b show the frequencies of length as a function of azimuth. In both data sets there is a preference of long linears (length greater than the modal values) in the range of N.10-40W. and a weaker preference at N.20E., N.60E. and N.85E. It is concluded that within a trend the frequencies at the modal length of the data are greater than in non-trend areas, and that lengths greater than the modal length occur much more frequently at azimuths within the major trends. Hypothetically, the best way to extract structural information from ERTS linears is to determine modal values from data sets of all linears and then determine structural trends by analyzing the trends of the linears of length greater than the modal length (super-modal linears).

A frequency analysis of the super-modal linears (length class greater than 2) of E-1172-17141 yields 4 significance trends: (I) N.20-40W., (II) N.5-20E., (III) N.40-50E., and (IV) N.85E.-N.70W. These trends are plotted for the image subdivisions in Figure 40a. They are also extrapolated to subdivisions outside the area of the Pueblo relief map. They are further extrapolated to the local linear trends of E-1154-17143. Trends I and II are associated with the trends of the large folds and faults of the central Colorado area (Figure 34). Subdivisions 22, 32, 33, 34 are underlain mostly by Precambrian rocks which
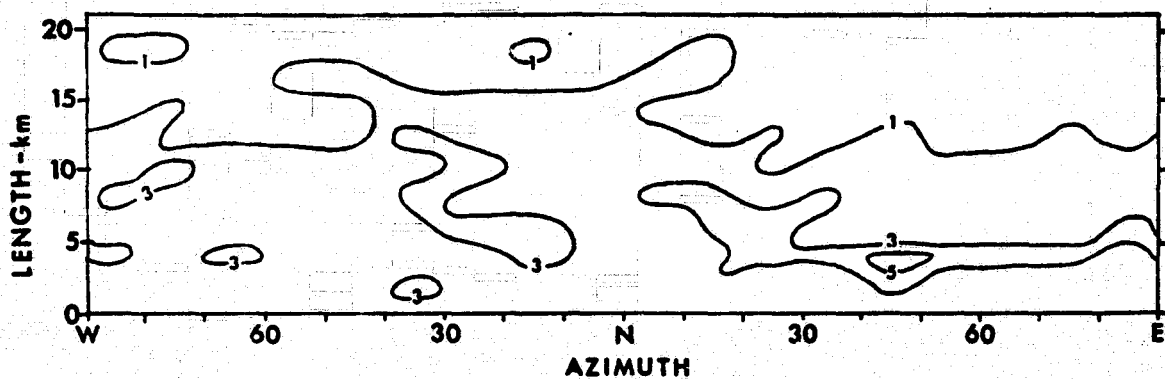
(a) E-1172-17141 image
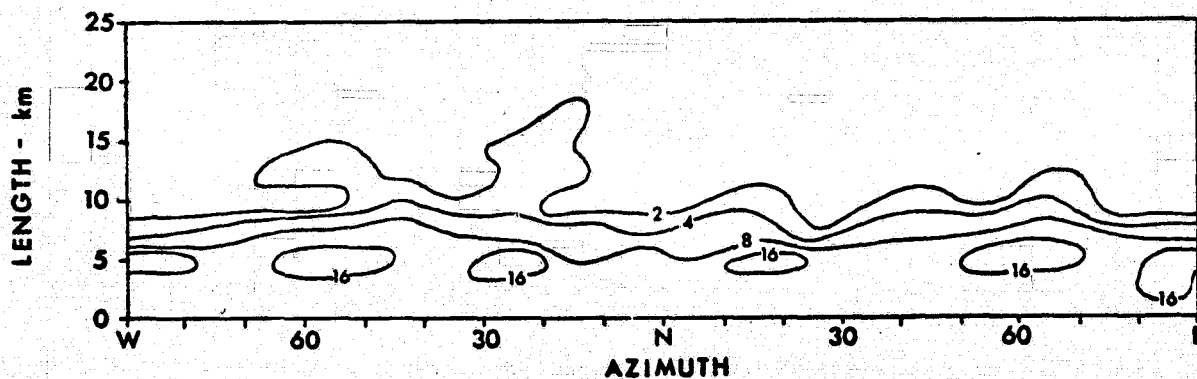
(b) Pueblo relief map

Figure 39. Graphs of frequencies of linears for given length and azimuth for 10 degree intervals.
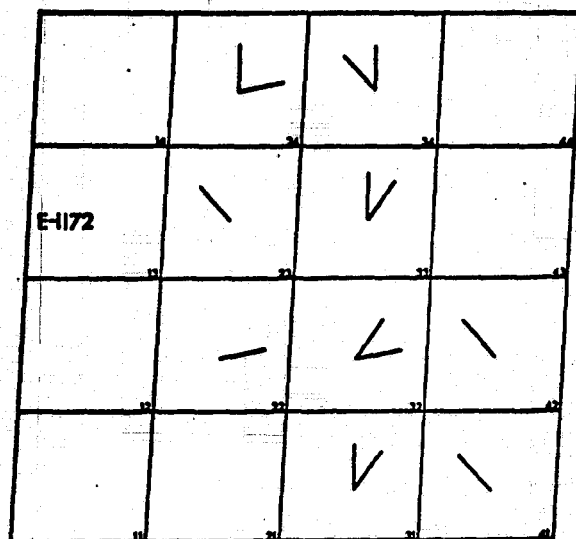
(a)   ERTS image E-1172-17141
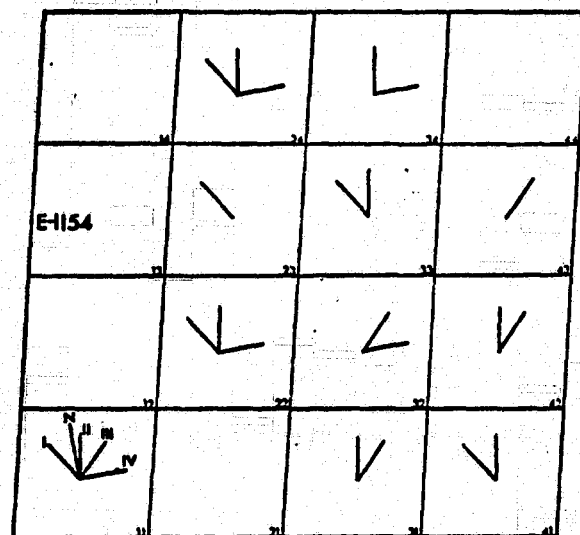
(b)   ERTS image E-1154-17154

Figure 40.   Occurrence in areal subdivisions of four super-
modal trends of length-weighted linears.

contain trends I and II. Subdivisions 23, 24 and 42 are underlain by younger sedimentary rocks folded at least by Cenozoic diastrophism. In subdivision 22 Cenozoic volcanic rocks lie upon Precambrian metamorphic rocks and Paleozoic and Mesozoic sedimentary rocks.

Subdivisions 22 and 32 also contain trend IV which is dominant in the Cenozoic volcanic terrains. This trend may be ascribed to non-topographic linears discussed in the following section. Trend IV is also found in subdivision 24 outside the area of the length-trend analysis. In this subdivision, the trend can be ascribed to deep topographic valleys in the Tarryall Mountains and the area of the North Fork of South Platte River.

TOPOGRAPHIC AND NON-TOPOGRAPHIC LINEARS

Analysis of the Pueblo relief map was done primarily to evaluate the dominance of topographic linears in ERTS imagery over other linears. To make the trend sampling as complete as possible, and diminish the azimuthal filtering effect, linear azimuths and lengths from four illumination directions were collected. The results of the analyses of all linears and super-modal linears is shown in Figures 38 and 41. Trends I, II, III, IV appear in Figure 38a, though trend IV is weak. In the length-weighted data (Figure 38b), trend IV is not present, indicating that
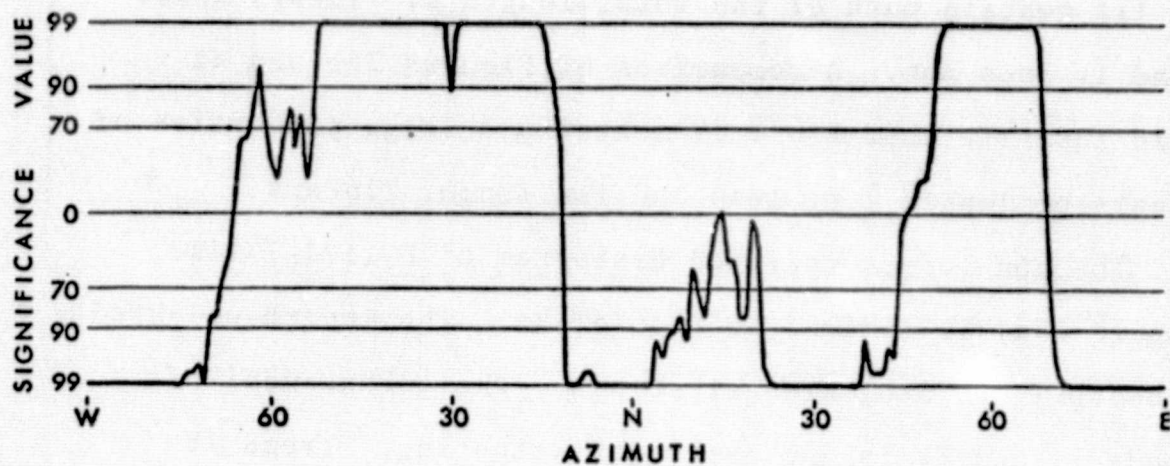
Figure 41. Length-weighted, super-modal linear trends in Pueblo relief map.
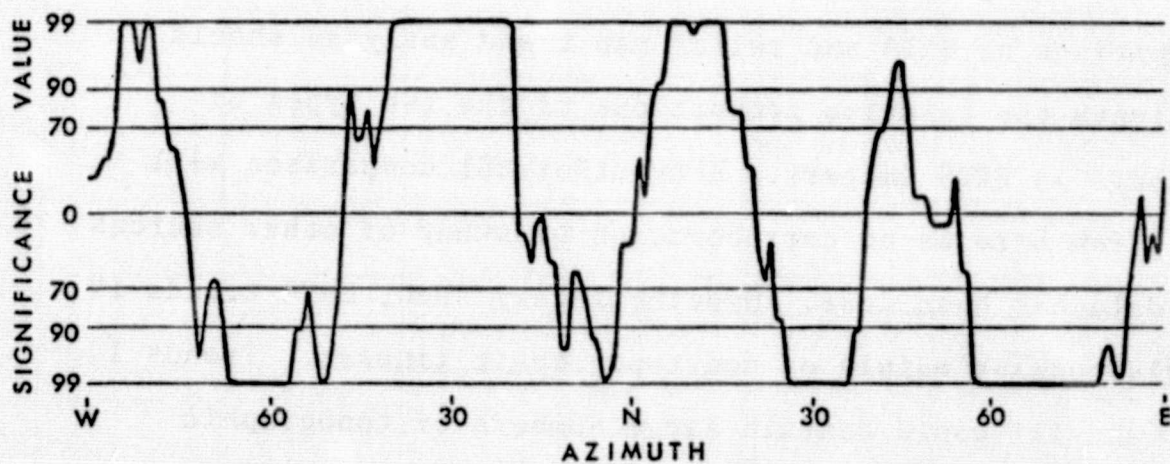
Figure 42. Length-weighted, super-modal linear trends in E-1172-17141 for area of Pueblo relief map.

long linears are few in this trend. The same is true for the super-modal trends (Figure 41b). Thus, trends I, II, and III contain much of the total length of linears while trend IV does not. A comparison of Figures 38b and 41 would indicate that trend IV contains a large proportion of linears of length 2 or less and few longer linears.

The non-length-weighted histogram of E-1172-17141 (Figure 37a) is similar to Figure 38a. The length-weighted trends (Figure 38b) are all strong. The enhancement of trends II and IV is due to length-weighting. Trend IV enhancement is due to length-weighting of a few long linears as further indicated by the super-modal trends in Figure 42.

Because the ERTS image records non-topographic linears (these will include topographic linears of low relief) as well as topographic linears (mostly moderate to high relief), comparison of ERTS and relief map trend analyses should indicate the relative proportions of the two types of linears in ERTS imagery. A hypothetical comparison will be given here as no corroboration by study of other sources of data has been done. Hypothetically then, ERTS trends IV could consist mainly of non-topographic linears. Trends I II, and III could contain large numbers of topographic linears. The idea could be extended further to compare the trends of snow-free and snow-covered scenes of an area

in the same season. The snow-covered scene would approximate
the painted relief map in the enhancement of topographic
linears.

LINEARS AND JOINTS

Measurements of attitudes of joints from the area of
subdivisions 32, 42, 33, 24, and 34 were also analyzed for
trends. Many of the joints were provided by Dr. Robert M.
Hutchinson of Colorado School of Mines from uncompleted
research and were available only in synoptic form. The
following discussion considers the correspondence of joints
for the entire data set covering the five subdivisions and
for a data set from the southern Front Range south of
Pikes Peak.

Figure 43 shows that the dominant trends in the two
groups of joints are N.0-30W. and N.55-90E; they are
approximately orthogonal. In the southern Front Range, the
ERTS trends are I, II, and III, (Figure 40a), but not IV
since the area lies outside the Cenozoic volcanic terrain.
The correspondence of the joints trends with the orthogonal
ERTS trends I and III is the most favorable one but is 20
degrees out of register for both. Nevertheless, the
tendency is to correlate the NNW joint trend with the major
structural trend (Trend I) in favor of topographic control
by joints. The ENE joint trend correlates with the major
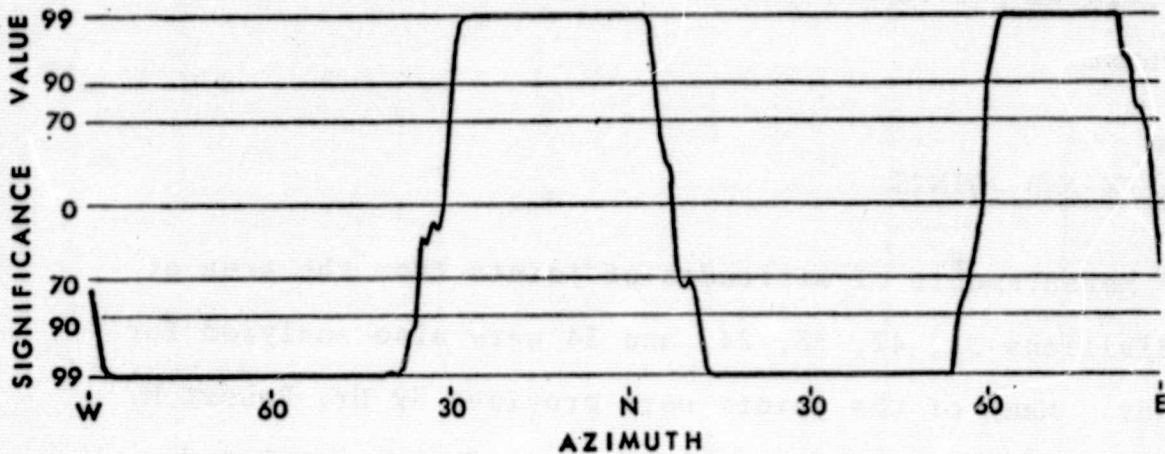
(a) Southern Front Range south of Pikes Peak, 18 degree smoothing
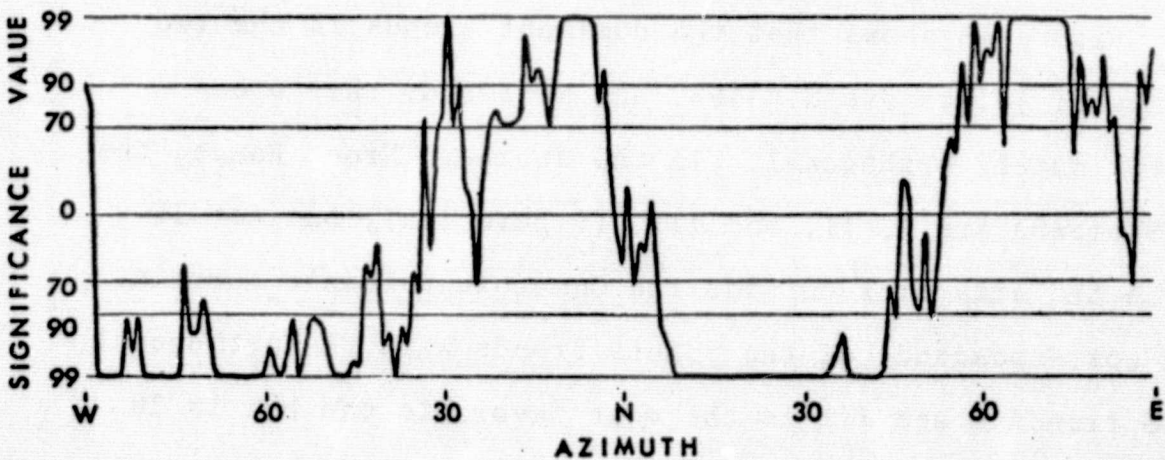
(b) Subdivisions 32, 42, 33, 24, and 34 of imaged area of
     E-1172-17141, 5 degree smoothing.

Figure 43. Azimuth trends of joints in area of central
            Colorado.

faults that transect the southern Front Range, again in favor of topographic control by joints.

The ERTS trends for the larger area of joint coverage are dominated by the local trends of the subdivisions, trends I and II (Figure 43b). The major structures parallel these trends, as does the NNW joint trend. However, the ENE joint trend does not seem to strongly affect topography and enhance or produce trend III. A joint analysis in the Devil's Head Quadrangle (1:24,000) is subdivision 34 by (7) indicates two strong trends: N-S and E-W. The latter trend does appear on E-1154-17143 in subdivision 34 (Figure 40). Three major faults in the Rampart Range parallel trend II and do have fault-line topography (Figure 34). It is entirely possible that in this area trend II contains a large percentage of topographic linears. Comparison of ERTS trends with relief map trends and length-weighted analyses could be done for this area as was done to the south.

APPENDIX--METHOD OF DETERMINING SIGNIFICANCE LEVELS OF
FREQUENCY MAXIMA.

The method calculates the deviation of a particular
value of frequency from the most likely frequency that
would occur in azimuthally uniform, randomly distributed
data set consisting of the same number of linears. This
deviation is expressed as a significance value that is
defined here and is not to be confused with "significance
level" widely used elsewhere. The azimuthally uniform
distribution refers to a distribution of equal frequencies
over the azimuthal half-circle (Figure 44). A frequency
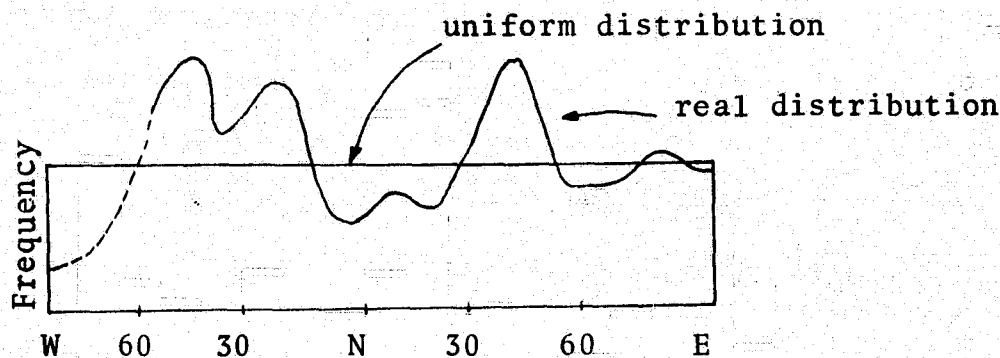
Frequency ≡ no. per n-degree interval

Figure 44. Uniform and non-uniform distribution over
the azimuth half-circle.

value at or near the uniform frequency value will have a
low significance value or may be considered of "low
significance". A frequency value with large deviation from
the uniform frequency value has a high significance value

and may be considered of "high significance" if the significance value is greater than 90% - 95%. A significant frequency value may lie within a maximum or minimum in the real frequency curve.

The method is especially applicable where azimuthal data are smoothed by a running sum over a fixed interval of azimuth. To obtain the significance value of a frequency value, we need the probability that that frequency value will occur if the data set of N values is drawn from an azimuthally uniform, randomly distributed universe of azimuths. This is calculated from the binomial distribution which gives the probability P_f that an event (f) of a given probability (p) will occur in N trials. The most likely value u is determined by the product Np.

For this application, the symbols are defined as follows:

f = number of azimuths per smoothing interval

N = total number of linears

p = degree interval/180 degrees

$$P_f = \frac{(N-f)!}{f!} \ p^f(1-p)^{N-f}$$

u = NP

The significance level S.V. is defined then,

$$\text{if} \quad f<u \qquad S.V. = 1 - \frac{\sum\limits_{n=o}^{f} P_n}{\sum\limits_{n=u}^{u} P_n} \ X \ 100;$$

if $f>u$
$$\text{S.V.} = 1- \frac{\sum\limits_{n=f}^{N} P_n}{\sum\limits_{n=u}^{N} P_n} \times 100.$$

As the frequency f deviates from the most likely value u, the probability that $n \geq f$ decreases and the quotient in the formula decreases, increasing the difference from 1 and increasing the significance value.

SUMMARY AND CONCLUSIONS

Method of Analysis

1. Estimating azimuth data to nearest degree, smoothing over 15-20 degree moving intervals and plotting in strike frequency histograms is an effective way to determine azimuthal trends of linears.

2. The method used for determining significance values provides a measure of the likelihood of non-random origin of the frequency values in a trend.

3. Detectability of linears and trends in ERTS images varies greatly between image generations and depends on sun attitude and surficial tonal contrasts due to seasonal vegetation effects, snow cover, etc.

4. The high resolution of ERTS imagery allows detection and connection of longer linear features than is possible with relief maps or topographic maps.

5. Length-weighted linears produce more distinct trends, and can reveal trends based on a few, very long linears.

6. Short linears contribute a large number of random azimuths and, as a result, decrease the signal (trend)-to-noise ratio.

7. More distinct trends can be produced from length-weighted linears greater in length than the modal length.

Data Characteristics

1. The strike-frequency histogram of linears from the total imaged area is not isotropic, but contains one distinct broad trend.

2. In subsets of the imaged area based on geologic distinctions 4 trends exist.

3. Trends are localized to less than 50 percent of the total area and are related to large geologic features.

4. In small areas of the image, the existence of only one or two trends in typical.

Correspondence with Geologic Trends

1. The analysis was confined to a portion of the imaged area of two ERTS images of central Colorado and four linear trends were found.

2. An overall broad trend reflects a change from south to north of the trends in major geologic structures from N.40W. to N.10E.

3. All four linear trends have geologic trends associated with them.

4. Trend I (N.20-40W.) and II (N.5-20E.) correspond to the trends of the major geologic folds and faults as well as one regional joint set.

5. Trend III (N.40-50E.) corresponds to a second regional joint set (perpendicular to the other) and several major faults.

6. Trend IV (N.85E.-N.70W.) corresponds to a few long, linear depositional features in a volcanic terrain.

7. The localization of trends in smaller areas is strongly related to the underlying major lithologic terrains.

Speculations

1. Trends of linears of length greater than modal length may yield the most information about geologic trends.

2. All geologic trends are not expressed as linear trends in a given small area, but might be on opposite sides of the area. In other words, all geologic trends are expressed somewhere as linear trends.

3. Intersections of linear trends in an image do not necessarily indicate a localized or unique intersection of geologic trends.

4. The trends of geologic structures in younger sedimentary strata strongly parallel linear trends in older metamorphic and igneous terrains.

LANDFORMS

The morphology of the earth's surface provides abundant information on the geologic history of the underlying crust. This information is contained in the landforms present at the surface and can be read by skillful photogeologic interpreters. Landforms are topographic phenomena produced by 1) tectonic forces (youthful fault scarps), 2) constructional geologic processes (stream terraces, alluvial fans, volcanic cones, etc.), and 3) destructional geologic processes primarily involving differential erosion between rocks with different weathering characteristics (hogbacks, cuestas, mesas, fault-line scarps, etc.).

The areal analysis of landforms can lead to an understanding of the geomorphic processes responsible for the present topographic configuration of an area or a region. In addition, landforms can be studied from the viewpoint of what they mean in terms of the lithology and geologic structure of exposed crustal rocks.

During the investigation of ERTS-1 imagery of central and western Colorado, landform analysis was aimed primarily

at the interpretation of the location and distribution of rocks and geologic structures, rather than rigorous study of the processes involved in the evolution of the landforms. This not to say that regional landform mapping and subsequent analysis pointed towards synthesizing the geomorphic evolution of a region is not possible with ERTS-1 imagery, but that both lines of investigation were not feasible with the time and funding of our contract. Indeed, the results of our investigation indicate that the regional geomorphic analysis of landforms using ERTS-1 imagery can, and should, be pursued in the future.

Landforms can be recognized on ERTS-1 images by the shape or geometry of tonal and textural patterns. These patterns are mostly the result of topographic and vegetative phenomena. Figures 45 and 50 illustrate some of the variety of landforms identified on ERTS-1 imagery of central and western Colorado.

By and large, landforms are most easily seen on low sun-angle, wintertime ERTS-1 imagery of Colorado. Notable exceptions to this are prominent terraces and pediments associated with streams. These features have relatively low relief, particularly in view of the scale of ERTS-1 imagery, but they can be discriminated on high sun-angle imagery because of vegetation differences that commonly produce sharp tonal contrasts.
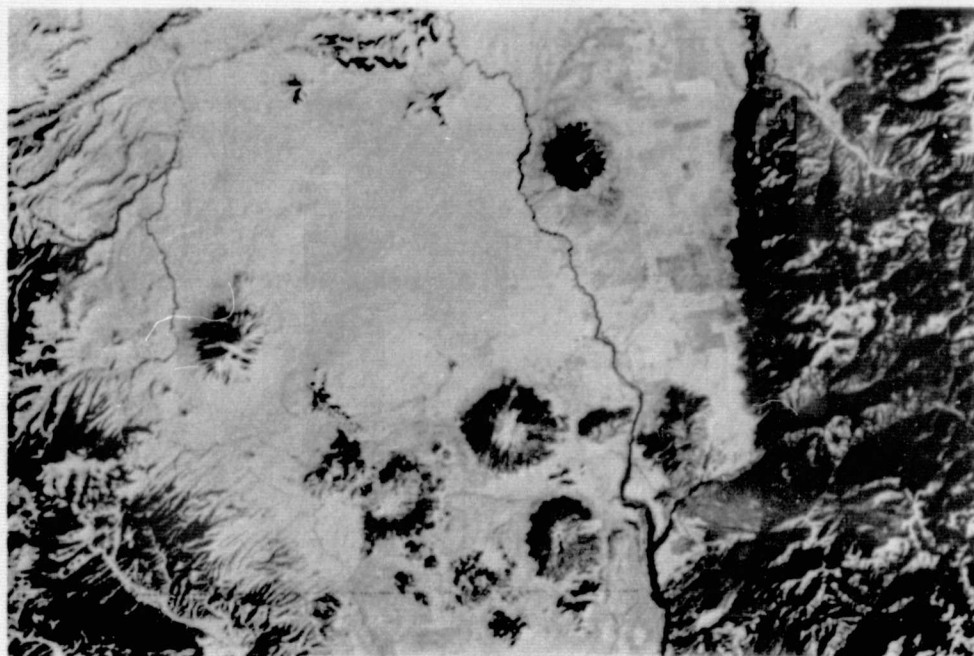
Figure 45. Volcanic cinder cones in the southern San Luis Valley, Colorado-New Mexico. Image 1172-17144-6
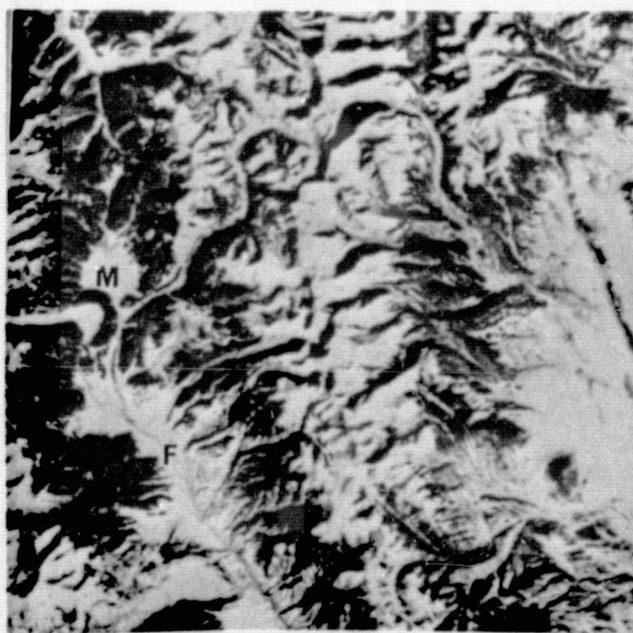
Figure 46. Terminal moraine (M) and alluvial fan (F) in northern Upper Arkansas Valley. Image 1172-17141-7.
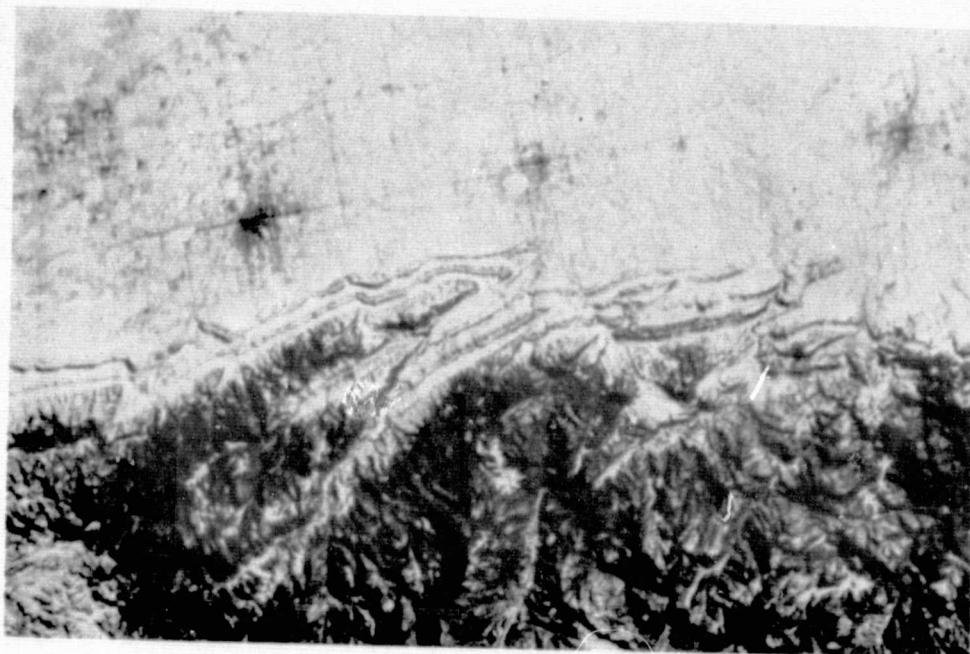
Figure 47. Topographically-expressed folds on the east
flank of the Front Range near Fort Collins,
Colorado. Image 1172-17135-5.
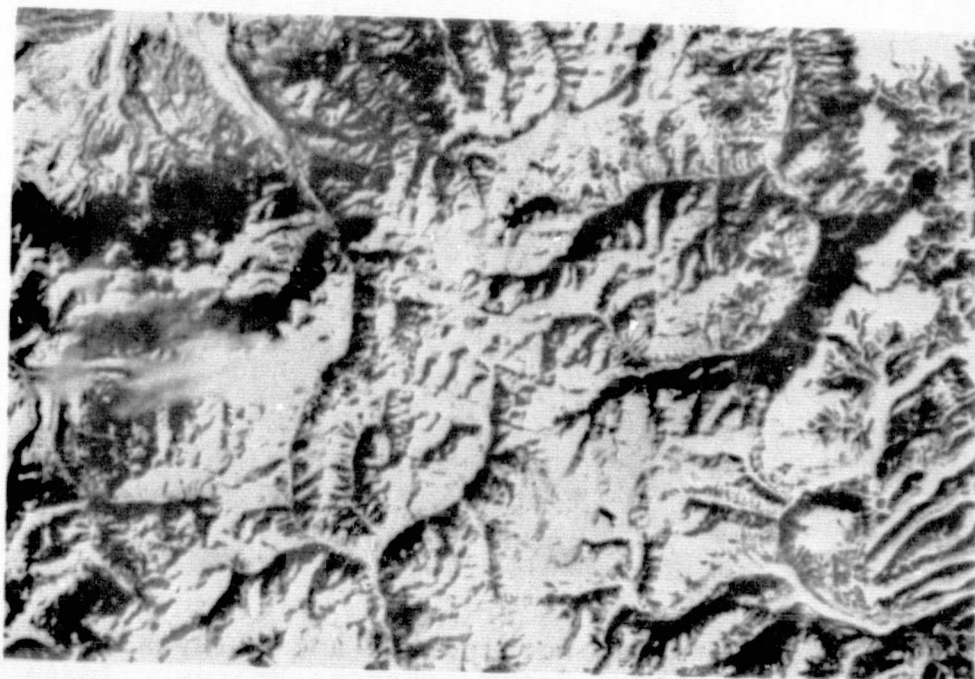
Figure 48. San Juan volcano-tectonic depression containing
Silverton and Lake City calderas, San Juan
Mountains, Colorado. Image 1191-17204-5.
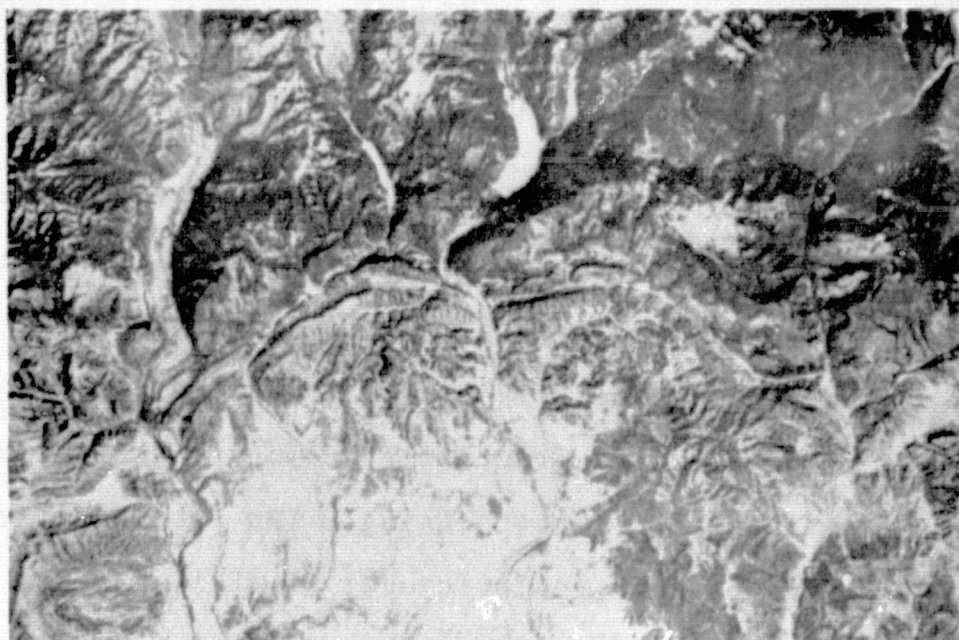
Figure 49. South-dipping hogbacks along the north rim of
the San Juan basin, Colorado. Image 1191-17204-5.

Figure 50. Fine-textured, dendritic drainage pattern in
the Green River Shale of the Piceance basin,
Northwestern Colorado. Image 1156-17253-7.

GEOLOGIC INTERPRETATION AND ENHANCEMENT TECHNIQUES

During the studies of the basic geologic information content of ERTS images, various interpretation and enhancement techniques were employed. Efforts at the Colorado School of Mines were generally restricted to techniques that could be used by the practicing geologist who has a minimum of training in remote sensing. The rationale for this is that the primary geologic user of ERTS imagery, that is, the practicing geologist affiliated with industry, a governmental agency, or a university, does not ordinarily have the budget or the sophisticated laboratory facilities necessary to pursue high-powered data processing and enhancement techniques. Therefore, efforts at the Colorado School of Mines were concentrated toward the following:

1. Conventional photo-geologic interpretation
2. Photo/optical image enhancement

Even with these relatively simple and inexpensive techniques, the amount of basic geologic information that can be extracted from the ERTS imagery of central and western Colorado has far exceeded expectations.

PHOTO-GEOLOGIC INTERPRETATION

The basic principles of photo-geology that are applied during aerial photointerpretation can also be applied to the

interpretation of ERTS imagery. However, the interpreter must be constantly aware of how the very small scale at which he is working affects the basic recognition elements of size, shape, tone, and texture and the relationship of these elements to the types of geologic phenomena that can be expected to be detected on ERTS-1 imagery.

Positive transparencies are better than prints for lithologic and structural interpretation of ERTS-1 images because they are of superior quality. The standard 9" by 9" (1:1,000,000) positive transparencies can be studied most effectively through a high quality optical viewing system (such as the Bausch and Lomb 240R zoom stereoscope) and can take at least 4X magnification before image degradation becomes significant. However, the amount of geologic information that can be interpreted commonly exceeds the ability to annotate it on the 1:1,000,000-scale images, so it is recommended that photographic enlargement prints (1:500,000 to 1:250,000) be used for annotation. Viewing of ERTS-1 transparencies is best on a rheostat-controlled light table since variation in illumination intensity commonly increases the interpretability of an image.

Use of the available stereoscopic viewing capability on ERTS-1 imagery cannot be overemphasized. In central and western Colorado, consecutive ERTS-1 ground tracks provided

imagery with approximately 35% sidelap such that about 70% of each image can be stereoscopically analyzed (Fig. 51).

As stated previously, in the examination of ERTS imagery, lithology and structure must be interpreted largely from the geomorphic expression of the terrain. Because geomorphology involves the recognition and proper interpretation of land forms, the ability to perceive the relationship of topographic features, their relative elevation, slope, or roughness is vital. The use of stereo is particularly valuable in the discrimination of relief, relative rock resistance and qualitative dip estimation.

Stereo viewing provides a number of additional advantages over monoscopic viewing. Since adjoining images (sidelap) are separated by a minimum of one day in time, clouds which obscure ground detail in one image are often absent in its "stereo-pair". Thus the interpreter, while viewing both images simultaneously, tends to filter out the "image-noise" of the cloud and is left free to concentrate on the ground detail. The absence of a stereo model in the limited region covered by clouds on one of the two images of the stereopair does not seriously disrupt the continuity of the entire three-dimensional scene, once a mental image of the overall scene is established. The same process of "noise-filtering" applied to film scratches and processing imperfections of all kinds as well as to differences in illumination (cloud
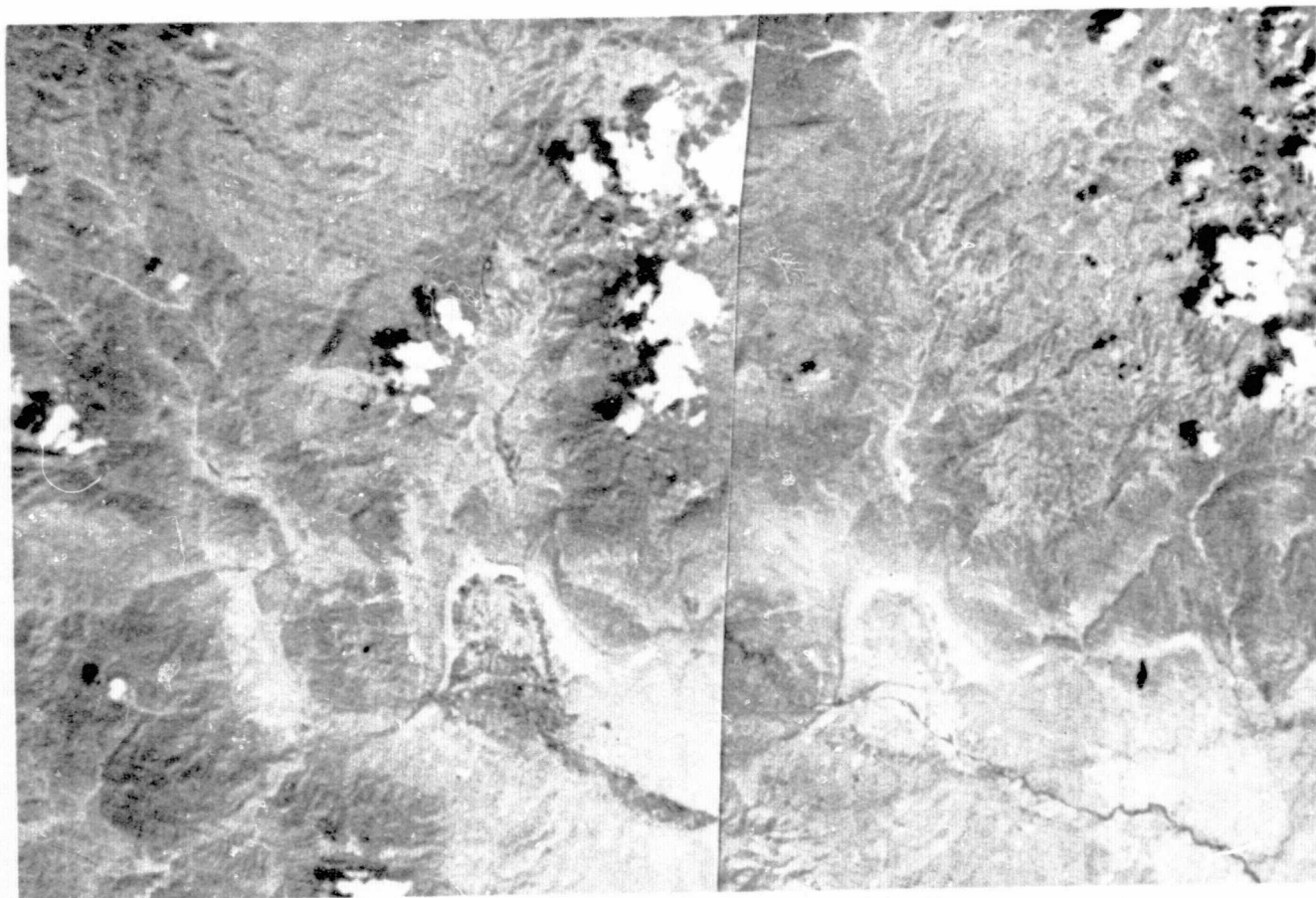
Figure 51.   ERTS-1 stereopair of the southern Front Range-
Canon City area.   Images 1334-17142-7 and
1333-17084-7.

shadows) or other visibility-limiting phenomena such as
thin, virtually indistinguishable layers of cirrus clouds
or snow cover. A serious loss of interpretability is noted
when going from a stereoscopic model on the two edge strips
of each image to a monoscopic mode on the center 1/3 part
of each strip (satellite track). The alteration of orbital
path to provide a minimum of 55% sidelap coverage of each
track or the addition of a second scanning system looking
fore or aft could provide 100% stereo coverage from future
ERTS systems.

The central, no-stereo portion of each image or images
where no stereo coverage has been obtained can be studied
by pseudostereoscopic viewing. This procedure simply uses
two bands of imagery of the same scene for a stereopair.
Relief perspective is less pronounced than with sidelap
stereopairs, but the improvement over monoscopic viewing is
significant for geologic interpretation.

PHOTO/OPTICAL IMAGE ENHANCEMENT

Several methods of enhancing ERTS-1 imagery were studied
during this investigation. In each case, the goal of
image enhancement was to produce images that were superior
to the standard, single-band, black and white ERTS-1 images
for general geologic interpretation. Results of the
studies indicate that none of the various enhancement

techniques used produce an image that is <u>in all respects</u> superior to single-band, black and white ERTS-1 images. However, each technique appears to produce enhanced imagery that is better than single-band, black and white ERTS-1 images for studying one or more specific types of surface phenomena related to geology.

The conclusions drawn from the image enhancement studies can be simply stated: the various enhancement techniques used cause enhancement of one or more geology-relate surface phenomena at the expense of serious image degradation resulting in images that are less useful than standard, single-band, black and white ERTS-1 images for general geologic interpretation. A discussion of each technique follows.

COLOR ADDITIVE VIEWING (CAV)

All direct color additive viewing (CAV) at the Colorado School of Mines was done with an I^2S viewer. Although many color renditions were looked at, the most useful was found to be a "true-color" rendition formed by projecting band 4 with green, band 5 with red, and band 6 with additional green in order to further bring up vegetation. One drawback to this particular color rendition is that water bodies are not easily seen. One way to rectify this situation, without destroying the "true-color" rendition of

the rest of the scene, is to add a negative of one of the infrared bands to the optical system and project it with blue light with the result that water bodies can be plainly identified, and the rest of the scene is essentially unchanged. Some caution must be used in interpreting such a color rendition since cloud and terrain shadows also will appear blue. However, shadows generally appear much darker blue in relation to water bodies.

The color reconstituted images projected on the ground glass screen of the I^2S color additive viewer are greatly degraded in clarity and sharpness compared to 1:1,000,000 positive transparencies of single bands of ERTS-1 imagery. However, the color contrast between some lithologic units can be somewhat enhanced by CAV, but the enhancement is minor in terms of rock discrimination capability. A single notable exception was found during the study of a moderately-dipping sedimentary sequence in central Colorado. The "true color" rendition of the area did not allow more stratigraphic units to be discriminated than could be seen on the 1:1,000,000 black and white positive transparency of band 5, but CAV provided a means of identifying areas underlain by red rocks. This capability is significant in that a geologist can infer much about the composition of a sedimentary rock by knowing only that it has a red color. Use of CAV, then, provided a means of taking a small step from rock discrimination towards rock identification.

The results of this study suggested that perhaps other areas of red ground could be enhanced and identified using CAV techniques. Therefore, a follow-on study was conducted to determine whether areas of red and red-brown staining associated with hydrothermal alteration and mineralization could be found using CAV. The results of this study are given in the section of Applications of ERTS Imagery in this report.

COMPOSITES FROM COLOR SEPARATES

A method of producing color and false color ERTS-1 composites by sandwiching color separates made from several bands of imagery was tried. This process involves exposing the various ERTS bands on colored Diazo proofing film. The Clark systems multispectral projector Model 5005 was used to establish the band/color/intensity combinations which seem to best enhance the features of interest. Many combinations can be examined rapidly with this system although the resulting format (image as projected onto a ground-glass screen) is not suitable for detailed analysis.

The best results using the colored Diazo film has been in simulating color-IR images. The initial relative color intensity to be used with each band was established with the multispectral projector. The exposure of the Diazo film is controlled, within limits, by regulating the operating

speed of the Diazo machine. First generation composites were made using relatively thin Diazo film exposures that appeared to have the most tonal variations. However, it was found that superior renditions result from using relatively dense exposures. Most of the composites used bands 4 and 5 plus either band 6 or band 7 but a very good composite was constructed using bands 4 and 5 plus both infrared bands (MSS 6 + 7).

The color-IR composites allow discrimination of general vegetation type and variations. This ability results in high detectability and enhancement of drainage systems due to characteristic vegetation variation associated with slope and moisture.

DENSITY SLICING AND CONTRAST ENHANCEMENT

A method of increasing the contrast, and interpretability, of an originally low-contrast scene of ERTS-1 imagery of southwestern Colorado was investigated. Basically, the method consists of first making contact negative trans-parencies of a scene (1:1,000,000) on Dupont Cronar Ortho-S Litho film (high contrast copy film) at different exposures. The exposure sequence tested consisted of exposures separated by 1 full F-stop. This sequence provides for successive density slices of 0.30.

Positive transparencies were then made from the entire sequence of negatives. Selected positive and negative slices were then color coded on Diazo film. The colored density slices were then registered producing a color composite of the density sliced image. The resulting image consisted of four discrete colors each representing a specific density slice of one or two steps of the step wedge that appears at the bottom of every ERTS scene.

It appears that with patience and practice, specific steps in the gray scale of an ERTS image can be isolated and color coded using this method. The ERTS scene used in this study was initially a fairly low-contrast scene of the San Juan Mountains in southwestern Colorado (Image #1407-17190). The pseudo-color separation produced with this method greatly increased the contrast of the original image and some of the topographic and geomorphic features were greatly enhanced, especially drainage textures and the annular drainages of the Silverton, Lake City and Creede Calderas. This method may definitely be an aid to an interpreter by bringing out the more obscure detailes present in originally low-contrast ERTS scenes.

It should be noted that a number of the high contrast negatives and positives (Fig. 52) of this scene greatly enhanced the fine details of topography and geomorphic features very much in the way low sun-angle photography or winter ERTS imagery enhances topography because of increased
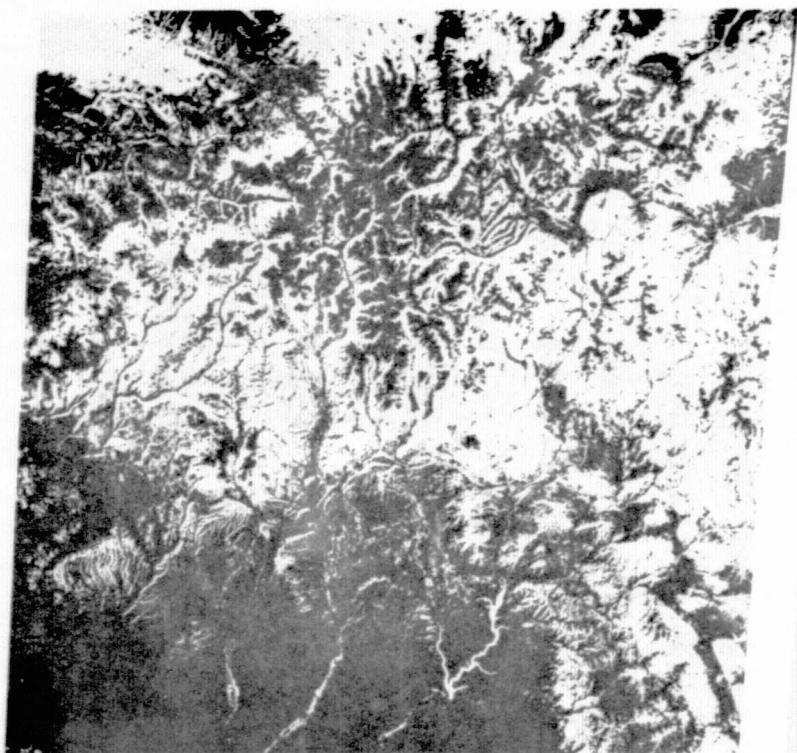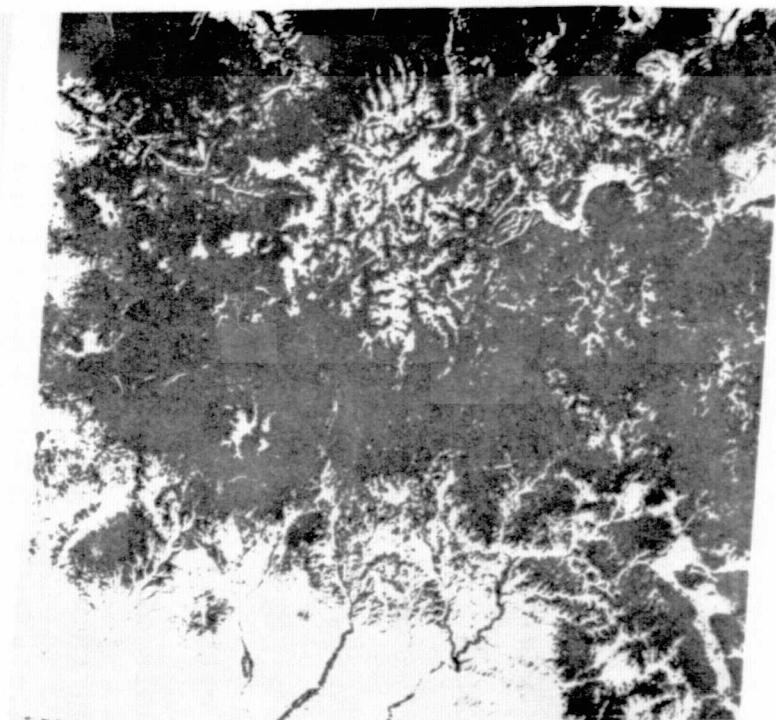
HIGH CONTRAST NEGATIVE   HIGH CONTRAST POSITIVE

Figure 52. High contrast positive and negative prints made from ERTS-1 image
1425-17190-7. Note the general enhancement of drainage lines and
topography.

terrain shadows. More work is needed in this area of photographic enhancement to fully develop the technique and its applications to geologic studies.

COLOR COMPENSATING FILTERS FOR PHOTOINTERPRETATION

The use of Kodak color compensating (CC) filters for photogeologic interpretation was suggested by NASA personnel in the fall of 1972. By way of investigating the use of these filters, two sets of metal clips were designed to fit over the stereo lenses of a Bausch & Lomb Zoom 240 stereoscope. These clips hold from one to three CC filters mounted in 35mm slide frames and allow rapid and easy removal and replacement of the filters. A variety of Kodak CC filters was purchased and tried on supporting color and color infrared aircraft photography.

In general, it was found that CC filters having number designations of less than 20 (CC10M, CC5R, etc.) were of little or no value in photointerpretation. Those filters having number designations of 20 or greater (CC20M, CC50R, etc.) were found to be of value in photointerpretation either when used alone or when used in combination. In general, the CC filters were found to be useful for the following purposes:

1. Adjusting or changing the color balance of the photography without expensive reporcessing.

2. Yellow CC filters (absorb blue) were found to be useful for enhancing areas of hydrothermal alteration or iron stain in color photography.

3. Cyan CC filters (absorb red) were found to be useful for enhancing lineaments above timberline in color photography.

4. Good results were obtained by using combinations of green, yellow, and cyan CC filters with color photography to first enhance the affects of vegetation, then, turning around and using combinations of red, blue, and magenta CC filters to subdue the affects of vegetation. A similar procedure was followed with CIR photography, also with good results.

5. Similarly, other combinations of CC filters can be used to enhance or subdue any other affects that can be attributed to colors, such as rock or soil color.

6. There seems to be a beneficial "phychological enhancement" produced when, after looking at a stereo pair of photographs for some period of time, any CC filter is inserted. The photography then appears to be somehow new and different, and additional information can be seen. This affect exists, whether or not any real enhancement of these features occurs, as once a feature is detected

in this manner, it can often be seen equally-well
with or without the presence of the CC filter.

The CC filters were used in routine photogeologic
interpretation of stereo pairs of color and color infrared
transparencies (they would have no value for use with black
and white photography). The results obtained would probably
apply equally well to color and color infrared prints. A
similar method could, no doubt, be devised to use CC filters
with a mirror stereoscope or even a small pocket stereoscope.
The filters, mounts, clips, etc., are cheap and easily pur-
chased or made, hence, this technique is a simple and
inexpensive method of extracting additional information
from available color and color infrared photography.

GEOLOGIC APPLICATIONS OF ERTS-1 IMAGERY

The ultimate worth of the ERTS-1 satellite is likely to be judged by the usefulness of its data products, and "usefulness" is a difficult parameter to evaluate. Potential usefulness of ERTS-1 imagery in solving geology-related problems appears to be a function of two primary factors: (1) the nature and amount of the readily-extractable geologic information and (2) the skill and imagination of the geologist/interpreter.

The basic geologic information content of ERTS-1 imagery of central and western Colorado was previously discussed in this report. In general, the amount of lithologic and structural information that can be extracted from the imagery has far exceeded expectations. Consequently, it seems that the burden of demonstrating the usefulness of the imagery now falls on the users of ERTS imagery.

Two types of geologic applications were studied during this investigation. The first involves broadening the base of areal geologic understanding, and includes such activities as geologic mapping and tectonic analysis; these applications were discussed in the section of this report on Basic Geologic Information. The second type was concerned with applying basic geologic information to the specific geologic problems discussed below.

MINERAL EXPLORATION WITH ERTS IMAGERY

Mineral exploration is an often-cited potential application of orbital remote sensing data. However, before a new method, system or instrument is employed by industry, it must show potential use and economic feasibility. In this light, studies were conducted to evaluate the potential usefulness of the geologic information extracted from ERTS-1 imagery of two highly mineralized areas of the state--the central Colorado mineral belt and the San Juan Mountains.

CENTRAL COLORADO MINERAL BELT

An experiment was conducted to test the application of photo-lineament information obtained from ERTS imagery of central Colorado to the selection of potential target areas for mineral exploration. The objectives of the experiment were:

1) To select potential target areas based on the distribution of photo-lineaments and their intersections, as obtained from the ERTS image.

2) To evaluate the target areas.

3) To determine what relationships, if any, exist between the distribution of photo-lineament intersections and the location of mineral districts.

The test area was defined by a single ERTS image of central Colorado (Fig. 53), which includes a part of the Colorado
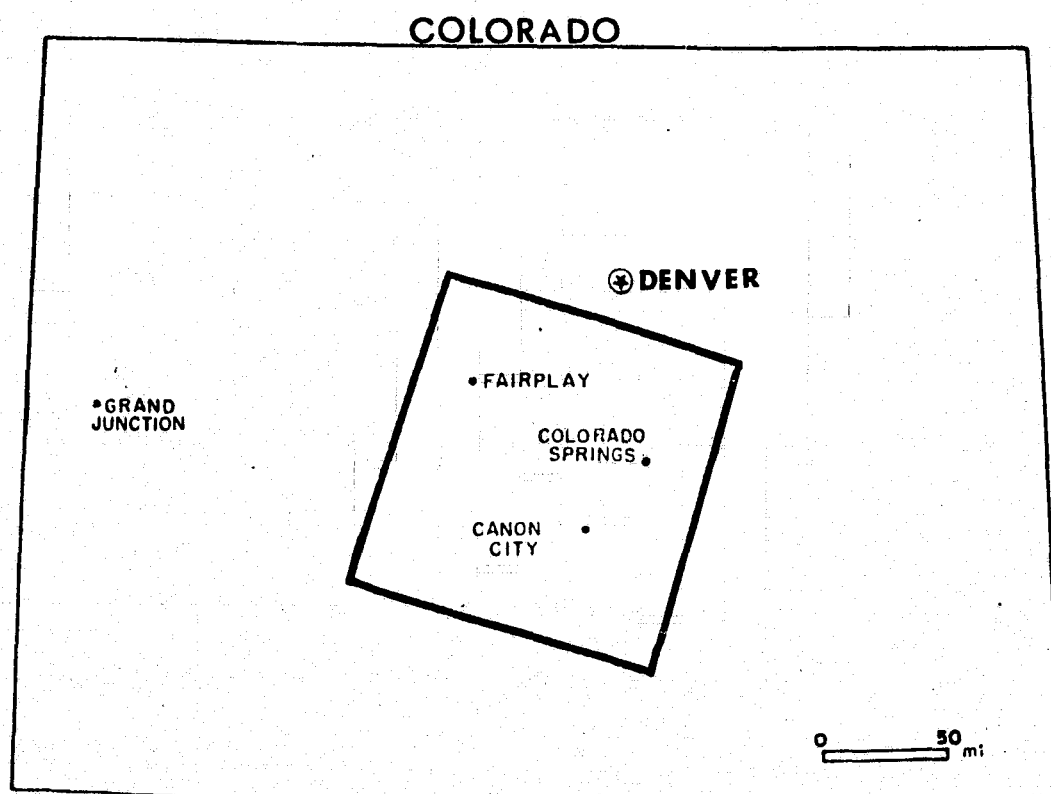
Figure 53. Colorado index map. Geographic location of the ERTS image 1172-17141.

Mineral Belt and, thus, several major mining districts. The northeast-trending mineral belt is characterized by intrusive porphyries of late Cretaceous and early Tertiary age (1). Ore deposition, in most cases, was structurally controlled by faults and shear zones.

PHOTOINTERPRETATION

Photointerpretation was performed on the 11 January 1973 image 1172-17141 (Fig. 54) using a Bausch & Lomb zoom stereoscope in both stereoscopic and monoscopic modes. The 9-x9-inch positive transparencies of all four MSS bands were used; however, most of the data was obtained from band 7. This image was chosen over other images of the same scene because the topography is enhanced by the low-angle solar illumination (23° elevation) and snow cover in the mid-winter imagery. The first step of the experiment consisted of interpreting the ERTS image and plotting the photo-lineaments on an overlay (Fig. 55). Two types of elements were plotted: straight lineaments and curvilinear or circular features.

TARGET AREA SELECTION

Potential reconnaissance target areas were selected on the basis of the lineament data. Selections were made under the following assumptions:

Figure 54. ERTS-1 image 1172-17141-7 of central Colorado
(11 January 1973).

Figure 55. Photo-lineament overlay. Solid lines are well-
defined linears; dashed lines are possible or
moderately expressed linears; dotted lines are
curvilinear or circular features.

1) We are looking for metallic mineral deposits

2) Mineralization is probably structurally related to
    faults and shear zones, which may, in turn, be spatially
    related to intrusive stocks, plugs and volcanic centers.

Target selection consisted of two steps. First, about 40
small, specific targets were chosen based on the numbers
and kinds of photo-lineament intersections. Next, the 10
best target areas (Fig. 56) were selected from the first
group. Each target area corresponds to a circular area
on the ground about 14 km (9 mi) in diameter or approximately
165 sq km (64 sq mi). The 10 final target areas were
broken down into three orders of priority (1, highest, etc.)
based on the complexity, type and strength of the inter-
sections and the presence or absence of curvilinear or
circular features. Of these criteria, complex areas of
intersections and intersections of photo-lineaments with
curvilinear or circular features were felt to be the most
important.

TARGET AREA EVALUATION

A map of Colorado mineral deposits (8) was used to
evaluate the target areas. The location of the larger
mineral districts and the selected target areas are shown
in the overlay in Figure 57. Most of the annotated mineral
districts have produced over $100,000 in metals; however
the combined production of Climax, Leadville and Cripple
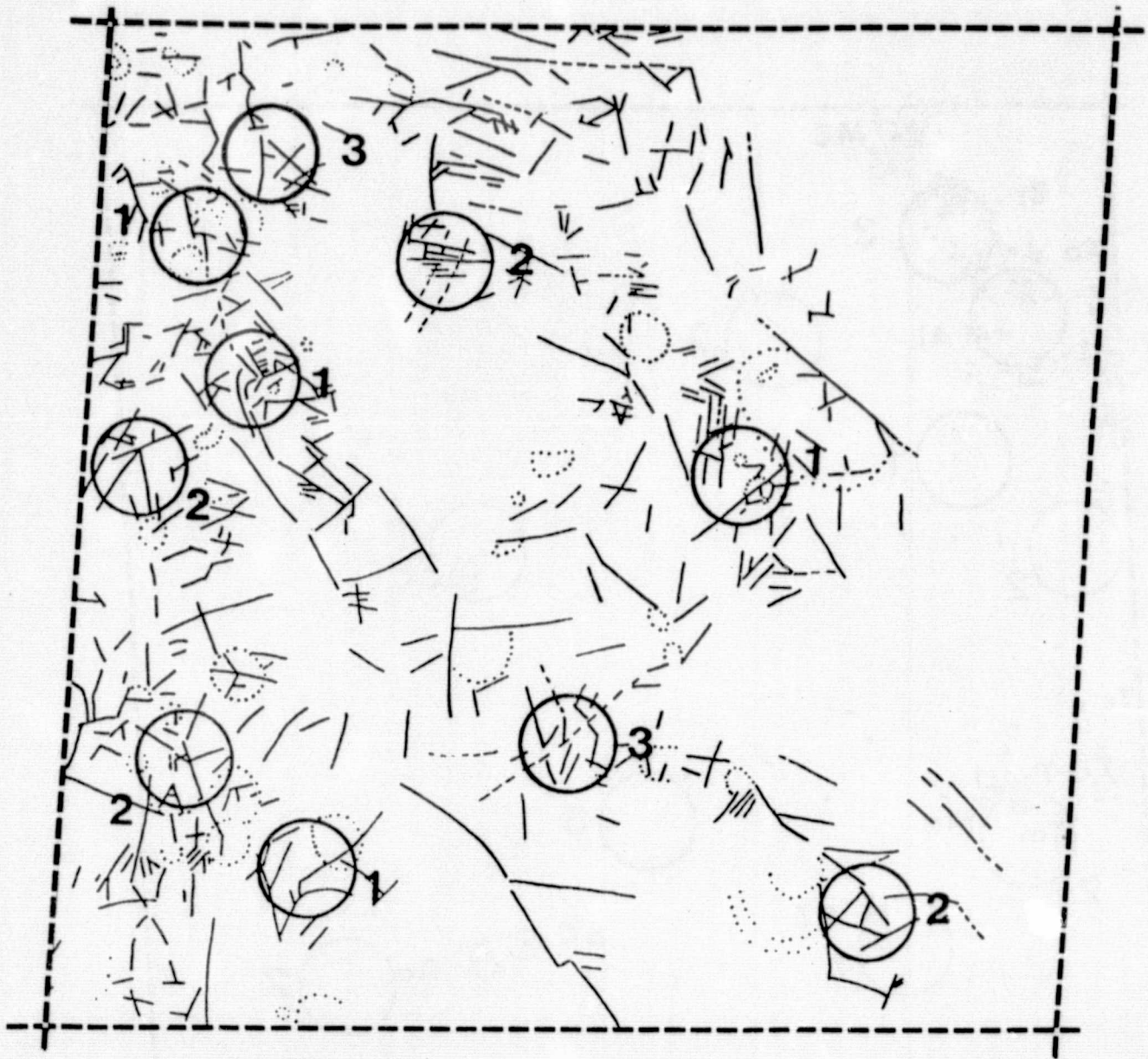
Figure 56. Location of target areas selected on the basis of
photo-linears. The priorities (1, highest, etc.) are
indicated by the number next to each target area.
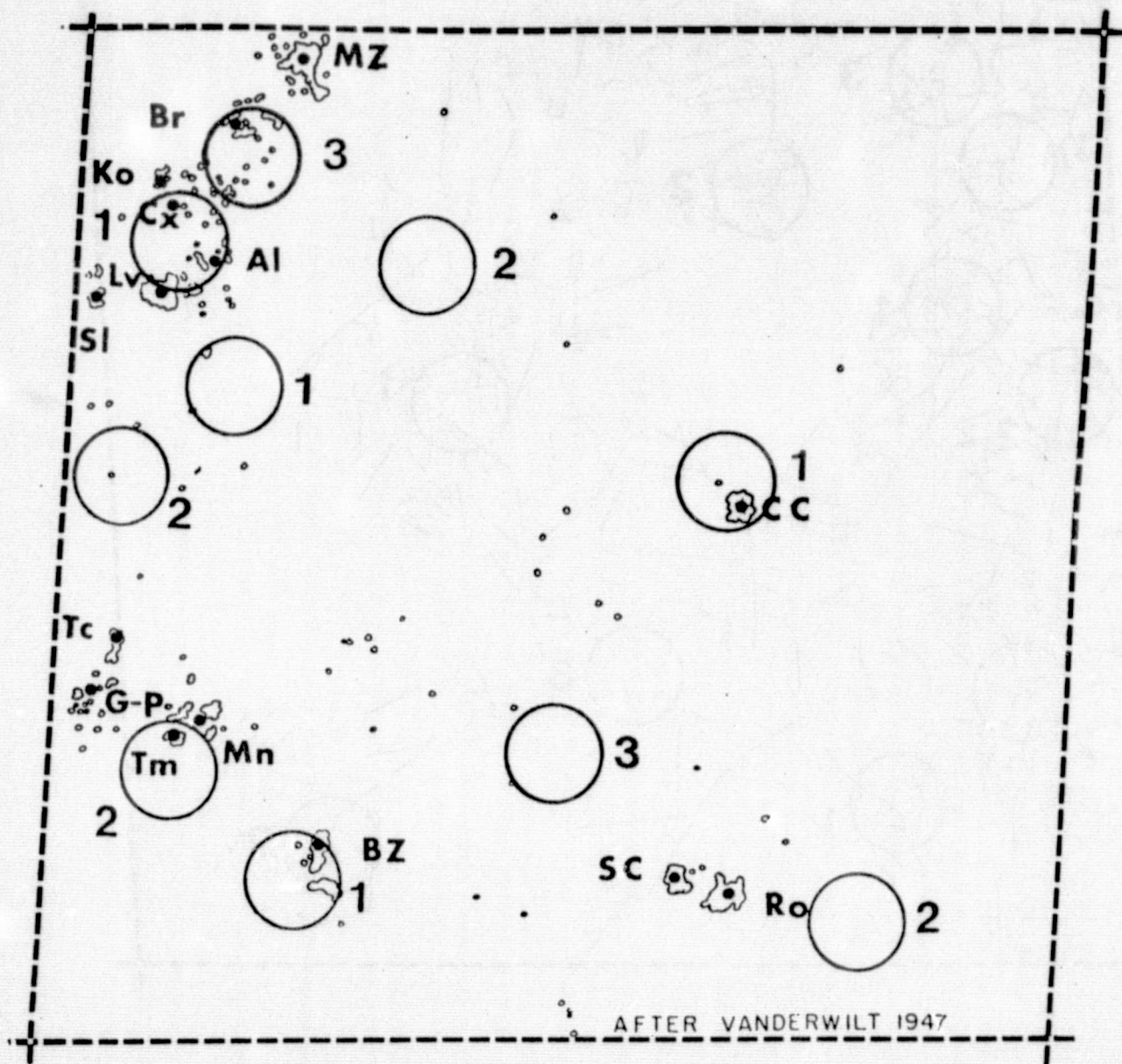
Figure 57. Location of major mineral districts and selected
target areas. The small circles are isolated areas of
mineral production, generally of low value. The
larger mineral districts indicated by a black dot have
irregular outlines and are annotated by an abbreviation:
MZ-Montezuma, Br-Breckenridge, Ko-Kokomo, Cx-Climax,
Al-Alma, Lv-Leadville, Sl-Sugarloaf, Tc-Tincup, C-P-
Goldbrick-Pitkin, Tm-Tomichi, Mn-Monarch, BZ-Bonanza,
CC-Cripple Creek, SC-Silver Cliff, Ro-Rosita.

Creek has been over $1,000,000,000 in precious and base metals. Other important mineral districts which have had production figures over $1,000,000 include Breckenridge, Kokomo, Alma, and Bonanza.

Five of the 10 target areas coincide with the following mineral districts: Breckenridge, the Leadville-Climax-Alma area (covered by one target area), Tomichi, Bonanza, and Cripple Creek. These results were better than expected, so the influence of prior geologic knowledge of the test area on target selection was tested.

BIAS IN TARGET SELECTION

Copies of just the lineament interpretation were distributed to a test group of 15 Colorado School of Mines professors and graduate students. After being instructed on the basic assumptions made during the selection of the Phase I target areas (those chosen in the first part of the experiment), each member of the group was asked to select 10 circular, 14 kilometer-diameter target areas. Analysis of the test group's selections (Phase II target areas) showed a remarkably strong agreement for 8 target areas, 5 of which coincide with mineral districts; 4 of these 5 were also picked during Phase I of the experiment. The test group's successful targets (i.e. coincidence with a mineral district) are tabulated and compared with the

successful Phase I targets in Table 13. There is a fairly strong agreement among members of the test group for the target areas that outline the following mineral districts: the Leadville-Climax-Alma area, Tomichi, Monarch, Bonanza and Cripple Creek districts.

Statistical analysis was used to evaluate both the test group's results and the method of target selection used in the experiment. The probability of selecting one successful target area in ten tries by random process is .32; this value decreases to .01 for selecting five successful target areas. In addition, the probability of 5 people choosing the same successful target area by random process is a mere 1.4×10^{-7}. The analysis was performed by placing a square grid with the approximate dimensions of a target area (9-x9-mile squares) on the lineament interpretation and the mineral district overlays. The probabilities were calculated assuming that there are 12 chances for a target area to coincide with a mineral district and there are 70 possible choices (target areas-squares) which coincide with photo-lineaments occurring on the overlay.

Analysis of the test group's results indicate that bias had very little, if any, effect on the selection of the Phase I target areas, and suggests that some of the mineral districts are defined by photo-lineament information.

TEST GROUP RESULTS

MINERAL DISTRICTS	A	B	C	D	E	F	G	H	I	J	K	L	M	N	O	P	%
MONTEZUMA																	
BRECKENRIDGE												X				0	13
KOKOMO				X	X	X							X		X		31
CLIMAX	X			X	X	X	X	X		X	X		X	X	X	0	75
LEADVILLE	X		X	X	X	X	X	X	X	X	X			X		0	75
ALMA	X		X	X	X	X	X	X		X	X		X	X	X	0	81
SUGARLOAF																	
TINCUP									X								6
GOLDBRICK-PITKIN					X												6
TOMICHI			X		X	X		X			X	X		X	X	0	56
MONARCH	X	X			X	X	X			X				X			44
BONANZA	X					X	X	X		X				X		0	44
SILVER CLIFF																	
ROSITA																	
CRIPPLE CREEK			X	X		X	X	X	X	X		X	X	X	X	0	75

Table 13. Test group's successful target areas. Each letter across the top corresponds to a member of the test group. Coincidence of a mineral district with a target area is indicated by the letter X. The letter 0 in column P represents the successful target area selections of Phase I. The last column indicates the percent agreement for successful target areas selected during Phase I and Phase II of the experiment.

PHOTO-LINEAMENTS AND MINERAL DISTRICTS

To determine what relationships exist between mineral districts and photo-linears, the frequency of photo-lineament intersections was plotted using a computer program originally designed to plot stereonet data in a form suitable for contouring. The contoured plot shows the density, or concentration, of all types of intersections on the photo-lineament overlay (Fig. 58).

The Cripple Creek district is well defined by a high density of lineament intersections, and the Kokomo, Climax-Alma, Goldbrick-Pitkin and Tomichi districts are moderately-well defined. The Leadville and Bonanza districts were not discriminated by this method. It should be noted that the Kokomo and Goldbrick-Pitkin districts do not coincide with the previously-selected Phase 1 target areas, but they are discriminated by a high density of photo-lineament intersections. It is also interesting to note that the 8 target areas that show good agreement among members of the test group, also coincide with areas having a high concentration of lineament intersections.

SUMMARY

A promising approach to the selection of mineral exploration targets using ERTS imagery has been demonstrated. This study reduced an original search area of 33,500 sq km
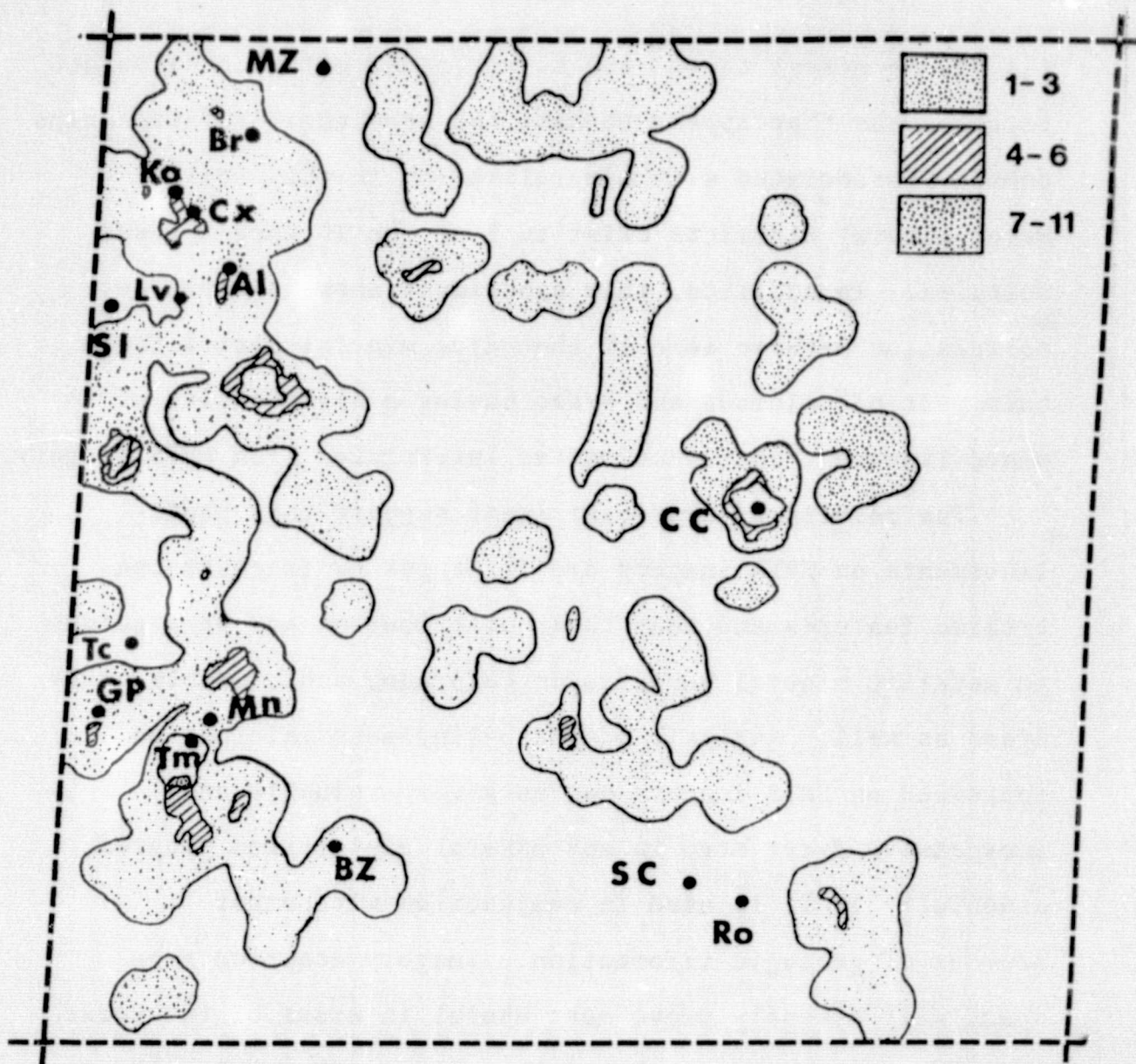
Figure 58. Density of photo-lineament intersections and the location of major mineral districts. The numbers in the legend represent the number of photo-lineament intersections per unit area.

(13,000 sq miles) to ten 165 sq km (64 sq mi) reconnaissance
target areas that appear to have the structural relationships
commonly associated with mineralization in this region.
Major mineral districts exist in 5 of the 10 target areas
selected. In addition, this experiment shows a definite
correlation between some of the major mineral districts in
this part of Colorado and areas having a high density of
photo-lineament intersections as interpreted from ERTS imagery.

The results of this experiment suggest that photo-
lineaments on ERTS imagery are fractures or fracture-con-
trolled features and that their distribution may be a guide
to metallic mineral deposits in Colorado, and probably other
areas as well. Analysis of photo-lineament information
contained on ERTS imagery can be a very valuable and
inexpensive first step in any mineral exploration program,
especially if it is used in conjunction with other
sources of geologic information. Imagery acquired from
space will probably prove most useful in areas of the world
in which less is known about the geology. Moreover, the
favorable results of this study suggest that those target
areas that do not correspond with known areas of mineraliza-
tion may, in fact, be new targets for mineral exploration
in Colorado.

SAN JUAN MOUNTAINS

A follow-up experiment was conducted with the ERTS imagery of the San Juan Mountain region of southwestern Colorado. This time, color anomaly data derived from the ERTS imagery was added to the regional geologic and photo-lineament data prior to target area selection. Two basic assumptions were made:

1) Very little detailed geologic information exists for the region.

2) Mineralization in this region is generally associated with the volcanic terrain and is structurally controlled by faults and fissures, which may, in turn, be related to intrusive stocks and plugs and volcanic centers and calderas.

COLOR ANOMALIES

The ability to detect and map color anomalies on a regional scale could be an important factor in the evaluation of the possible mineral potential of an area. More specifically, it could be a very useful aid in the selection of mineral exploration target areas, especially in the reconnaissance of the lesser known regions of the world. Color additive viewing of a snow-free, cloud-free ERTS scene 1425-17190 (Fig. 4) was performed in an attempt to detect color anomalies. Of the various color combinations

tried, a psuedo-true color rendition (band 4 is projected in green, band 5 in red and band 6 also in green) was found to be the most useful. With this color combination it was possible to locate and map many of the major and some of the minor red to reddish-brown color anomalies occurring in the western San Juan Mountains.

Using the colors of known anomalies as guide (for example the Red Mountain near Silverton, Colo.), thirteen additional anomalies were mapped. These anomalies were plotted on a 1:250,000 base map and then checked in the lab on low-altitude color photography (NASA Mx 213). Nine of the thirteen anomalies mapped on the color additive viewer were confirmed on the photos. The remaining 4 anomalies could not be confirmed due to the lack of photographic coverage. However, two of the four uncon-firmed anomalies are located in areas of known mineralization: the La Plata Mountains and the Platoro-Summitville area.

Seven of the fifteen color anomalies mapped (two known; thirteen unknown) on the ERTS scene occur within the Ophir Quadrangle. The color anomalies in the southern part of the quadrangle are apparently related to hydro-thermal alteration within the Grizzly Peak stock and along its contact zone with the country rock. The highest concentration of color anomalies mapped on the ERTS scene is alligned along the large northeast-trending lineament which may have been a controlling factor in the location and

formation of the Silverton-Lake City Caldera complex and its associated mineralization and alteration.

The color anomalies, as seen on the color additive viewer, are generally very small, irregular patches that have a subtle to a very-definite orange, pink, or red tinge with respect to the colors of the surrounding area. The boundaries of most color anomalies are somewhat diffuse. When checked on the color aerial photographs, the color anomalies mapped on the ERTS imagery were found to represent fairly large areas that are characterized by a high concentration of small individual color anomalies. An important factor in the detection of these areas on the ERTS imagery is the tendency for much of the color of an anomaly to be spread-out over very extensive talus slopes. These colored talus slopes increase the effective detectable size of some of the smaller color anomalies.

In order to check the reproducibility of the results and to evaluate any possible bias, four geologists, who were relatively unfamiliar with the western San Juan Mountains, were asked to map possible color anomalies on the same ERTS scene, with the same color combination. In addition to selecting the Red Mountain and Pilot Knob-Vermillion Peak known areas, the test group had very good agreement for 12 of the 13 unknown anomalies previously selected in this study. Of the 11 confirmed anomalies, 6 anomalies had 100% agreement, 3 had 80% agreement and 2 had 60% agreement. This

good agreement indicates that it is definitely possible to detect and map color anomalies on ERTS imagery using color additive viewing techniques.

TARGET SELECTION

Two types of target areas were selected: (1) reconnaissance target areas and (2) smaller, detailed exploration target areas. Both types of target areas were selected on the basis of the information derived from the ERTS imagery. Each target area was given a priority (1, highest etc.) with respect to its apparent mineral potential. The factors considered important in the selection of both types of target areas and in the assignment of target priorities are:

1) Presence of color anomalies (alteration), confirmed and unconfirmed.

2) Proximity of color anomolies to a large photo-lineament or circular or curvilinear features.

3) Overall complexity of the structural fabric (density and distribution of photo-lineaments and their intersections).

Three large reconnaissance target areas and ten smaller specific target areas were selected and assigned priorities as shown in Figure 59.

The reconnaissance targets were selected as a first step in isolating those areas on the ERTS imagery appearing to have the highest potential for successful mineral exploration.

RECONNAISSANCE

EXPLORATION

COLOR ANOMALY

Figure 59.   Location of target areas selected on the basis
of geologic information derived primarily from the
ERTS images 1191-17204 and 1425-17190. The
priorities (1 highest etc.) are indicated by the
number within the target area.

The smaller target areas, most of which are located within the reconnaissance target areas, represent starting points for more detailed mineral exploration.

TARGET EVALUATION

A map of Colorado mineral deposits (8) was used to evaluate the target areas. The location of the larger mineral districts and the selected target areas are shown in Figure 60. Most of the major mineral districts are located within the priority 1 reconnaissance target area. However, mineral districts are also located in the other two reconnaissance target areas.

Five of the 10 exploration target areas covered the following mineral districts: Ophir, Red Mountain-Eureka, Lake City, La Plata and Summitville-Platoro. Except for Eureka, no other major mineral districts coincided with a selected target area. However, Ouray, Telluride and Silverton lie just outside of the small priority 1 exploration target areas.

It should be noted that the selection of the exploration target areas was strongly influenced by the presence of color anomalies interpreted from the ERTS imagery and that the exact placement of the target circles was somewhat arbitrary. This was especially true in the selection of the target areas in the La Plata and Summitville-Platoro
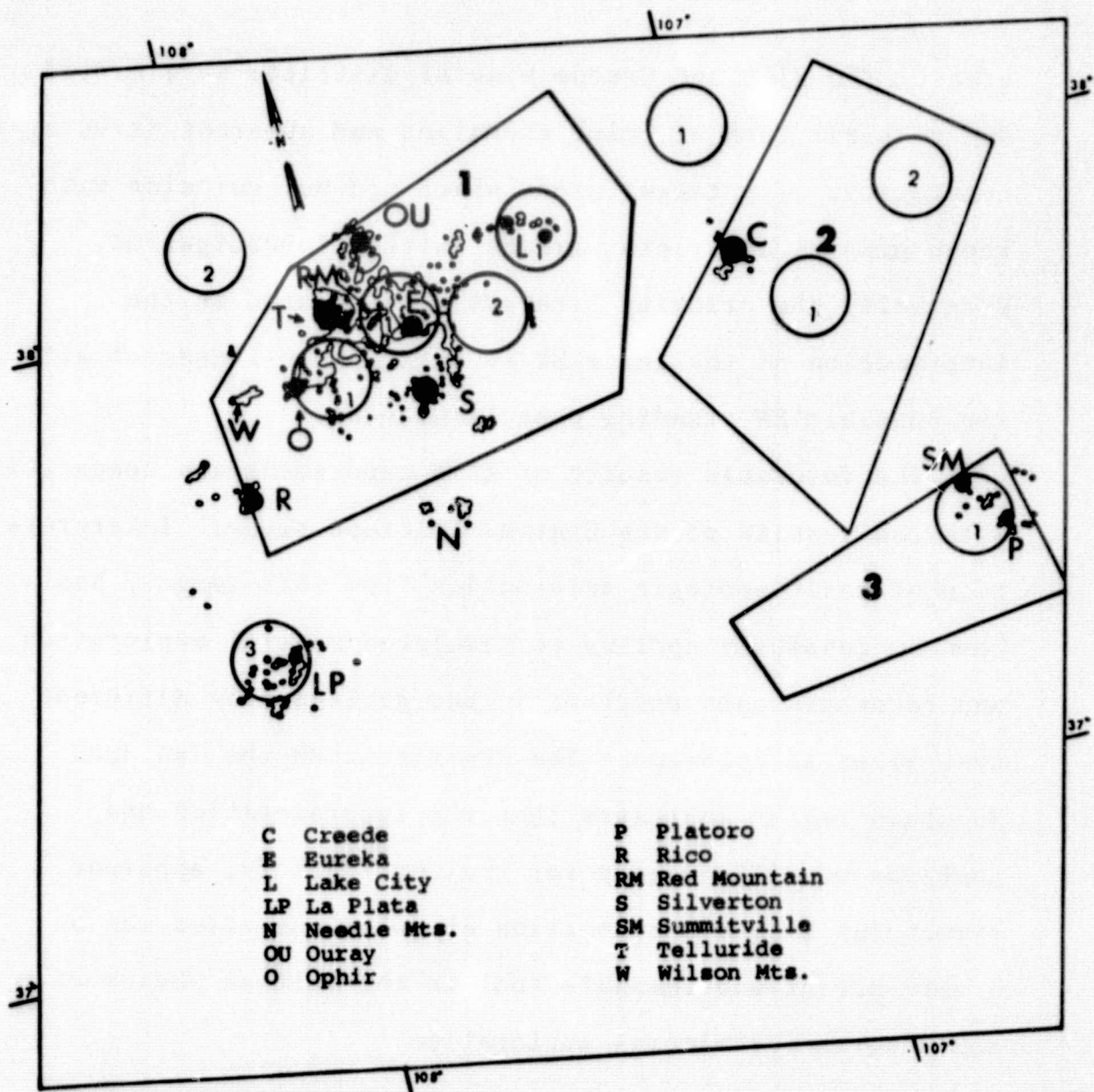
EXPLANATION

○   Less than $100,000 production

•   More than $100,000 production

⬤   Mining district; relative importance
      is indicated by the size of the circle

Figure 60. Target areas and the location of metallic
                mineral production in the San Juan Mountains,
                Colorado.

areas. The Rico and Creede mineral districts were missed due to their lack of color anomalies and apparent structural complexity. The target areas which did not coincide with known mineral districts warrent further investigation, especially the priority 1 target area located at the intersection of the large NE-trending photo-lineament with the possible EW-trending photo-lineament.

The favorable results of this experiment are comparable with the results of the Central Colorado study. Interpreta tion of basic geologic information from ERTS imagery has been successfully applied to simulated mineral exploration and reconnaissance programs in two geologically different test sites in Colorado. The experiment in the San Juan Mountain region indicates that the interpretation and analysis of ERTS imagery for regional geology, apparent structural fabric and location of color anomalies can be a very useful and feasible tool in the initial phases of any program for mineral exploration.

STUDIES OF VOLCANIC PHENOMENA

Studies of the San Juan Mountains suggest that ERTS-1 imagery can be successfully employed in locating volcanic centers, calderas and associated intrusive bodies. The San Juan Mountains are composed of a thick, layered sequence of Tertiary volcanic rocks overlying Tertiary, Mesozoic and Paleozoic sedimentary rocks and Precambrian metamorphic rocks

Studies conducted by the United States Geological
Survey (9) have defined 14 calderas within the San Juan
Volcanic field (Fig. 61). Of these 14, 3 calderas--
Silverton, Lake City and Creede calderas--are very well
expressed on the ERTS imagery because of the annular
drainages that have developed on or near the ring faults
bounding the calderas (Fig. 4). In addition, the Cochetopa
caldera and the Summer Coon volcanic centers are well-
expressed on the imagery as large circular depressions with
a raised portion in their centers. A large dike swarm
originating near the Platoro caldera and trending south-
southwest into New Mexico is also easily discriminated on
the ERTS imagery.

A number of fairly subtle circular and arcuate features
mapped on the ERTS imagery appear to lie close to other
calderas discovered by the United States Geological Survey.
The Platoro, Lost Lake and Mt. Hope calderas may correspond
to three of the circular features mapped (Fig. 24).

Most of the intrusives thought to be associated with
the late stages of the volcanic activity could not be
detected on the ERTS imagery because the landforms developed
over them are similar to the landforms developed in the
volcanic rocks. Some of the intrusives which have penetrated
the sedimentary rocks fringing the San Juan Volcanic field
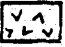were detected and mapped (Fig. 6).

Legend:
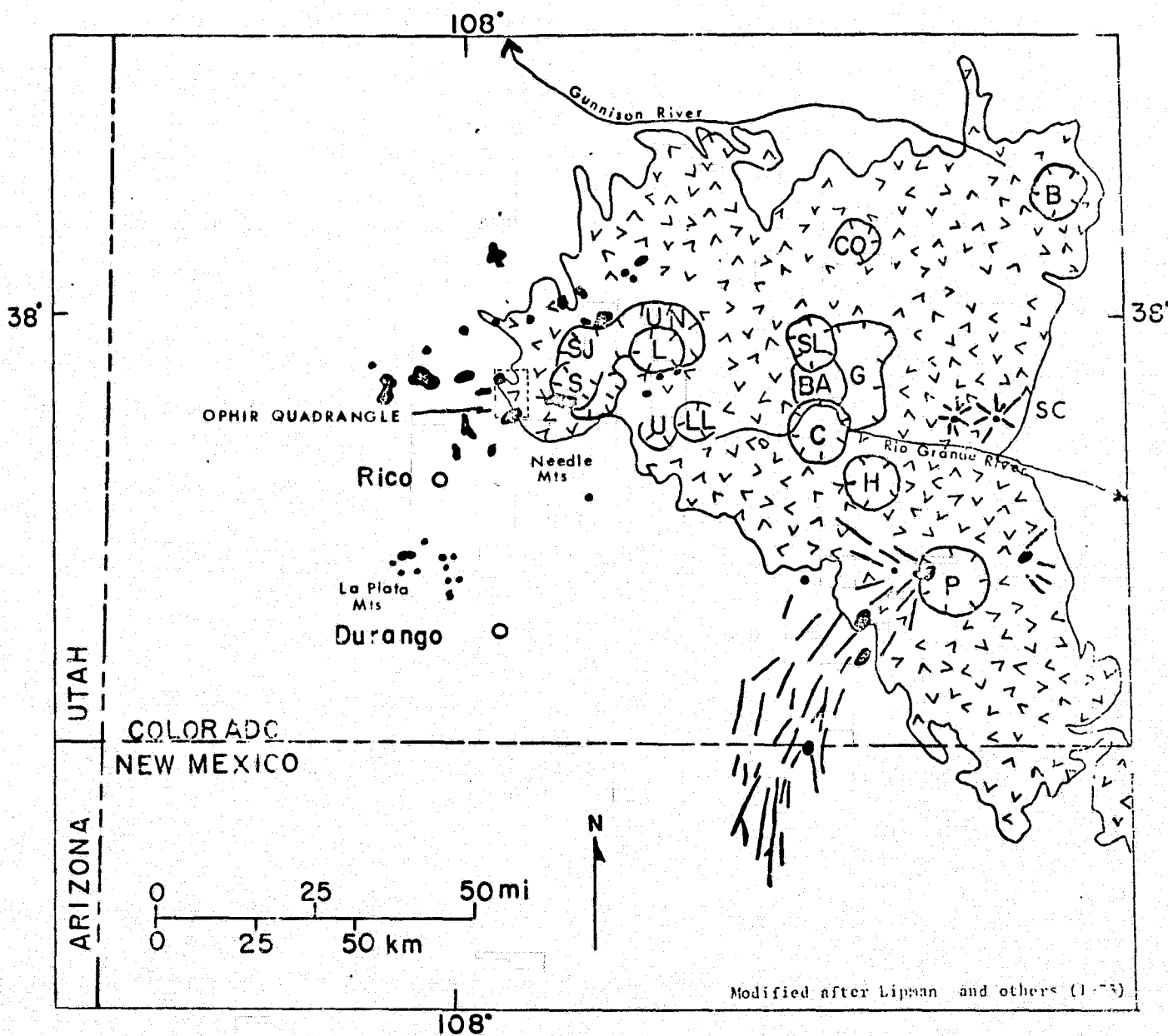
- Volcanic Rocks
- Intrusive Rocks

SC, SUMMER COON CENTER

CALDERAS

B, BONANZA
BA, BACHELOR
C, CREEDE
CO, COCHETOPA
G, LA GARITA
H, MT. HOPE
L, LAKE CITY

LL, LOST LAKE
P, PLATORO
S, SILVERTON
SJ, SAN JUAN
SL, SAN LUIS
U, UTE CREEK
UN, UNCOMPAHGRE

FIGURE 61. Calderas of the San Juan Mountains.

Finally, a large northeast-trending lineament passing through the Silverton, Lake City and Cochetopa calderas was mapped. It possibly coincides, at least in part, with the northeast-trending lineament (10) appears to be the surface expression of a deep-seated zone of weakness that controlled the location and formation of the Silverton, Lake City and Cochetopa volcanic centers and their attendent mineralization and intrusive activity.

The boundaries of the San Juan volcanic field could be mapped fairly accurately in areas where the volcanic rocks are in contact with sedimentary rocks. However, because of similarities in weathering characteristics and vegetation, the contacts of the volcanics with the Precambrian crystalline rocks and Tertiary intrusive rocks are obscure on the imagery.

It was impossible to map individual stratified volcanic units on the ERTS imagery. Although the drainage textures of the eastern and western San Juan Mountains are somewhat different, and probably reflect different volcanic formations, the boundary is not clear.

SURFACE WATER RESOURCES

The drainage basin of the Arkansas River between Leadville and Salida, Colorado is the beginnings of one of Colorado's major river systems (Fig. 62). This portion
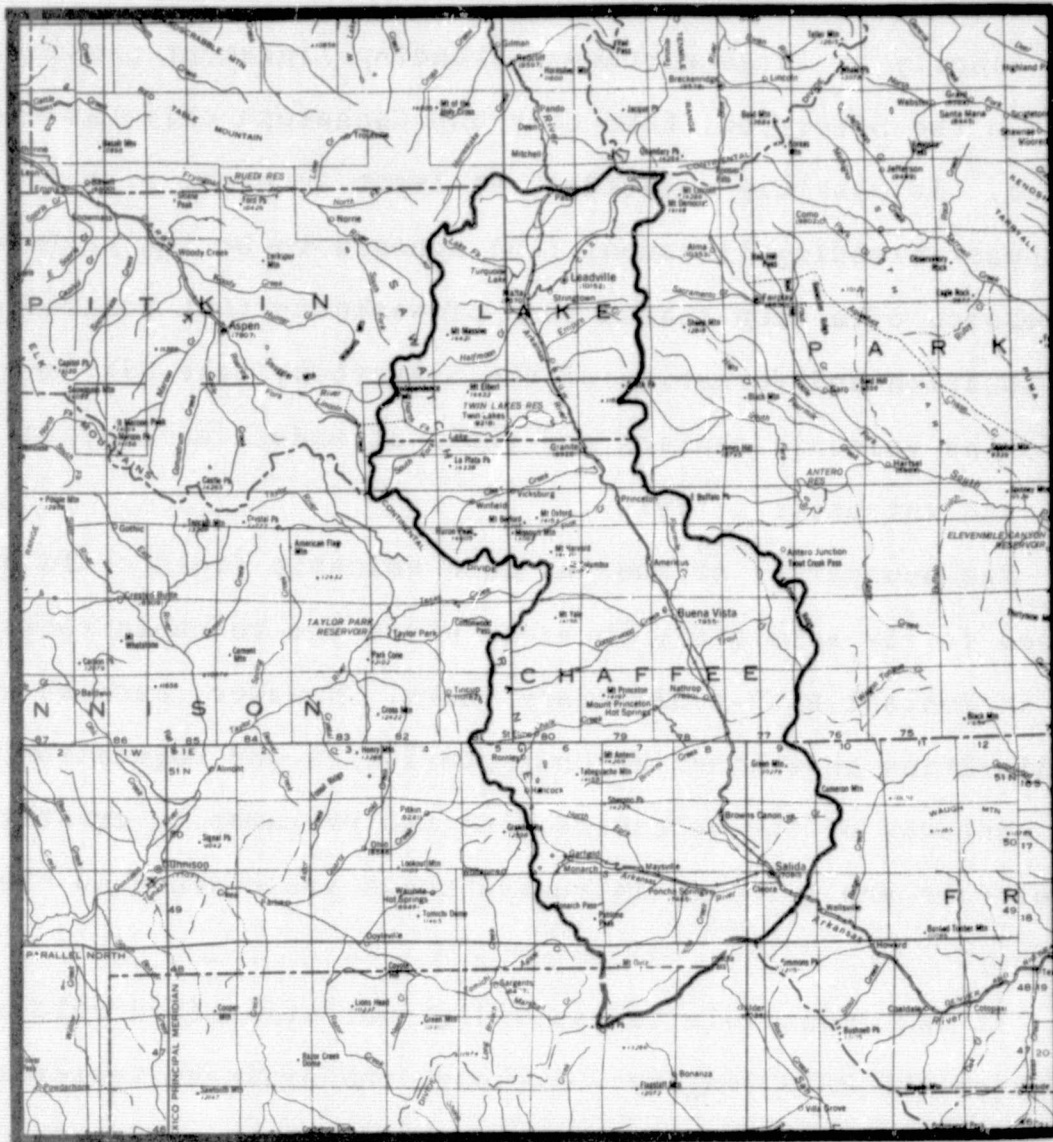
Figure 62. Index map of the Upper Arkansas drainage basin, central Colorado.

of the Arkansas River, termed the Upper Arkansas River, flows along the northern extension of the Rio Grande rift zone, a major Late Cenozoic topographic and structural depression extending 965 km from northern Mexico into central Colorado. In addition to the importance of the Upper Arkansas drainage basin as source of water for irrigation and numerous community water supplies, the Upper Arkansas drainage basin is currently one of the most actively investigated areas for geothermal energy in Colorado.

ERTS MSS imagery of the Upper Arkansas drainage basin was studied to investigate:

1)   the capability of the photo-interpreter to map the primary drainage net work and to correctly map and identify bodies of standing surface water,

2)   the interpretative techniques most useful for studying surface water phenomena, and

3)   the types of ERTS imagery useful for studying surface water phenomena.

This study was not undertaken to discover new geologic data about the Upper Arkansas drainage basin but, rather, to investigate the ability of ERTS imagery to provide information on surface water phenomena in the Colorado Rocky Mountains; the Upper Arkansas drainage basin served only as an area in which to investigate these phenomena.

Much of the Upper Arkansas drainage basin falls in
the alpine-glaciated areas of the Sawatch and Mosquito
ranges and, hence, contains many natural tarns and morainal
lakes as well as larger, man-made reservoirs. Existing
large and small-scale topographic maps of the area allowed
the ERTS imagery interpretations to be easily checked.

METHOD AND APPROACH

The available ERTS imagery of the Upper Arkansas
drainage basin was examined and two sets of imagery were
chosen for more detailed study (Table 14 and Fig. 63).
Snow-covered winter imagery (low sun elevation) depicts an
enhanced topographic model of the drainage basin area;
snow-free fall imagery depicts subtle soil moisture and

Table 14. Characteristics of the two sets of ERTS MSS
images used in this study.

IMAGE I.D.	DATE	SUN EL.	SUN AZ.	COMMENTS
1172-17141	11 Jan. '73	23°	150°	Snow-covered
1424-17125	20 Sep. '73	45°	142°	Snow-free

vegetation changes that are related to surface water
phenomena. Preliminary study of the fall imagery indicated
that band 7 (0.8-1.1μm) best displays the surface water
bodies in the drainage basin area; there was no clear-cut
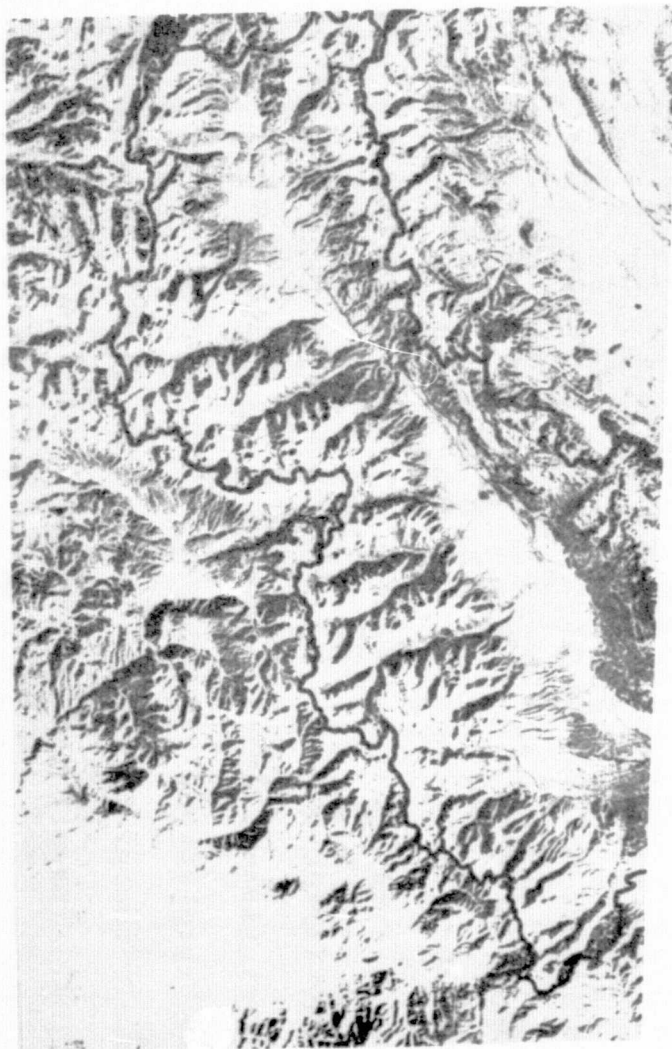
1172-17141-7 (Winter)   1424-17125-7 (Fall)

Figure 63.   Winter and fall ERTS-1 imagery of the Upper Arkansas drainage basin.

best band in the winter imagery as bands 5, 6 and 7 all show high contrast between snow and shadows. Band 7 from both sets of imagery was used for the photo-interpretations.

Initial interpretation of 10" x 10" positive transparencies of the drainage basin area indicated that the 1:1,000,000 scale images were too small to be adequately annotated. Consequently, enlarged prints at a scale of 1:360,000 were prepared. All subsequent interpretations were conducted on the enlarged prints. In addition, enlarged prints were also made of the drainage basin area from the ERTS images acquired the day after the test images were acquired; these prints provided stereo pairs that covered nearly all of the drainage basin area.

Photo-interpretation of the ERTS MSS imagery consisted of 3 steps:

    (1)   Outlining the divide of the Upper Arkansas drainage basin

    (2)   Tracing the network of streams in the drainage basin area

    (3)   Identifying and mapping the bodies of standing water (lakes, ponds, reservoirs).

The photo-interpretations were compared to existing small- and large-scale topographic maps of the area to determine whether the ERTS imagery interpretations provide a reasonable picture of the general surface water conditions.

DRAINAGE NETWORK

Both the winter and the fall ERTS images were studied to define the primary drainage network of the Upper Arkansas drainage basin. The final interpretation (Fig. 64) was made on the fall imagery because snow and terrain shadows obscured many drainage lines on the winter imagery.

The drainage network prepared from the ERTS imagery is much more detailed than the existing 1:1,000,000 scale map of the area (Fig. 62), but it is inferior to the 1:250,000 and larger scale maps. Accuracy of the photo-interpreted drainage net is very good compared to the 1:250,000 scale topographic map.

Mapping of the drainage net was done in two modes: non-stereoscopic and stereoscopic. The non-stereoscopic interpretation was generally worse than the stereoscopic interpretation in detail and accuracy. Consequently, stereoscopic analysis is deemed essential if the optimum job of mapping drainage networks is to be accomplished. This is particularly true in high-relief terrains.

WATER BODIES

Lakes, ponds and reservoirs cannot be identified on the winter ERTS imagery because they are frozen and covered by snow and do not contrast with their surroundings. On the fall imagery, however, 97 standing water bodies were
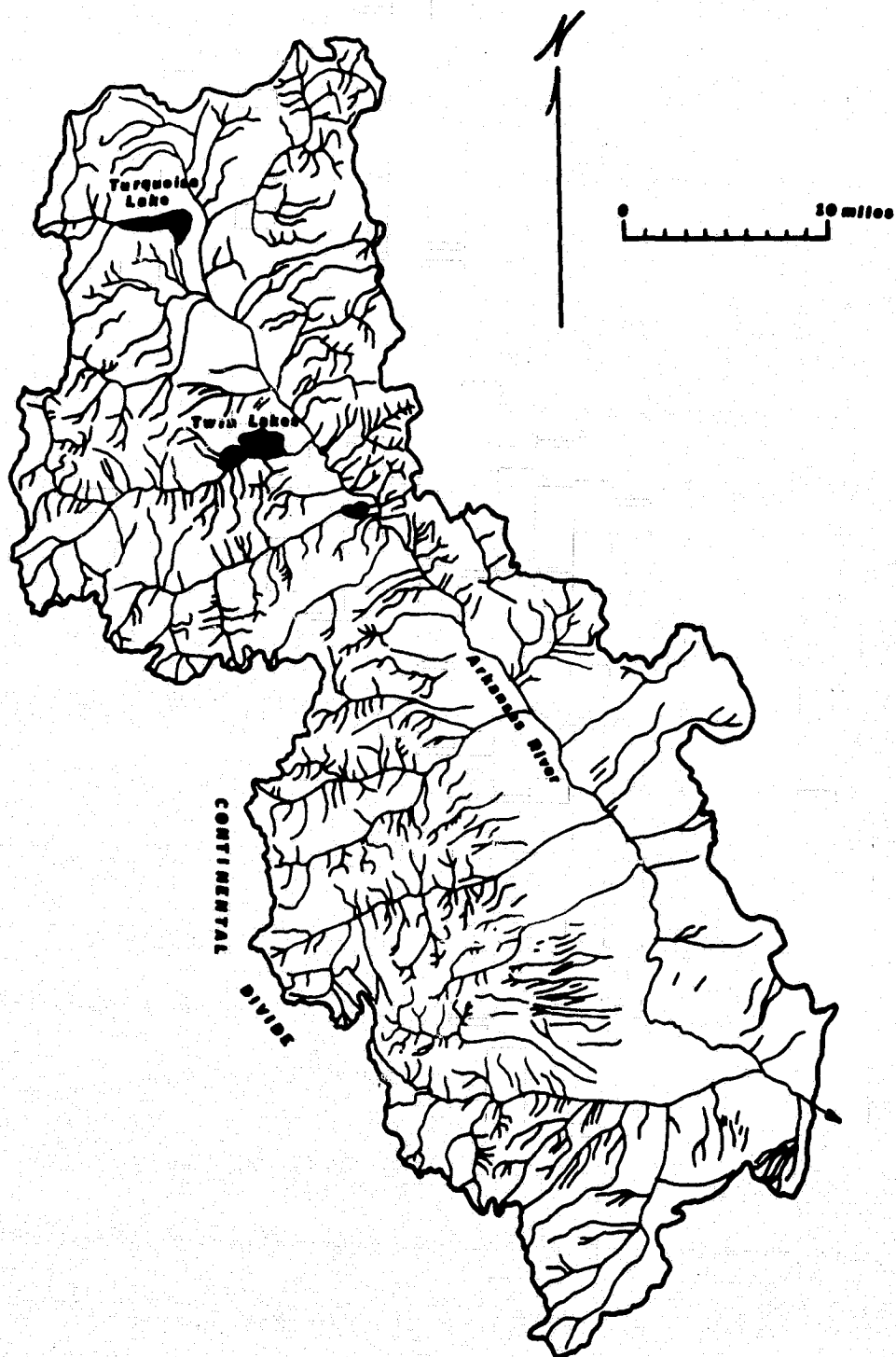
Figure 64.   Drainage network of the Upper Arkansas drainage
basin mapped from ERTS-1 image 1424-17125-7.

mapped.   The smallest water body mapped is about
85 meters in diameter.

The photo-interpretation was compared to the 1:250,000
scale topographic map of the drainage basin area. The
topographic map showed 99 lakes to be present in the area
and 61 of the lakes were correctly identified on the ERTS
imagery (61.6%). However, 38 of the lakes shown on the
topographic map (38.4%) were not identified on the ERTS
imagery and 36 of the 97 lakes mapped on the imagery
were not shown on the topographic map.

To determine whether any of the 36 unconfirmed lakes
mapped on ERTS imagery were real, existing topographic maps
at scales of 1:62,600 and 1:24,000 were checked. Of these
36 unconfirmed lakes, 25 were found on the larger scale
topographic maps and 11 apparently were not water bodies.

In total, 86 of the 97 (88.7%) ERTS-mapped water
bodies were confirmed as real and 11 (11.3%) either are
not real or are not shown on the large-scale topographic
maps, most probably the former. These figures indicate
only that a large percentage of the water bodies mapped
on ERTS imagery are actually water bodies; they say nothing
about the ability to map all the water bodies of an area
using ERTS imagery. Casual inspection of the large-scale
topographic maps of the drainage basin area indicates that
less than 50% of the water bodies in the area were actually

observed on the ERTS imagery. The primary factors in
this rather poor showing is the relatively small size of
many of the water bodies and the fact that many of the
small water bodies are hidden in shadows in the rugged
mountainous terrain.

SUMMARY

In the rugged terrain of the central Colorado Rocky
Mountains, relatively detailed drainage networks can be
mapped from ERTS imagery acquired in the fall; winter
imagery is less useful because of snow and terrain shadows.
Lakes, ponds and reservoirs can also be identified on the
fall imagery, although all of the water bodies in the
area cannot be found. The limiting factors appear to
be the size of the water bodies (>85m) and their position
with respect to shadows and trees; small water bodies are
difficult or impossible to identify if they are on the
north side of a steep, north-facing slope (shadows and
low scene radiance) or if they are surrounded by dense
coniferous forests.

In general, ERTS MSS band 7 (8-1.1µm) imagery shows
the best contrast between water bodies (dark) and their
surroundings (light gray to white). Image interpretation
using the available stereoscopic capability is necessary to
gain the maximum amount of information and avoid ambiguities

in identifying water bodies. Prints or transparencies enlarged to a scale of 1:360,000 or larger are necessary to accommodate the annotation of detailed information.

ERTS imagery should provide a quick means of evaluating the surface water resources of areas of the world where good topographic maps at a scale of 1:250,000 or larger do not exist. In the better known areas of the world, the major usefulness of ERTS imagery will probably lie in the ability to use repetitive imagery to monitor changes in surface water conditions and predict water availability.

ATMOSPHERIC EFFECTS

The Colorado School of Mines participated in a coopera-
tive study aimed at determining the effects of the atmosphere
on ERTS MSS imagery. This research was conducted by scientists
at the Martin Marietta Corporation-Denver Division under
subcontract to the Colorado School of Mines, and in coopera-
tion with the Environmental Research Institute of Michigan
(ERIM) and Dr. Harry Smedes of the U.S. Geological Survey.
The Colorado School of Mines portion of this cooperative
study consisted basically of the following:

1. Spectral measurements of direct, diffuse, and
    total solar radiation in the ERTS MSS bands.

2. Spectral reflectance measurements on selected
    broad outcrops in central Colorado.

These data were used by the ERIM to re-calculate the
radiance recorded by the MSS and to thereby generate
atmospherically-corrected MSS tapes. Dr. Smedes will
evaluate the utility of atmospherically-corrected ERTS
data by comparing computerized terrain recognition maps
generated with corrected and non-corrected MSS data. The
generation of atmospherically-corrected tapes is still in
progress (May 1975), so the results of this study will not
be known for several months.

The Colorado School of Mines completed the data col-
lection and passed the data on to the others for study and
evaluation. The following is a chronological summary of
the atmospheric studies.

PRE-LAUNCH ACTIVITIES

Two field trips were conducted for the purpose of
collecting baseline atmospheric data prior to ERTS I
satellite launch. Dr. H. Smedes and R. Watson, USGS,
accompanied Martin Marietta Corporation personnel on
these trips. Two objectives were set:

1) To locate suitable candidate atmospheric measure-
    ment sites for the overall geographic range of
    our area of interest, i.e., from Florissant north
    of Cripple Creek to the Great San Dunes.

2) To record first measurements of atmospheric
    parameters at ten individual locations within
    our selected ERTS test sites.

Candidate sites for measuring atmospheric parameters
during ERTS-1 overpasses were selected. Each site was
chosen on the basis of altitude and geologic, topographic
and vegetative environment; geographic position within the
overall test site was also considered. Actual measurements
made pertain to the optical transmission properties of the
atmosphere above each of the sites as well as the atmospheric
clarity above each site. Optical transmission was determined
using a Kahlsico pyrheliometer filtered to the following
spectral bands:

1) 300 to 2800 nanometers   6) 300 to 630 nanometers

2) 525 to 2800 nanometers   7) 300 to 700 nanometers

3) 630 to 2800 nanometers   8) 525 to 630 nanometers

4) 700 to 2800 nanometers   9) 525 to 700 nanometers

5) 300 to 525 nanometers   10) 630 to 700 nanometers

Atmospheric clarity was measured using a Kahlsico pyranometer to establish the ratio of diffuse-to-total solar radiation. In addition, pressure, temperature, relative humidity, and a plot of topographic elevations as seen radially to the test site were recorded in each case. Of the ten sites planned, only three sites were sufficiently cloud-free on the day of the field trip to allow solar measurements. These three were at Howard, at Hayden Pass, and at Gribble Run at the south end of the Thirtynine Mile volcanic field Pressure, temperature, relative humidity and topographic profiles were recorded at all ten sites.

Two specific geologic control sites were selected for field study. Site 1 is in the Granite Hills seven miles south of Florissant (105.27°W, 38.83°N). Surface outcrop is weathered granite of the Pikes Peak batholith. Site 2 is at Cross Creek at the north end of the Thirtynine-mile volcanic field, near Elevenmile Reservoir (105.60°W, 38.88°N). Surface outcrop here is Oligocene basalts apparently extruded from the Guffy Center.

SEPTEMBER 1972

Four persons occupied ground stations during the ERTS-1 satellite pass of 7 September 1972. Two persons manned Martin Marietta Atmospheric Sciences Mobile Laboratory at the Granite Hills site on 6 September. Data collection commenced on the afternoon of 6 September and included measurements of direct, diffuse, and total incident solar radiation, as well as reflectance spectra of the granite itself.

Additionally, during satellite overpass on 7 September, two persons occupied the second ground site located at Cross Creek. Measurements of solar radiation and rock reflectance were made over a four hour period.

FEBRUARY 1973

Atmospheric effects measurements were made during the 16 February 1973 overpass of ERTS-1. Measurements of direct, total, and diffuse solar radiation were made at two sites, Eleven Mile Reservoir (South Park) and Granite Hills. Spectral regions covered were those of the four bands of the ERTS MSS.

An ISCO spectroradiometer, modified somewhat for our specific applications, was used at the Granite Hills site, and a Bendix Model 100 Radiant Power Measuring Instrument (RPMI) was used at the Eleven Mile Reservoir

site. The use of the Bendix instrument was coordinated
with Dr. R. Rogers of Bendix, who is an ERTS-1 principal
investigator.

The atmospheric conditions for the 16 February overpass
were ideal; no clouds were present and atmospheric aerosols
appeared to be at a minimum. All measurements were analyzed
for optical depth and the absolute quantities of total and
diffuse solar radiation. There is a measurable difference
between the sites. This difference is attributed to an
altitude difference of 800 feet. The magnitudes and
differences of optical depth were compared to existing
atmospheric models published by A.F.C.R.L (11). These
comparisons indicate that the measurements were in the
general range of the 23 km visual range model. However,
the measured valued of optical depth for the Colorado Test
Site (Granite Hills and Eleven Mile Reservoir) are even
less than the most tenuous aerosol model (23 km visual
range). The measured values of optical depth and total and
diffuse solar radiation were forwarded to the Environmental
Research Institute of Michigan (ERIM). Dr. Thomson and
Dr. Turner of ERIM were to introduce these measurements
into their existing computer programs in order to correct
the 16 February MSS data for atmospheric effects. Dr. H.
Smedes of the U.S.G.S. was to compare the corrected and
uncorrected automatic computer terrain maps in order to
evaluate the impact of the atmospheric corrections.

In order to fully evaluate the radiative transfer programs used by ERIM for correcting the MSS data, measurements of snow reflectance were also made at the Eleven Mile Reservoir site. Measurements of snow reflectivity were made by viewing standard relfectance panels (gray and white), calibrated for each of the MSS bands using a Beckman DK2 reflectometer. The R.P.M.I. was used to measure the radiance of the gray panel, white panel and snow, and the reflectance of the snow was thus determined. In order to assess the degree of uniformity of the snow cover, a total of six different sites was measured. It was found that for RPMI band 1 (ERTS band 4), the reflectance varied from 83-86%, for band 2 (ERTS band 5) it varied from 83-87%, for band 3 (ERTS band 6) it varied from 82-87%, and for band 4 (ERTS band 7) it varied from 73-79%. The magnitude of the snow radiance during the actual overpass was measured to be: Band 1 - 42.0 watts per meter^2 per steradian; band 2 - 37.4 watts per meter^2 per steradian; band 3 - 31.8 watts per meter^2 per steradian; and band 4 - 55.5 watts per meter^2 per steradian.

The above measurements of snow relfectance, along with the corresponding measurements of atmospheric optical depth, at the Eleven Mile Reservoir site will allow ERIM to evaluate their computer corrections. This will be done

by first calculating the snow radiance and reflectance using the measurements of optical depth with the radiative transfer models, and then comparing these calculations with the actual measurements.

In order to perform the measurements of optical depth, reflectance, total radiation, and diffuse solar radiation, detailed laboratory calibrations were made for the Bendix R.P.M.I. and the ISCO. Calibration factors were derived that allowed absolute quantities to be obtained. These factors were compared to those derived by Bendix (Dr. R. Rogers) and NASA G.S.F.C. (using the Hovis Sphere). According to Bendix, all factors were in good agreement with each other.

In addition to the atmospheric measurements, spectral reflectance measurements were made of the Pikes Peak granite at time of the 16 February 1973 satellite overpass using the ISCO spectroradiometer and about four hours following overpass using the Bendix M-100 Radiant Power Measurement Instrument (RPMI). The RPMI measurements were calculated using spectral reflectance panels calibrated with a Beckman DK2 reflectometer. It is important to realize for purposes of comparison that the ISCO instrument measures hemispherical reflectance properties while the RPMI provides a directional measurement (FOV 6°). Both readings were taken 18 inches above the outcrop. Some loss of data was experienced due to ink freezing in the ISCO recorder.

Two field crews were on station during the 17 May 1973
ERTS-1 overpass. Hazy, thin cirrus clouds began appearing
over both the Granite Hills and Cross Creek stations about
0715 and continued progressively more dense. Finally, at
about 1100 MDT a heavy, solid cloud cover appeared overhead,
rendering solar radiation data at time of ERTS overpass
completely useless.

The same two stations were again occupied for the
21 June 1973 overpass. An ISCO Spectroradiometer was
used on each site with excellent results. The best data,
by far, of any obtained at time of ERTS overpasses were
recorded at both Granite Hills and Cross Creek on this
date. Measurements consisted of a repeating series of
the following data, recorded spectrally from 400 to 1100
nanometers:

A) Direct solar radiation

B) Total solar radiation as viewed through a BG-36
    filter for instrument calibration purposes

C) Diffuse solar radiation

D) Hemispherical reflectance (180°) of the outcrop

E) Directional reflectance of a spectrally-calibrated
    white card

F) Directional reflectance of the outcrop

G) Directional reflectance of a spectrally-calibrated
    gray card.

An ISCO spectroradiometer was used on each of the two sites to derive the above measurements. A Bendix Model 100 Radiant Power Measuring Instrument (RPMI) was used to derive optical depth. Such measurements are required in order to determine the effects of the atmosphere on the ERTS MSS data and to derive sensor corrections to be performed by the Environmental Research Institute of Michigan (ERIM). The radiance recorded by the ERTS MSS is related to the above measurements by

$$N_{MSS} = \frac{\rho \, He^{-\tau \, \sec \theta_o}}{\pi} + N_p$$

where ρ is the target reflectivity, H is the total solar radiation, τ is the optical depth, N_p is the atmospheric path radiance, and θ_o is the solar zenith angle. As discussed previously, H and τ were measured, along with ρ. The path radiance, N_p, will be calculated by ERIM. This will then allow the ERTS data to be corrected for atmospheric effects, and subsequent evaluation (by H. Smedes of USGS) of these effects on computerized terrain recognition routines.

The results of the measurements are shown in Figures 65 through 71, and in Table 15. The Granite Hills site had a slightly higher amount of total solar radiation which is most likely a result of the slightly higher ratio of diffuse to solar radiation. The optical depths at the two sites are similar. The optical depth is calculated by
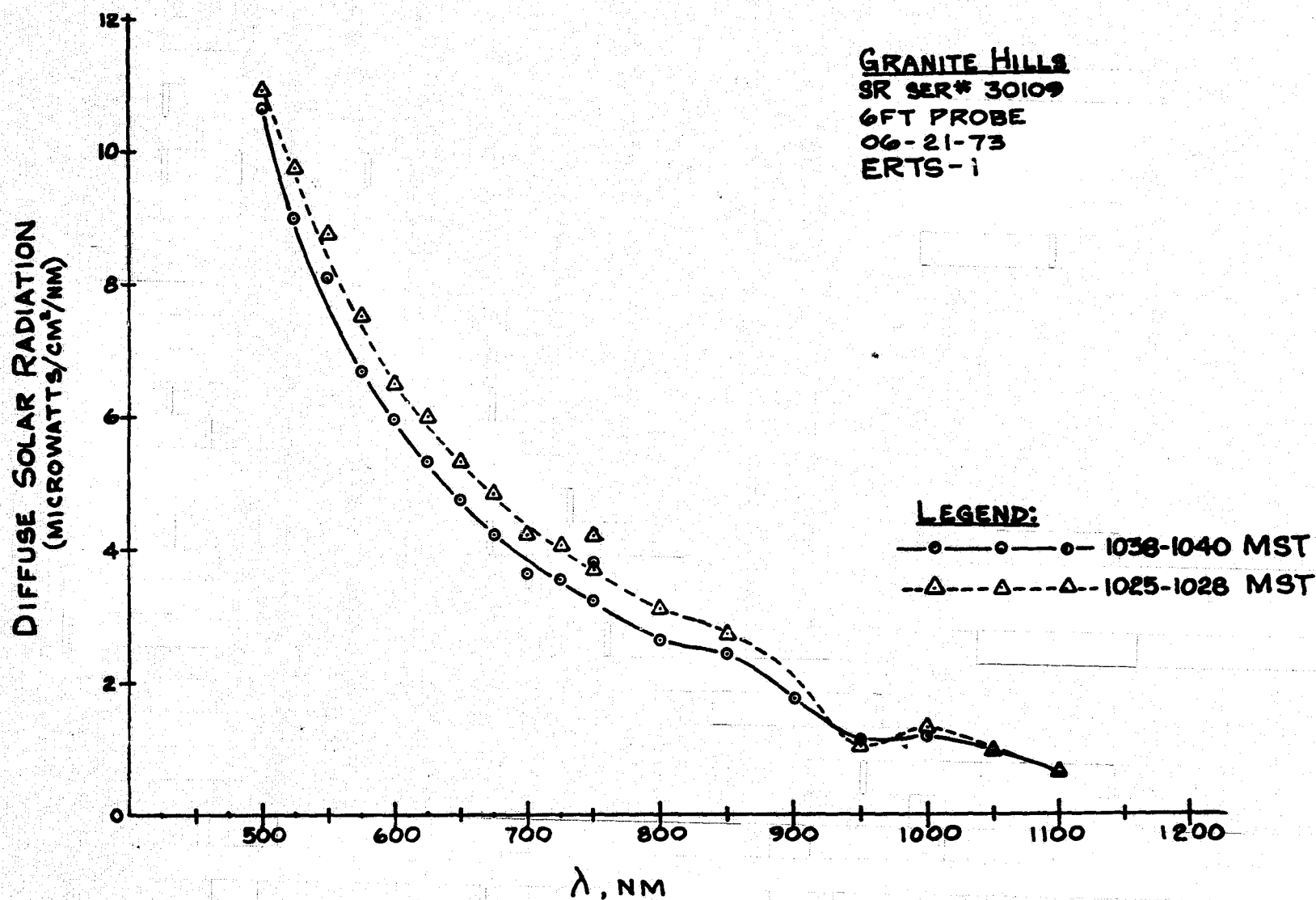
GRANITE HILLS
SR SER# 30109
6FT PROBE
06-21-73
ERTS-1

LEGEND:
—o——o——o— 1038-1040 MST
--△---△----△-- 1025-1028 MST

Figure 65. Diffuse Solar Radiation Incident on Granite Hills Test Site (Pikes Peak Granite) 21 June 1973.
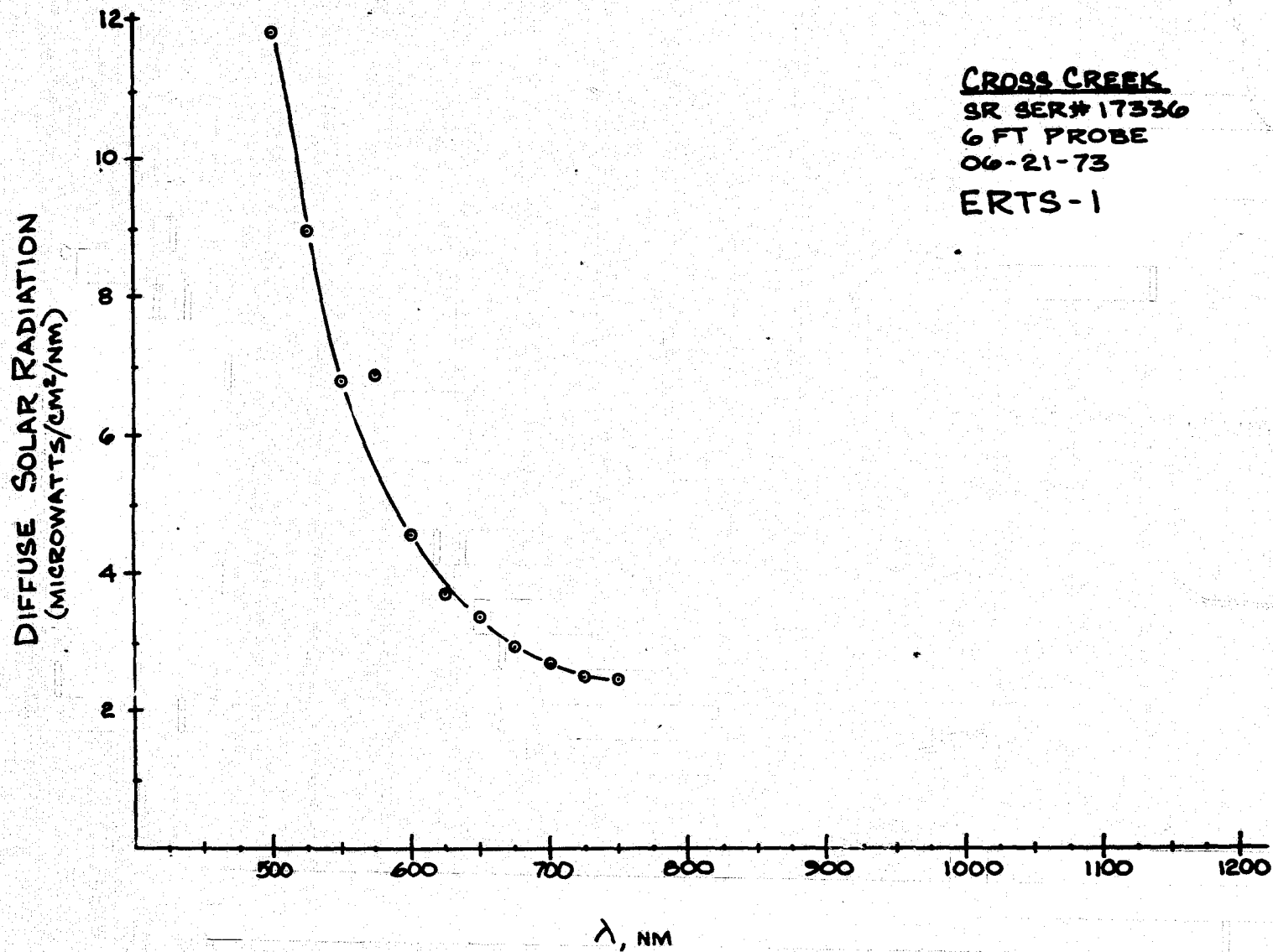
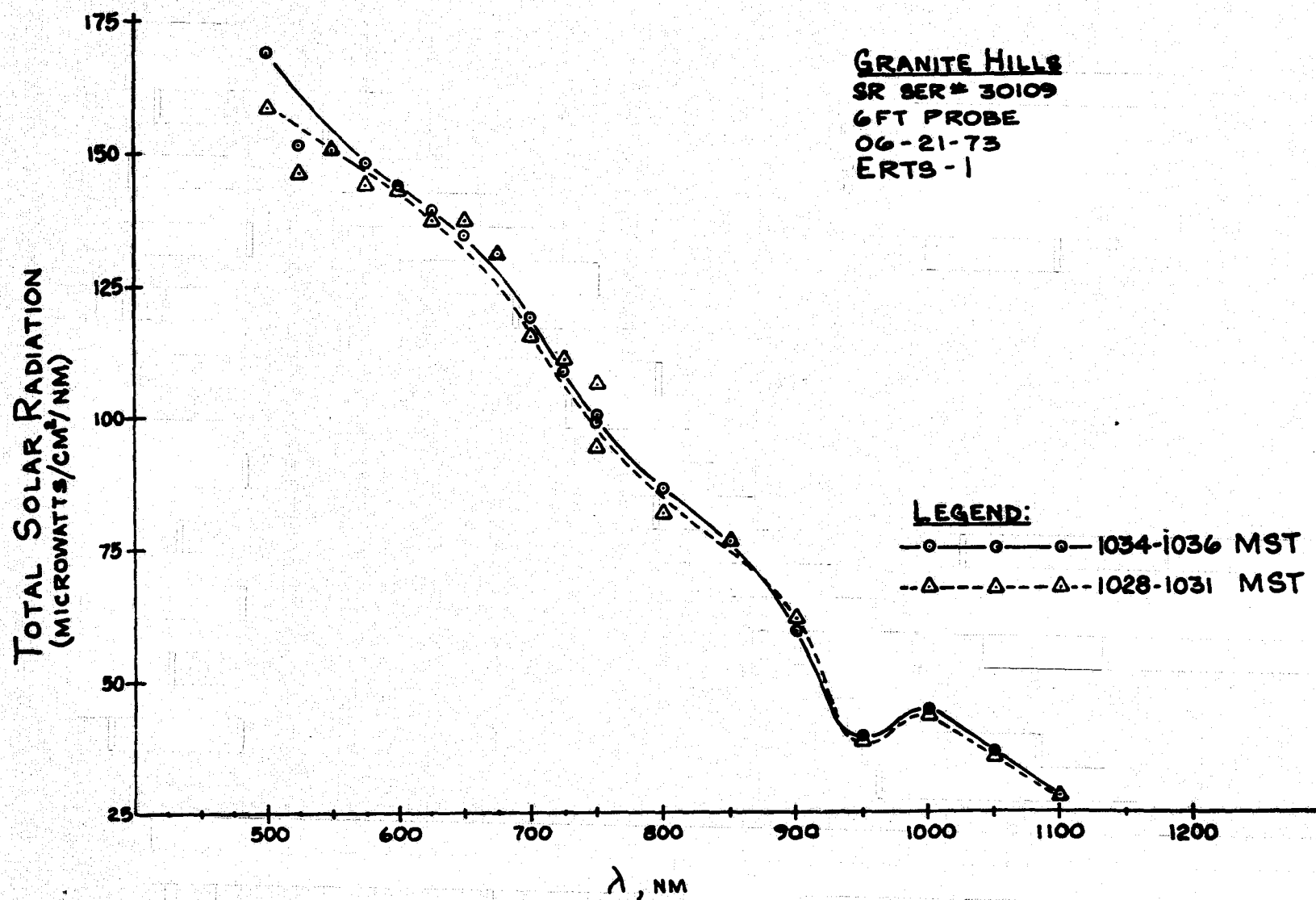Figure 66. Diffuse Solar Radiation Incident on Cross Creek Test Site (Thirtynine-Mile Basalt) 21 June 1973

Figure 67. Total Solar Radiation Incident on Granite Hills Test Site (Pikes Peak Granite) 21 June 1973
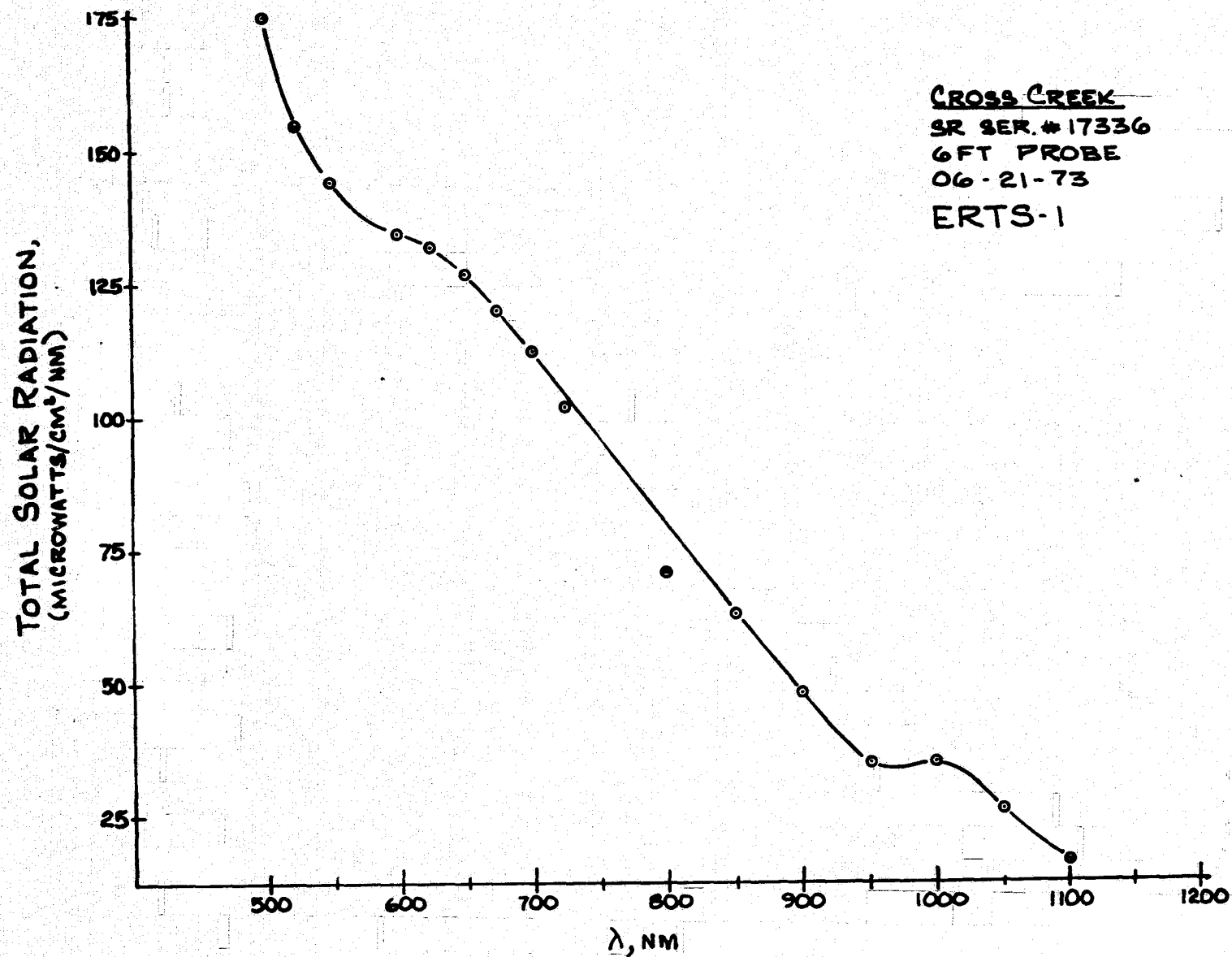
Figure 68. Total Solar Radiation Incident on Cross Creek Test Site (Thirtynine-Mile Basalt) 21 June 1973
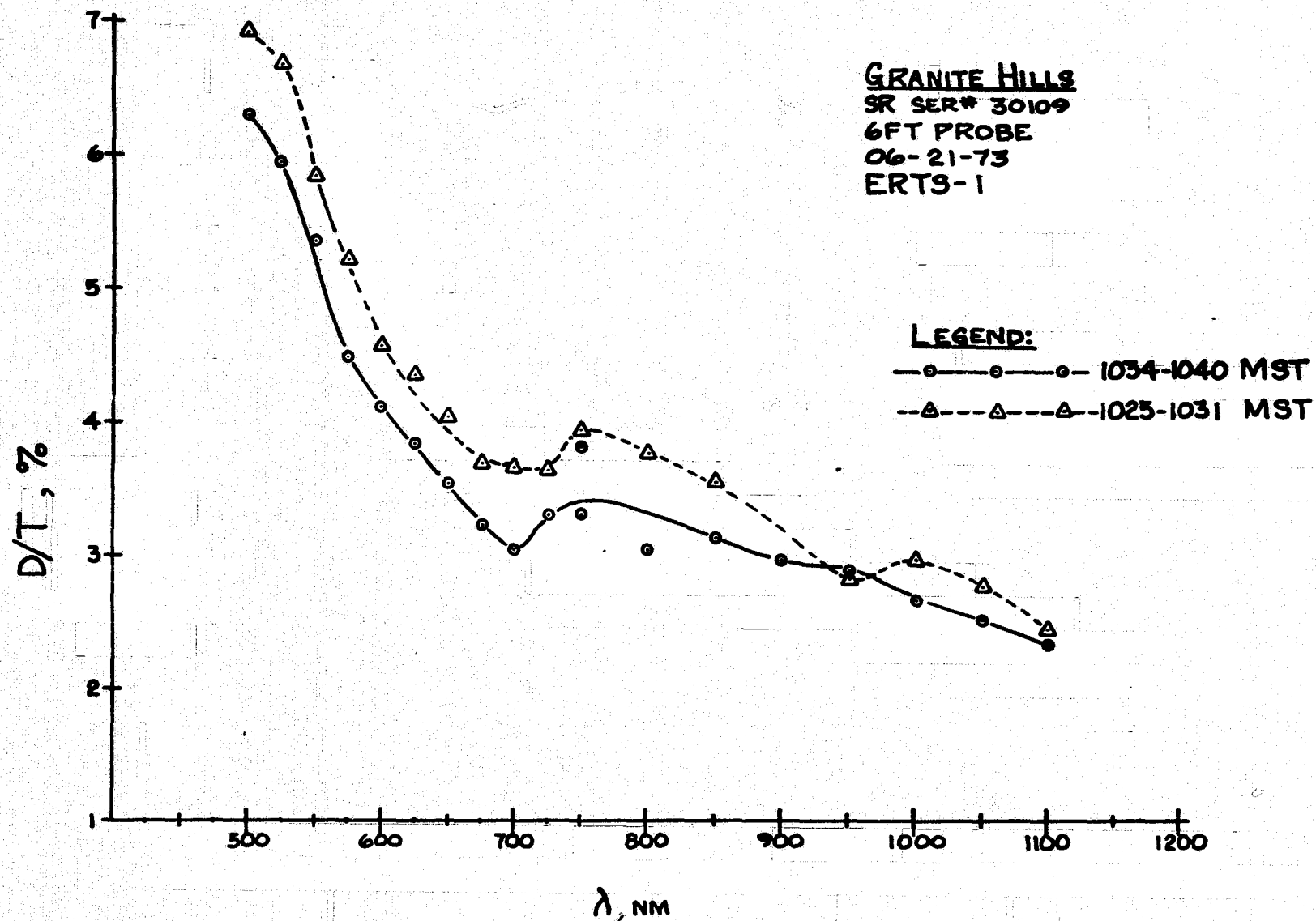
Figure 69. Ratio of Diffuse-to-Total Solar Radiation Incident
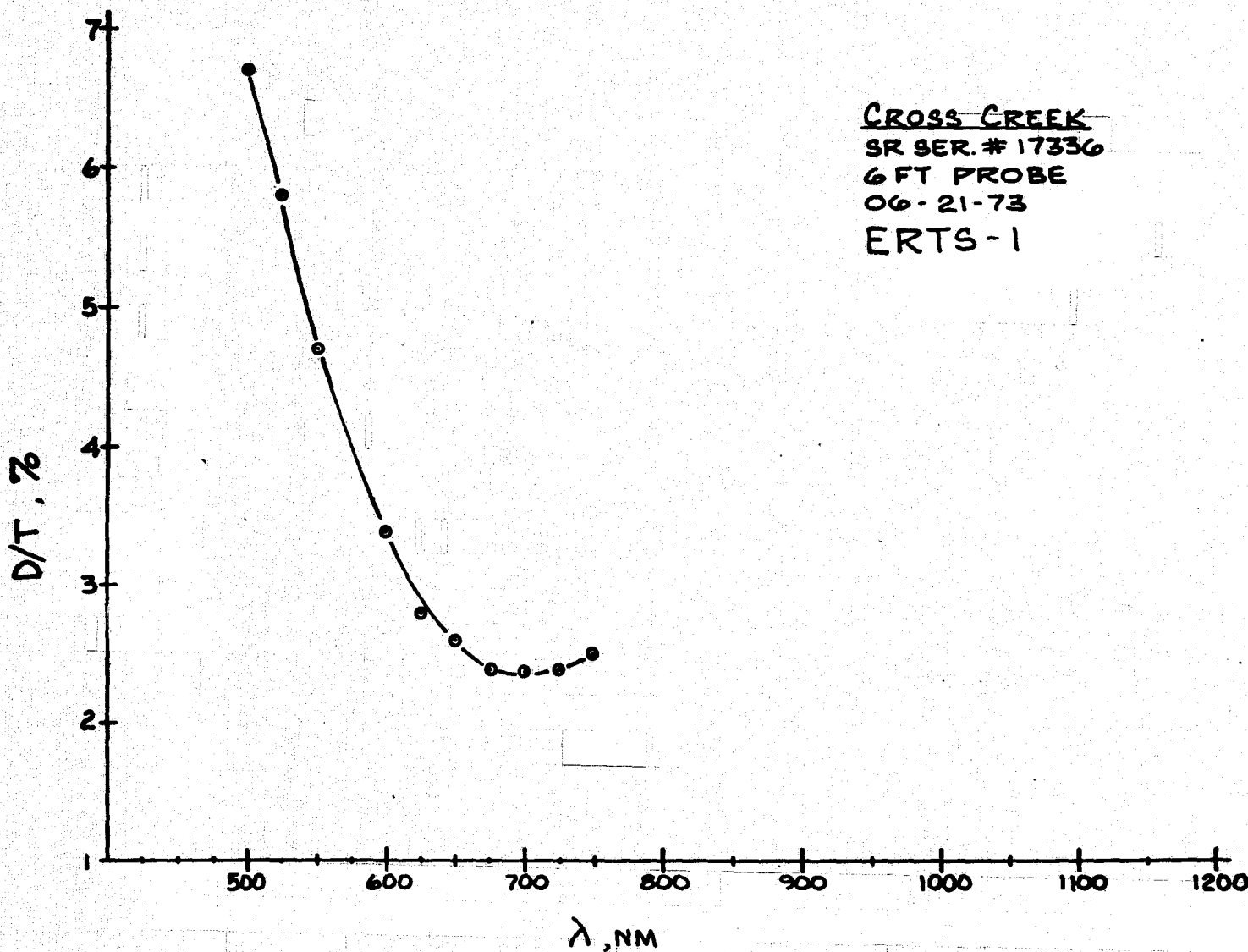on Granite Hills Test Site (Pikes Peak Granite) 21 June 1973

Figure 70. Ratio of Diffuse-to-Total Solar Radiation Incident on
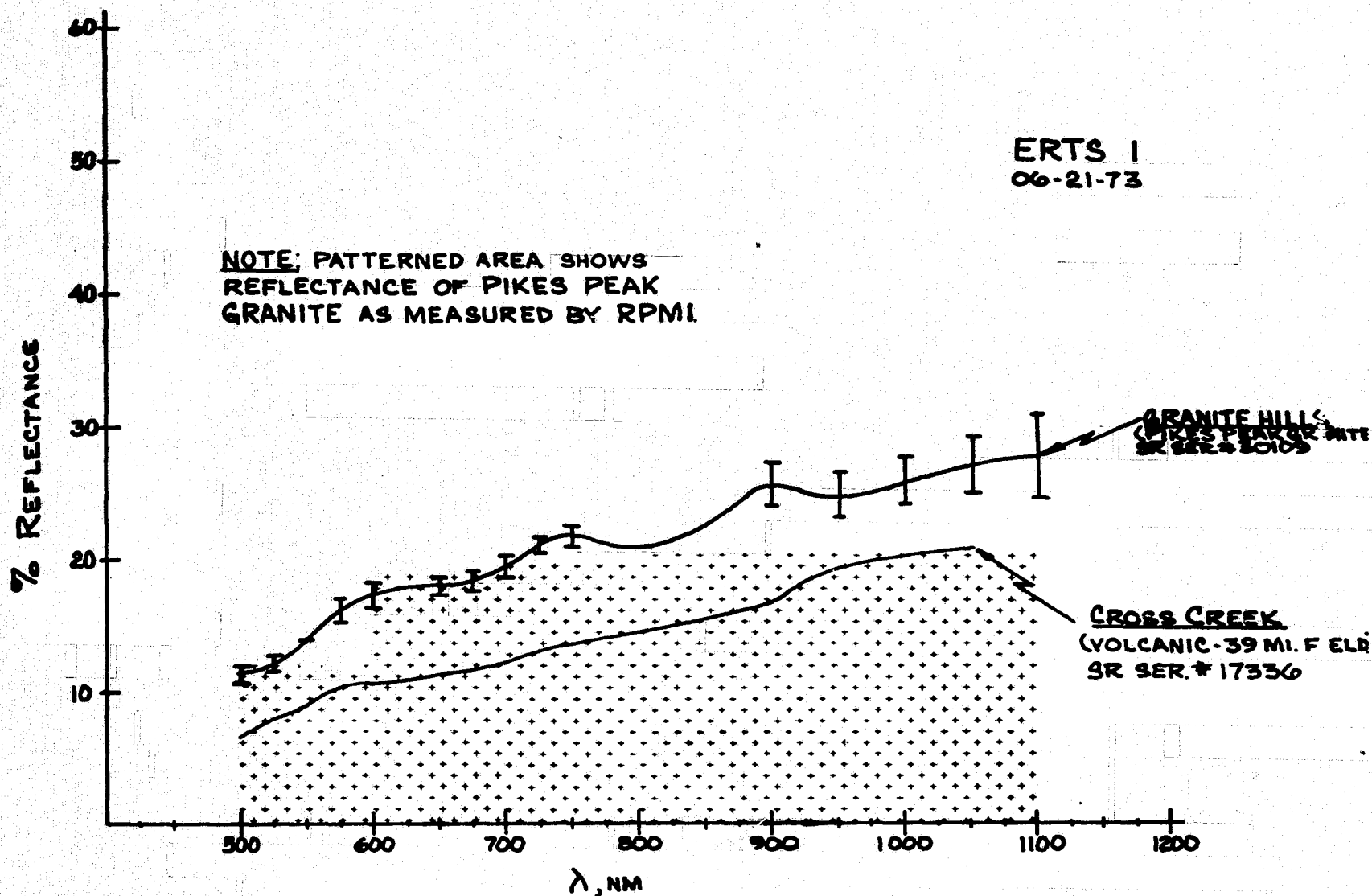Cross Creek Test Site (Thirtynine-Mile Basalt) 21 June 1973

Figure 71. Comparison of Spectral Reflectance of Pikes Peak Granite and Thirtynine-Mile Basalt, 21 June 1973

Table 15. Optical Depth Measurements at Two Locations Using Bendix Model 100 RPMI; 6-21-73

CROSS CREEK: Time - 1154 MST, Sec θ_0 = 1.04
Elevation: 9,400 Feet

ERTS-1 MSS Bands	B1	B2	B3	B4
Meter	1.39	1.40	1.18	.862
Scale	30	30	30	10
M-Intensity	13.9	14.0	11.8	8.62
M_0	16.4	15.9	12.8	9.15
τ	.159	.122	.078	.058

GRANITE HILLS: Time - 1030 MST, Sec θ_0 = 1.10
Elevation: 8,240 Feet

ERTS-1 MSS Bands	B1	B2	B3	B4
Meter	1.38	1.39	1.17	.853
Scale	30	30	30	10
M	13.8	13.9	11.7	8.53
M_0	16.4	15.9	12.8	9.15
τ	.157	.122	.082	.063

$$\tau = \frac{\ln M_o - \ln M}{\sec \theta_o}$$

where M is intensity as measured by the RPMI for each ERTS band, and M_o is the calculated intensity that would be measured by the RPMI outside of the atmosphere. M_o was determined using data from the ERTS overpass of 16 February 1973. M_o is calculated by taking several intensity readings at varying airmasses ($\sec \theta_o$). Intensity, M, is plotted (semilog) vs. airmass, $\sec \theta_o$ (linear axis) to extrapolate M_o to an airmass of zero intensity outside of the atmosphere.

In addition to the measurements of solar radiation and rock reflectivity described above, a Bendix RPMI was used to record spectral reflectivity in each of the four ERTS-1 bands at a number of field outcrop locations. These outcrops included; Pikes Peak Granite, Cripple Creek Granite, mine tailings at the Mollie Kathleen gold mine at Cripple Creek, undisturbed, altered Cripple Creek granite near the mined area, sandstones of the Dakota Formation and Carlisle Shale.

During all of these measurements, the Bendix RPMI worked flawlessly, was extremely portable and easy to use, and it produced consistently good data.

CONCLUSIONS

The major goals of this investigation were to evaluate the geologic information content of ERTS-1 imagery and to study some possible geologic applications of the extracted information. Results of several independent studies conducted within the Colorado School of Mines ERTS-1 investigation provide the basis for the following conclusions:

1) The amount of geologically-relevant information that can be interpreted from ERTS-1 imagery far exceeds initial expectations.

2) Most of the geologic information in ERTS-1 imagery can be extracted from bulk processed black and white transparencies by a skilled interpreter using standard photogeologic techniques. Stereoscopic analysis is invaluable.

3) Various image enhancement techniques, including color additive viewing, color separation and density slicing, can be effectively used to selectively enhance certain geologic phenomena on the original imagery. The enhancement processes, however, produce an overall degraded image; enhanced images are unsatisfactory for general geologic interpretation.

4) In central and western Colorado, the detectability of lithologic contacts on ERTS-1 imagery is closely related

to time of year the imagery was acquired. Furthermore, some contacts are most easily detected on wintertime imagery; others are best expressed on summertime imagery.

5) The lithologic information content of ERTS-1 imagery is also strongly sensitive to the time of imagery acquisition; the band of imagery used is unimportant. Most of the information capable of being extracted can be found by interpreting imagery from only the winter and summer seasons together, thereby eliminating the need to examine great volumes of imagery.

6) Geologic structures are the most readily extractable type of geologic information contained in ERTS-1 images. The usefulness of this information appears to be limited only by the skill and imagination of the investigator.

7) Major tectonic features and many associated minor structures can be rapidly mapped from ERTS-1 images, allowing the geologic setting of a large region to be quickly accessed.

8) The detability of linears and trends in ERTS-1 images varies greatly between image generations and depends on sun attitude and surficial tonal contrasts due to seasonal effects.

9) The high resolution of ERTS imagery allows detection and connection of longer linear features than is possible with relief maps and topographic maps.

10) The trends of geologic structures in younger sedi-
mentary appear to strongly parallel linear trends in
older metamorphic and igneous basement terrain.

11) Landforms can be recognized on ERTS-1 images by the
shape of tonal and textural patterns. These patterns
are mostly the result of topographic and vegetative
phenomena. Low sun-angle, wintertime ERTS-1 imagery
is best for studying landforms in central and western
Colorado.

12) Linears and color anomalies mapped from ERTS-1
imagery are closely related to loci of known minerali-
zation in the Colorado Mineral Belt. Plotting frequency
of linear intersections, combined with the location of
"reddish-brown" color anomolies, appears to be a
relatively quick and effective way of isolating primary
target areas for metallic mineral exploration.

REFERENCES CITED

1. D.L. Bruns. Geology of the Lake Mountain northeast quadrangle, Saguache County, Colorado. Unpublished Colo. School of Mines M.S. Thesis, T-1367, 1971. 79 p.

2. D.L. Bruns, R.C. Epis, R.J. Weimer, and T.A. Steven. Stratigraphic relations between Bonanza center and adjacent parts of the San Juan volcanic field, south-central Colorado. New Mexico Geol. Soc. Guidebook 22nd Field Conf., 1971, p. 183-190.

3. Irwin Miller and J.E. Freund. Probability and statistics for engineers. Prentice-Hall, Inc., Englewood Cliffs, New Jersey, 1965. 432 p.

4. Ogden Tweto and J.E. Case. Gravity and magnetic features as related to geology in the Leadville 30-minute quadrangle, Colorado. U.S. Geol. Survey Prof. Paper 727-C, 1972.

5. D.L. Sawatzky and Keenan Lee. New uses of shadow enhancement. Remote Sensing of Earth Resources, v. 3, 1974. p. 1-18.

6. R.C. Epis, G.R. Scott, and R.B. Taylor. Petrologic, tectonic, and geomorphic history of central Colorado. Geol. Soc. America, Rocky Mtn. Section, Guidebook for Field Trip 8, 6 May 1973. 22 p.

7. D.H. Johnson. Geology of the Devil's Head quadrangle, Douglas County, Colorado. Unpublished Colo. School Mines D.S. Thesis, 1961.

8. J.W. Vanderwilt. Mineral resources of Colorado. Colorado Mineral Resources Board, 1947. Plate 4.

9. Lipman, P.W., Steven, T.A., Luedke, R.G., and Burbank, W.S., 1973, Revised volcanic history of the San Juan, Uncompahgre, Silverton, and Lake City calderas in the western San Juan Mountains, Colorado: U.S. Geol. Survey, Jour. Research, v. 1, no. 6, p. 627-642.

10. R.G. Ludke and W.S. Burbank. Volcanism and cauldron development in the western San Juan Mountains, Colorado. Colo. School Mines Quart., v. 63, n. 3, p. 175-208.

11. L. Elterman. Vertical-attenuation model with eight surface meteorological ranges 2 to 3 kilometers. AFCRL, 1970.

BIBLIOGRAPHY OF CONTRACT-SUPPORTED

PUBLICATIONS

Evans, J.L., 1973, Geology of the upper Marshall Creek drainage basin, Saguache County, Colorado: Unpublished Colorado School of Mines M.S. Thesis T-1529, 78 p.

Hutchinson, R.M., 1973, Pikes Peak Batholith: A composite batholith [abs.]: Geol. Soc. America Abstracts with Programs, v. 5, no. 6, p. 486.

Knepper, D.H., 1974, Lithologic mapping with ERTS-1 imagery (in preparation).

Lee, Keenan, Knepper, D.H., and Sawatzky, D.L., 1974, Geologic information from satellite images: Remote Sensing of Earth Resources, v. 3, p. 411-448.

Nicolais, S.M., 1974, Geology of the south Ophir mining district, San Miguel County, Colorado: Unpublished Colorado School of Mines M.S. Thesis T-1640 (in progress).

Sawatzky, D.L., and Lee, Keenan, 1974, New uses of shadow enhancement: Remote Sensing of Earth Resources, v. 3, p. 1-18.

Trexler, D.W., 1974, Fold structures in northwestern Colorado from ERTS-1 imagery [abs.]: Geol. Soc. America Abstracts with Programs, v. 6, no. 5, p. 480.

_____, 1974, Fold structures in Piceance Basin, Colorado, from ERTS-1 imagery: Rocky Mountain Assoc. of Geologists 1974 Guidebook (in press).